CHARACTERIZING THE ROLE OF CENTRAL CARBON METABOLISM AND CELL WALL STRESS RESPONSES IN *BACILLUS SUBTILIS* CELL WALL SYNTHESIS

A Dissertation

Presented to the Faculty of the Graduate School

of Cornell University

in Partial Fulfillment of the Requirement for the Degree of

Doctor of Philosophy

By

Vaidehi Bhupendrakumar Patel

December 2018

Characterizing the role of central carbon metabolism and cell wall stress responses in *Bacillus subtilis* cell wall synthesis

Vaidehi Bhupendrakumar Patel, Ph.D.

Cornell University 2018

The cell wall is an essential organelle for many bacteria since it provides mechanical strength and prevents bacterial cell lysis due to internal turgor pressure. Additionally, the cell wall is the first line of defense against various external stresses. The mesh of peptidoglycan is a major component of bacterial cell wall that surrounds the outer membrane. The cell wall of the gram-positive rod-shaped bacterium *Bacillus subtilis* consists of a thick peptidoglycan (PG) layer and phosphate containing anionic polymers called teichoic acids. To maintain the rod shape, *B. subtilis* elongates its lateral cell wall first, followed by cell division. Both tasks are carried out by distinct but coordinated machineries termed as elongasome (also termed as the Rod complex) and divisome, respectively. The synthesis of peptidoglycan is a dynamic process that is affected by various factors such as the availability of nutrients and external stresses. I have characterized the physiological role of an essential gluconeogenic factor GlmR (previously known as YvcK) in *B. subtilis*. Homologs of GlmR present in bacteria from different phyla and preliminary observations hint towards a conserved role of GlmR in different organisms. Except the phenotypic observations, for a long-time the function of GlmR has been a mystery. In my dissertation, I show that GlmR functions at the interface of the central carbon metabolism and the peptidoglycan biosynthesis

pathway. I have discovered that under gluconeogenic growth condition, GlmR plays an essential role in diverting carbon from the central carbon metabolism to the peptidoglycan biosynthesis, putatively by activation of GlmS- the first enzyme in PG precursor biosynthesis. Additionally, I have studied a *B. subtilis* signaling nucleotide, cyclic diadenosine monophosphate (c-di-AMP), and an extracytoplasmic function (ECF) σ-factor, σ^M, in peptidoglycan homeostasis in response to beta-lactam stress.

GlmR as well as c-di-AMP are known to be important for virulence in many pathogenic bacteria. GlmR is essential for establishing infection in *Listeria monocytogenes* and *Mycobacterium tuberculosis*. Many pathogens use c-di-AMP to modulate the host immune system to facilitate the infection. Taken together, this dissertation adds to the current understanding of the effects of nutrient availability and stress on peptidoglycan homeostasis in *B. subtilis* which can be further applied to understand bacterial virulence.

BIOGRAPHICAL SKETCH

Vaidehi Patel was born and brought up in the Ahmedabad city of India. She obtained her undergraduate degree in microbiology from M.G. Science Institute of Gujarat University in the same city. She then moved to USA to pursue a Master of Science degree. While pursuing her MS degree, she joined Dr Max Gottesman's lab in Columbia University as a volunteer student researcher. She graduated with an MS in Biotechnology from the NYU Tandon School of Engineering in NYC in 2011. She continued working in Columbia University until July 2012. In August of that year, she joined the PhD program in the department of microbiology at Cornell University. After completing the mandatory lab rotations, she decided to join Dr John D Helmann's lab to pursue her PhD research. There she has studied regulation of early steps peptidoglycan synthesis and cell wall stress response in the model organism *Bacillus subtilis*.

For Mom, Dad and Naman

ACKNOWLEDGEMENTS

My journey through Doctor of Philosophy wouldn't have been possible without guidance and support of many. I would like to express my gratitude for the people who have made this journey possible.

I would like to begin by thanking my advisor, Dr. John D Helmann for his superlative guidance that has shaped me into the scientist I am today. He has always been very encouraging and ready to discuss science whenever I needed him. Moreover, he has been very supportive of me and understanding when things didn't go as planned. I really appreciate his immense faith in me. In the past few years, I have learned a great deal from him including but not limited to, scientific communication, critical thinking, experimental design and mentoring skills. Thank you, John, for being the most amazing mentor a graduate student can hope for!

Next, I would like to thank my committee members: Drs. Eric Alani and Holger Sondermann for always taking time out from their busy schedules to attend my research seminars and committee meetings and providing me with valuable feedback and new ideas. I am greatly appreciative of the guidance they have provided me in the past few years, whether it be scientific or related to career development.

I would also like to thank all the amazing members of the Helmann lab who provided an incredibly supportive, fun filled and positive working environment. I would like to thank the past lab member, Dr. Ahmed Gaballa, for teaching me many scientific techniques and always being there to trouble shoot my experimental procedures, especially during the early stages of my PhD.

Lastly, I would like to thank my parents and my brother for their love, encouragement and unflinching support. I would also like to thank my husband, Naman, for always being supportive of my endeavors and standing by me through thick and thin. My time at Cornell University and in the microbiology department has been very enjoyable, comfortable and full of great memories. Thank you to all the people that I have had the pleasure of interacting with in the department and the university in the past 6 years. And lastly, thank you to Cornell University for providing me with a very inclusive, friendly and open environment that proved to be very conducive to my successful research work.

TABLE OF CONTENTS

LIST OF TABLES

LIST OF FIGURES

Chapter 1

Peptidoglycan biosynthesis and its regulation in bacteria

1.1 Bacterial cell-wall

The bacterial cell-wall is a complex and rigid multilayer structure that plays a crucial role in maintaining the cell shape and integrity. Due to its essential nature, the bacterial cell wall is a target for various antibiotics and there is a long-standing interest in understanding the mechanism of cell wall synthesis and regulation. There are two major classes of bacteria based on how their cell-walls stain when subjected to a specific stain, gram-positive and gram-negative. Gram positive bacteria have a multilayer, 30-100 nanometers (nm) thick peptidoglycan (PG) mesh surrounding the inner cell membrane which is a major component of a cell wall. This PG layer comprises of long glycan chains with repeating subunits of N-acetylglucosamine (GlcNAc) and N-acetylmuramic acid (MurNAc) linked by β1-4 glycosidic bonds. These glycan chains are crosslinked to neighboring strands by short peptide bridges consisting of a mixture of L- and D-amino acids. The peptide chain amino acid composition is L-Ala_1-D-Glu_2-$mDAP_3$ (or L-Lys)-D-Ala_4-D-Ala_5 in the nascent PG and the last D-Ala is lost in the mature PG [1]. In most bacteria, peptide chains are crosslinked by D, D-transpeptidases to D-Ala_4-$mDAP_3$ or D-Ala_4-L-Lys_3. Another significant portion of a gram-positive cell wall is negatively charged teichoic acids (TAs) that play a crucial role in cell shape determination and cell division. They are either embedded in the inner membrane or covalently attached to the PG layer. Wall teichoic acids (WTA) are covalently tethered to the PG layer and they are repeating units of glycerol 3-phosphate or ribitol 5-phosphate decorated with either hexose or N-acetyl hexosamine residues and alanine

substitutions[2, 3]**.** Membrane anchored lipoteichoic acids (LTA) comprise of poly glycerol or polyribitol phosphate with D-alanine and/or glycosyl substitutions [4]. Gram- negative bacteria also have PG surrounding the inner membrane, although it is thinner than gram-positive bacteria (2-3 nm) and contains only 2-3 layers of PG. The outermost layer of the gram-negative bacterial cell is a lipid-protein bilayer, also termed as outer membrane. This membrane comprises of proteins, phospholipids and lipopolysaccharides (LPS) [5].

1.2 Peptidoglycan biosynthesis

The biosynthesis of PG is a complex multi-step process involving series of highly coordinated enzymatic reactions that begin in the cytoplasm. PG biosynthesis can be divided into three parts: (i) Biosynthesis of PG precursors in cytoplasm, (ii) Biosynthesis of lipid linked intermediates at the inner side of cytoplasmic membrane, and, (iii) PG polymerization outside of cytoplasmic membrane.

Biosynthesis of PG precursors: The PG glycan monomers are synthesized in the cytoplasm as uridine nucleotides, uridine diphosphate-GlcNAc (UDP-GlcNAc) and UDP-MurNAc. Four consecutive reactions carried out by enzymes GlmS (glucosamine 6-phosphate synthase), GlmM (phosphoglucosamine mutase) and GlmU (glucosamine-1-phosphate acetyltransferase and *N*-acetylglucosamine-1-phosphate uridyltransferase) generate UDP-GlcNAc (Figure 1.1) [6]. Enzyme GlmS catalyzes the first rate-liming step in the pathway from central carbon metabolite, fructose 6-P (F6P) and amino acid glutamine to generate GlcN6P. In all organisms, there is a mechanism to regulate expression and/or activity of GlmS. In *B. subtilis*, a cis-acting self-cleaving ribozyme reduces the expression of *glmS* upon binding a GlmS catalysis product, Glc6P [7]. In *E.*

coli, glmS expression is controlled by binding of antisense RNA to *glmS* mRNA followed by RNAase dependent degradation [8]. UDP-GlcNAc can feed into PG synthesis as well as in WTA linkage unit to PG synthesis in gram positive bacteria [2]. A part of UDP-GlcNAc is converted to UDP-MurNAc in the first committed stage towards the creation of PG. The sequential activities of enzymes MurA (UDP-N-acetylglucosamine 1-carboxyvinyltransferase) and MurB (UDP-N-acetylenolpyruvoylglucosamine reductase) generate UDP-MurNAc from UDP-GlcNAc (Figure 1.1) [6]. Amino acid precursors for the peptide bridge are derived from the cytoplasm. The D-Ala and D-Glu are generated from L-Ala and L-Glu respectively by alanine and glutamate racemases. mDAP is a last intermediate in L-Lys biosynthesis pathway[9]. The Mur ligases, MurC, MurD, MurE and MurF, then sequentially add amino acids L-Ala, D-Glu, mDAP or L-Lys and D-Ala-D-Ala respectively to UDP-MurNAc forming UDP-MurNAc pentapeptide (Figure 1.1) [6].

Biosynthesis of lipid linked precursors: The phosphor-MurNAc pentapeptide moiety of UDP-MurNAc pentapeptide is now transferred to a membrane acceptor, undecaprenyl pyrophosphate by transferase MraY, yielding lipid I with concomitant release of UMP (Figure 1.1) [10]. Thereafter a transferase, MurG, adds GlcNAc moiety from UDP-GlcNAc to MurNAc residue of lipid I, generating lipid II. The PG precursor lipid II must be translocated (flipped) across the membrane by the lipid II flippase (Figure 1.1). The identity of the lipid II flippase has been a long-standing controversy. Ruiz first proposed that the membrane-anchored protein MurJ as the lipid II flippase in *E. coli* based on a bioinformatic analysis [11]. This notion was supported by the fact that MurJ is essential and required for PG biosynthesis in *E. coli*. This idea was challenged by another study that demonstrated that the purified cell division protein FtsW has a lipid II flippase activity *in vitro*. It was proposed that FtsW flips lipid II during cell division and RodA and SpoVE

can translocate lipid II during cell elongation and sporulation in *B. subtilis*, respectively [12]. The idea of MurJ being a lipid II flippase was challenged by the fact that MurJ and its homologs can be deleted from *B. subtilis*. The lipid II flippase is supposed to be universally essential. In a recent study, Meeske *et al.* carried out a transposon sequencing screen to identify a synthetic lethal partner of MurJ. They discovered that unknown function *ydaH* (now named *amj*) becomes essential in the absence of *murJ* [13]. It was later demonstrated that both MurJ and Amj possess lipid II flippase activity [14]. Interestingly, Amj bears no sequence or structural similarity to MurJ, therefore making it impossible to have predicted its function.

PG polymerization: Once outside the membrane, the disaccharide-peptide (GlcNAc-MurNAc pentapeptide) unit from lipid II is incorporated into the growing PG layer. This task is performed by enzymes possessing glycosyltransferase (GTase) activity, which generates glycan chains and transpeptidase (TPase) activity, leading to the peptide crosslinks (Figure 1.1). These two functions are achieved by groups of enzymes known as penicillin binding proteins (PBPs). PBPs were first identified because their TPase activity is inhibited by beta-lactam antibiotics such as penicillin. The first major group of PBP is high molecular weight (HMW) class A PBPs (aPBPs). Enzymes of this class possess GTase as well TPase activities. The second class consists of HMW Class B PBPs (bPBPs) that only possess TPase activity. Therefore, only aPBPs possess GTase activity. *E. coli* has two aPBPs and either one of them can be deleted due to their functional redundancy [15], however deletion of both is lethal, pointing to essentiality of GTase function. However, McPherson *et al.* reported that in *B. subtilis*, all four aPBPs can be deleted and this pointed to existence of another GTase [16]. In two independent studies, Meeske *et al.* and Emami *et al.* discovered that

an important cell shape and determination protein RodA possesses monofunctional GTase activity [17, 18].

The PBPs add precursors to growing PG in coordination with PG hydrolases. During active growth, the old PG layer needs to be remodeled by the activity of hydrolases to accommodate new PG. The hydrolases maintain thickness of the cell wall as well as facilitating separation of cell during cell division. There are two main classes of PG hydrolases: The glycosidases that cleave the glycan backbone and the amidases or peptidases that cleave the peptide chain. Each group can be further subdivided based on their cleavage site. Most bacteria encode multiple PG hydrolases. For instance, *E. coli* has approximately 13 known and *B. subtilis* has over 30 known PG hydrolases [19, 20]. In most cases deletion of a single or sometimes multiple hydrolases of the same class do not reflect any phenotypic change due to their functional redundancy. In *B. subtilis*, D, L-endopeptidases CwlO and LytE cleave the peptide bond between D-Glu_2 and $mDAP_3$ of the peptide chain. It has been demonstrated that *cwlO* and *lytE* are essential for the cell proliferation and that the double deletion of the pair cannot be constructed [21]. The localization study has revealed that CwlO plays a role in lateral PG synthesis and LytE is important for the lateral PG synthesis as well as cell separation process in coordination with the PG synthesis machinery [21]. The balance of PG synthesis and hydrolysis is imperative and in many instances perturbation in PG synthesis is coupled with early lysis phenotype due to higher PG hydrolase activity [20, 22, 23].

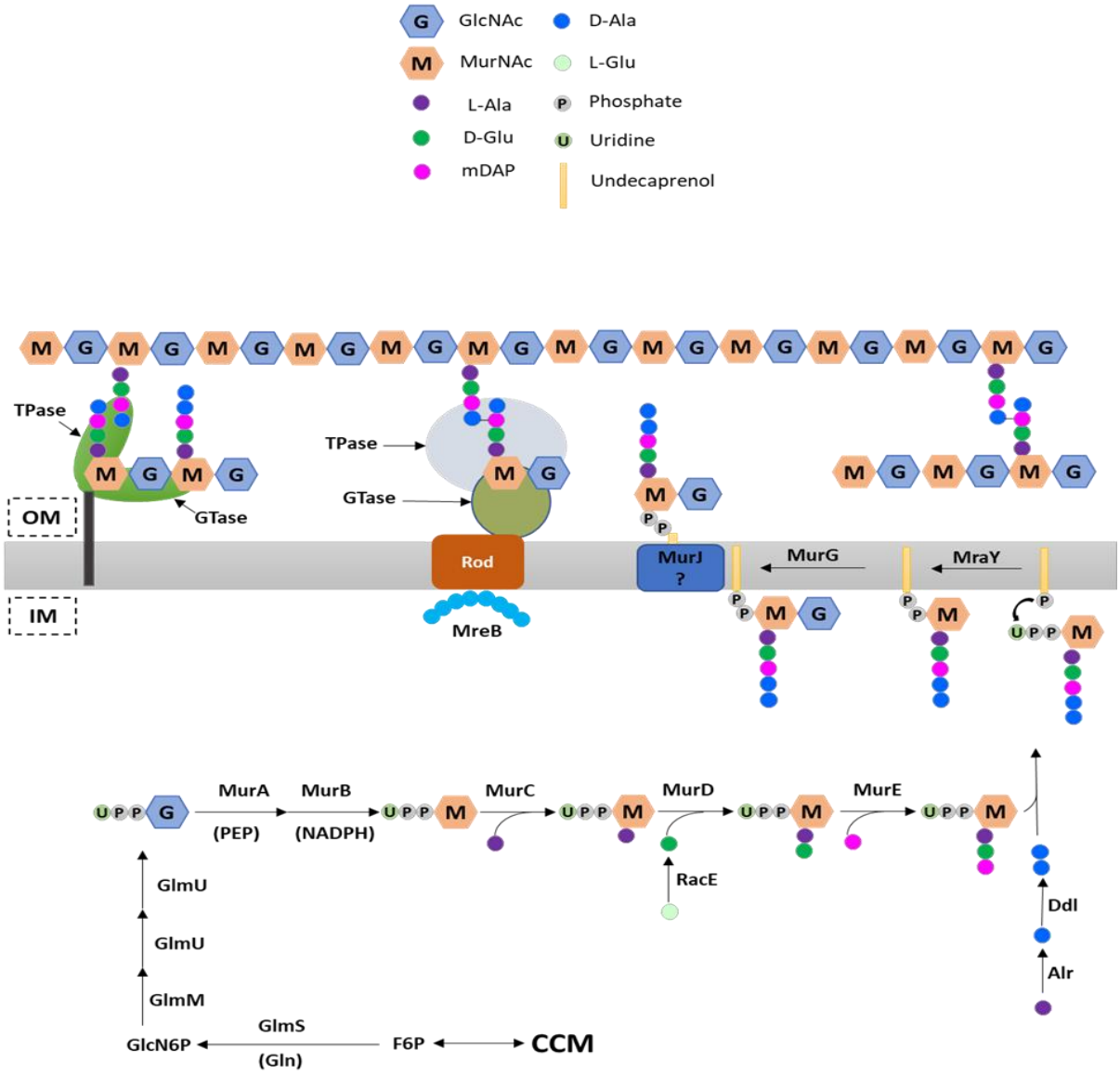

Figure 1.1: PG biosynthesis. The schematic depicts PG precursors biosynthesis in cytoplasm, biosynthesis of lipid linked precursors and lateral PG polymerization at the outer face of the membrane. Above figure also shows the membrane anchored PG synthesis complexes including the Rod complex and aPBPs. Abbreviations: IM= inner membrane, OM=outer membrane, F6P=fructose 6-phpsphate, Gln=glutamine, GlcN6P=glucosamine 6-phosphate, PEP=phosphoenolpyruvate, TPase=transpeptidase, GTase=glycosyltransferase, CCM= central carbon metabolism

1.3 Regulation of PG biosynthesis

Bacteria exist in characteristic shapes including spheres, spirals and cylinders. The shape of a bacterium is determined by complex interplay of many proteins that make up PG biosynthesis apparatus. Rod shaped bacteria like *B. subtilis* and *E. coli* first grow laterally and then divide after reaching a certain length. Two multi-protein membrane spanning complexes carry out these two apparently disparate tasks. Lateral cell wall synthesis is carried out by cytoskeleton protein MreB-associated multiprotein complex and independently acting bifunctional aPBPs (Figure 1.1) [24, 25]. The MreB associated multiprotein complex referred to as the 'elongasome' or the 'Rod complex' has PG hydrolases, monofunctional TPase bPBPs, GTase RodA, probably a lipid II flippase and other conserved membrane anchored proteins (MreC, MreD, RodZ) [24, 26]. The Rod complex moves around the cell diameter driven by RodA/bPBP in a persistent fashion carrying out processive insertion of long glycan chains at the outer face of membrane [24, 25]. At the inner face of the cell membrane, in RodA/bPBP-dependent fashion, short and curved MreB filaments rotate around the cell while remaining connected to the outer membrane complex via MreCD. The aPBPs function independent of the Rod complex and don't move directionally. Rather, the aPBPs exhibit a disorganized, diffusive pattern at the outer face of the cytoplasmic membrane with intermittent pauses and remain immobile for few seconds [24, 25]. Although spatially independent, the Rod complex and bifunctional aPBPs seem to function in synergy, as inhibition of either one reduces the insertion of new PG material by 80% [24]. It is, however, not clear how these two PG elongation machineries co-ordinate with each other. A recent study by Dion *et al.* demonstrates that the Rod complex and aPBP activities have opposing effects. The circumferentially moving Rod complex reduces the cell diameter, while aPBPs increase the cell diameter [27].

MreB is an actin-like cytoskeletal protein present in most rod-shaped bacteria. Deletion of *mreB* leads to the bacterium losing its rod shape followed by cell lysis, likely due to a failure to assemble the Rod complex [28]. MreB serves as a scaffold for proteins required for lateral PG elongation and it is also important for coordinating PG elongation with growth rate and cell cycle [24]. This model is corroborated by the fact that the speed of MreB patch is directly proportional to the growth rate [29]. Studies have shown that the Rod complex communicates with early steps of PG synthesis via MreB. Protein DapI which is involved in the synthesis of mDAP, an essential constituent of PG peptide chain, exhibits MreB dependent localization at the cell membrane [30]. Depletion of DapI leads to the reduction of MreB filament movement, ultimately bringing the filament to a complete halt. MreB is also required for spatial organization of several PG precursor biosynthesis enzymes such as MurB, MurG, MurC, MurE and MurF in *Caulobacter crescentus* [31]. Moreover, it has been demonstrated that the localization of MreB at the membrane is regulated by the availability of PG intermediate lipid II [32]. Whereas another study reported that the MreB filaments are required for the localization of the lipid II synthesis enzyme MurG at the membrane [33]. These observations suggest that MreB likely coordinates the PG precursor biosynthesis in cytoplasm and PG polymerization outside the membrane.

After the lateral cell wall synthesis is completed, cell division begins at the middle of the elongated cell. The timing of the division depends on the availability of nutrients and sometimes on external cell wall stress. When grown on a rich growth medium, the rod-shaped bacteria tend to be long in size. *B. subtilis* starts to elongate even before the division is complete, resulting in long chains of cells in the logarithmic growth phase [34]. When nutrition is sparse, the cell division is faster resulting in a smaller cell size. The cell division machinery consists of cytoskeletal protein FtsZ, other accessory cell division proteins, PG hydrolases and designated PBPs with GTase and

TPase activities. FtsZ forms a circumferential ring at the division plane at the inner face of the cytoplasmic membrane. This ‘Z ring’ also serves as a scaffold to recruit other accessory proteins for the cell division machinery to form the ‘divisome’[35]. The FtsZ movement guided divisome facilitates cytokinesis, membrane constriction, synthesis of new cell wall material and ultimately the daughter cell separation [36].

Although cell elongation and division are carried out by two separate multi-protein complexes, it is safe to say that they are highly coordinated processes. One study has shown that in *E. coli*, MreB is recruited to the division plane via direct interaction with FtsZ [37]. Additionally, a mutation in MreB that abolishes the interaction with FtsZ also blocks cell division process. However, there is no other evidence demonstrating cross talk between the elongation and the division processes. Lateral PG synthesis and timing of cell division is synchronized with cellular metabolism with reference to nutrient availability. Cell envelope stress is another factor that influences cell wall biosynthesis and cell cycle regulation. The impact of metabolism and cell wall stress in shaping bacterial cell wall are discussed further in the following section.

1.4 Metabolism and bacterial cell-wall

Metabolism is essential to every living being as it fuels various cellular activities with energy and building blocks. To grow, the cell needs to import nutrients, break them down to generate intermediate metabolites and create monomers to build macromolecules like proteins, cell wall, DNA and RNA. Metabolism of carbon forms the core of all cellular pathways. Carbon is metabolized through glycolysis/gluconeogenesis, tricarboxylic acid (TCA) cycle and pentose phosphate pathway (Figure 1.2) [38]. A catabolic pathway, glycolysis, breaks down six carbon

sugar-glucose-into two molecules of pyruvate and two molecules of ATP. Consequently, pyruvate is metabolized through the TCA cycle via conversion of acetyl-coA into citrate. The TCA cycle provides precursors for biosynthesis of certain amino acids as well as generates reducing agent NADH. Additionally, the TCA cycle intermediate oxaloacetate is a participant in the first gluconeogenesis pathway reaction (Figure 1.2). Organisms carry out gluconeogenesis when hexose sugars are not available from the environment and *de novo* glucose and other six carbon sugars need to be synthesized. A third major pathway of central carbon metabolism is the pentose phosphate pathway. A parallel pathway of glycolysis, pentose phosphate pathway generates reducing power NADPH and pentose sugars, especially ribose 5-phosphate, a precursor for nucleotide biosynthesis.

Central carbon metabolites are precursors for biosynthesis of various essential macromolecules in bacteria including bacterial cell wall. Components of bacterial cell wall are made in cytoplasm using central carbon metabolites as precursors. PG glycan chain precursors, GlcNAc and MurNAc, are generated from the glycolysis intermediate fructose 6-phosphate [6]. The first committed step of PG biosynthesis catalyzed by MurA needs phosphoenolpyruvate (PEP) to generate UDP-GlcNAc enol pyruvate from UDP-GlcNAc to ultimately generate MurNAc (Figure 1.2) [6]. Amino acids of PG pentapeptide chains are generated from TCA cycle and lower glycolytic pathway intermediates. The bacterial cell wall and thus its components are essential for most bacteria, and therefore synthesis of the cell wall needs to be finely coordinated with the availability of nutrients. In recent years, new evidence has emerged demonstrating cross talk between metabolism and PG biosynthesis as well as cell division.

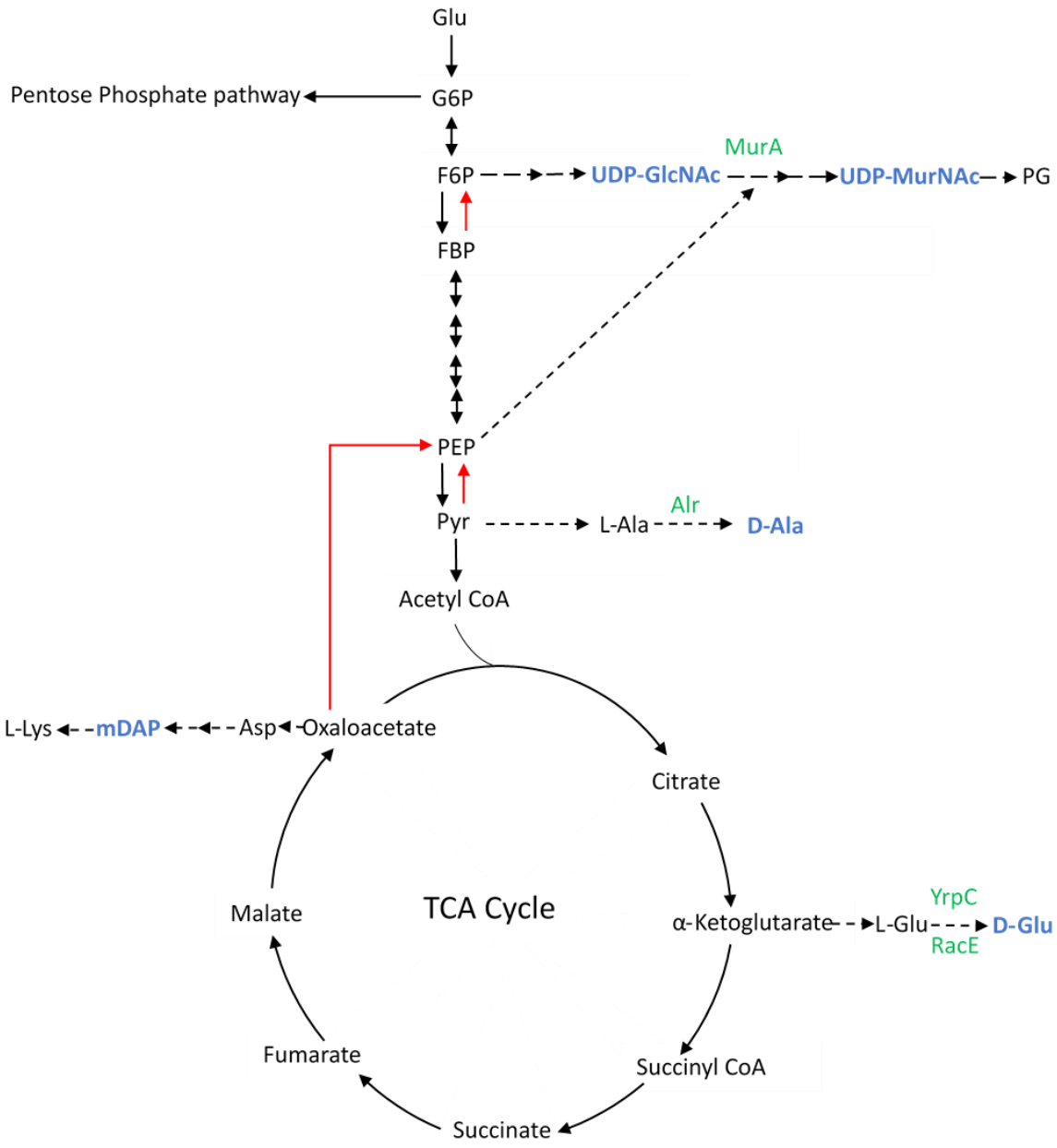

Figure 1.2: Central carbon metabolism and PG precursors biosynthesis. Above schematic depicts PG precursors (Glycan chain and pentapeptide) biosynthesis from glycolysis and TCA cycle metabolites as shown with broken arrows. PG precursors and selected enzymes are shown in blue and green color respectively. Black double headed arrows represent bidirectional enzymatic reactions, whereas open head arrows represent unidirectional reactions. (Black- glycolysis, Red- gluconeogenesis)

There are examples of metabolic proteins directly or indirectly affecting the PG biosynthesis. A significant part of my thesis involves understanding the role of protein GlmR (YvcK) in gram-positive model organism *Bacillus subtilis*. As detailed in Chapter 2, GlmR plays an essential role of diverting carbon in to PG biosynthesis from central carbon metabolism when cells are grown on gluconeogenic carbon source. Another recent study highlights that aspartate deficiency perturbs peptidoglycan biosynthesis and consequently *B. subtilis* exhibits increased susceptibility to antibiotics acting on the cell wall [39]. The aspartate transaminase (*aspB*) null mutant is auxotrophic for the amino acids aspartate (Asp) and asparagine (Asn). Thus, when grown on a medium with limited availability of Asp, *aspB* mutant strains exhibits an early lysis phenotype. The lysis phenotype can be suppressed by 2,6-diaminopimelete (DAP) chemical complementation. This study shows that *aspB* deletion mutant is deficient in the PG pentapeptide chain precursor mDAP and inability to efficiently synthesize PG results in early lysis. In *Caulobacter crescents*, a recent study demonstrates that deletion of Hfq, a global gene regulator alters central carbon metabolism and results in cell shape defect [40]. This phenotype has been attributed to accumulation in α-ketoglutarate (KG), an intermediate of TCA cycle. High KG in the cell reduces mDAP biosynthesis leading to reduced PG biosynthesis and thus, a cell morphology defect. In another example of cross talk between carbon metabolism and PG synthesis, a *B. subtilis* metabolic enzyme ManA, which is a part of mannose phosphotransferase system, has a secondary function when the bacterium is grown on a rich medium in absence of mannose sugar. In absence of *manA*, *B. subtilis* loses its characteristic rod shape and appears as an elongated sphere. This morphological abnormality results from mis-regulation of cell wall biosynthesis. Deletion of *manA* perturbs the coordination between cell wall biosynthesis and cell cycle in *B. subtilis* affecting the carbohydrate composition of cell wall [41].

Cell size and cell division is also coordinated stringently with the availability of nutrients. A study carried out by Kjeldgaard *et al.* showed that the cell size of *Salmonella typhimurium* varies depending on the growth rate [42]. They showed that when cells were shifted from rich growth medium to glucose containing minimal medium, the average cell size reduced to half. Despite long observed phenotypic changes associated with growth rate, the mechanism and knowledge of a nutrient-dependent cell size regulator has only started to emerge. In a recent study, Westfall *et al.* showed that cAMP is a contributor to nutrient-dependent reduction in cell width as well as cell length in *E. coli* [43]. Under non-glycolytic growth conditions cAMP binds to transcription factor Crp (catabolite repressor protein) and regulates the expression of more than 280 genes [44]. In *E. coli*, accumulation of cAMP-Crp under nutrient-poor condition reduces the cell width via impact on morphogenesis factor BolA, an inhibitor of *mreB* transcription. CAMP-Crp complex also impacts the FtsZ ring formation to maintain proper cell width-length ratio. In *B. subtilis*, the glycosyltransferase UgtP serves as a metabolic sensor for regulating cell size under nutrient rich condition by sensing its catalytic product UDP-Glucose (UDP-Glc). UgtP interacts with cell division protein FtsZ to inhibit Z ring formation when UDP-Glc levels are high. UDP-Glc in this instance is a sensor for nutrient availability. In *Escherichia coli*, a glucosyltransferase, OpgH, is also a nutrient dependent regulator of the cell size [45]. During nutrient rich conditions, OpgH localizes at the nascent division site upon sensing UDP-Glc levels and prevents Z ring formation and thus, increases cell size. Metabolite UDP-Glc thus indirectly co-ordinates central carbon metabolism to cell wall biosynthesis and division based on nutrient availability. UgtP and OgpH have distinct enzymatic activities and share no homology, however their role in nutrient dependent cell size regulation in *B. subtilis* and *E. coli* respectively show conserved aspect of cell size regulation. This explains why cells are longer in nutrient rich growth conditions. Another instance

of metabolism and cell division cross talk is the metabolite pyruvate affecting Z ring formation in *B. subtilis*. Pyruvate is a glycolysis pathway intermediate and a precursor for anabolic pathways such as fatty acid biosynthesis and some amino acids biosynthesis. In *B. subtilis*, deletion of gene encoding pyruvate kinase, *pyk* that catalyzes conversion of PEP to pyruvate, rescues the assembly defect of the temperature sensitive *ftsZ* mutant [46]. In the WT cells, loss of *pyk* interferes with normal function of FtsZ and disrupts Z ring assembly. Addition of exogenous pyruvate restores normal growth in *pyk* mutant. This is yet another example showing availability of central carbon metabolite regulating cell cycle in bacteria.

1.5 Cell wall stress response with emphasis on beta-lactams and PG remodeling:

The stress bearing PG layer of bacteria also protects the cell from various extracellular stresses. PG biosynthesis pathway is a target for various antibiotics and almost all major PG biosynthesis steps are inhibited by antimicrobial compounds. The beta-lactam antibiotic penicillin was the first antibiotic to be discovered in 1928 by the Scottish scientist Alexander Fleming from the fungus *Penicillium notatum*. Penicillin and other beta-lactams are widely used drugs to treat broad range of bacterial infections. Due to a broad clinical application, there has always been a lot of interest in uncovering the beta-lactam dependent changes associated with the bacterial cell as well as the counteractive resistance mechanisms. Beta-lactam antibiotics inhibit TPase activity of PBPs by covalently binding to the serine in the active site due to its structural resemblance to D-Ala_4-D-Ala_5 moiety of PG pentapeptide chain [47]. Various beta-lactam antibiotics have different affinities for the PBPs [48]. The lethality of beta-lactams is considered to stem from the loss of cell wall integrity accompanied by increased PG lysis [49]. The past studies have suggested that

the cell wall damage following beta-lactam treatment results from the drug-induced imbalance between PG synthase and PG hydrolase activities [22, 50]. Inactivation of PG hydrolase can prevent or delay beta-lactam induced cell lysis. Cho *et al.* have shown that in *E. coli*, beta-lactam mediated inhibition of TPase activity uncouples the GTase activity from TPase, thus generating noncrosslinked glycan chains. These noncrosslinked glycan chains are rapidly degraded by PG hydrolases resulting in futile cycles of PG synthesis and hydrolysis [23]. Various target bacteria have evolved resistance mechanisms against beta-lactam antibiotics. Many pathogenic bacteria have acquired beta-lactamase encoding gene by horizontal gene transfer that hydrolyses beta-lactams, rendering them inactive. In some gram-negative pathogenic bacteria like *E. coli* and *Pseudomonas aeruginosa*, an increased pool of muropeptide due to increase in PG hydrolysis activates the PG recycling pathway. Upon further degradation these muropeptides are sensed by the regulator, AmpR and that leads to the induction of beta-lactamase AmpC expression [51].

Some beta lactam resistant strains of the opportunistic pathogen *Staphylococcus aureus* have acquired extra transpeptidase termed as PBP2a that has a very low affinity for beta-lactams as its active site is hidden in the cleft and inaccessible to the antibiotic [52]. When exposed to beta-lactam, the transpeptidases are rendered inactive, *S. aureus* switches to PBP2a for PG synthesis. According to a recent study, the origin of the gene encoding PBP2a, *mecA,* can be traced back to other *Staphylococcus* species [52]. These are non-resistant variants of *mecA* that evolved due to exposure of beta-lactam in a human created environment [53]. There are examples of evolution or acquisition of low beta-lactam affinity HMW PBPs in other pathogenic bacteria like *Streptococcus pneumoniae*, *Neisseria meningitis* and *Enterococcus faecalis* [54].

Some other bacteria have other intrinsic mechanisms to resist beta-lactam stress. In gram-positive bacterium *B. subtilis*, beta-lactam resistance is conferred by an extra cytoplasmic function

(ECF) sigma factor, σ^M [55]. Deletion of *sigM* renders *B. subtilis* very sensitive to beta-lactam antibiotics [55]. Another ECF σ factor σ^X plays secondary role in beta-lactam resistance especially in the absence of σ^M. σ^M is one of the seven ECF sigma factors *B. subtilis* has that are involved in different kinds of cell envelope stress response. σ^M controls expression of over 30 operons and more that 60 genes [56]. *sigM* regulon is activated by heat, high salt, acidic pH and other cell-wall synthesis inhibiting antibiotics such as vancomycin [57, 58]. How the σ^M regulon confers resistance to beta-lactam and which genes are most important for the process is unknown. Interestingly, σ^M induces transcription of enzymes for the synthesis of PG precursors (MurB, MurF, Ddl), PG assembly (PBP1, PBPX), the Rod complex (MreBCD, RodA) as well as the divisome (MinCD, DivIB, DivIC) and an enzyme needed for lipid II carrier recycling (BcrC). The lipid II flippase MurJ functional homolog Amj is also part of the *sigM* regulon. To carry out PG synthesis, *B. subtilis* needs either MurJ or AmJ. σ^M upregulates PG biosynthesis pathway probably to increase thickness of PG against beta-lactam stress. Interestingly, previous studies have linked increased thickness of PG to counter cell-wall acting antibiotics in *Staphylococcus aureus* [59]. Although it has not yet been proven experimentally, *B. subtilis* using an increased thickness of PG can also be a beta-lactam counter mechanism. σ^M also induces genes for TA biosynthesis, like an alternate LTA synthase, LtaSa, and one of the enzymes that attaches WTA to PG, TagA. Signaling nucleotide c-di-AMP synthase, DisA, is also a part of *sigM* regulon. Interestingly, a moderate increase in the concentration of c-di-AMP reduces beta-lactam sensitivity of a *sigM* null mutant strain [55]. The role of c-di-AMP in beta-lactam resistance is yet elusive. Intriguingly, the major c-di-AMP synthase, CdaA, is part of the same operon as GlmS and GlmM, the enzymes that catalyze the first two cytoplasmic steps of PG precursor GlcNAc biosynthesis. Apart from the fact that CdaA and GlmM physically interact and GlmM modulates activity of CdaA [60], it is unclear

if c-di-AMP in any way controls PG precursors biosynthesis and how it is linked to beta-lactam resistance in *sigM* deletion mutant.

1.6 Dissertation summary

This dissertation focuses on characterizing PG biosynthesis in response to nutrient availability and the cell wall stress response using model organism *B. subtilis*.

Chapter 2 describes the role of GlmR in carbon partitioning between PG and central carbon metabolism. GlmR (previously known as YvcK) was known to be essential for the growth of *B. subtilis* on gluconeogenic carbon source. I have carried out a forward genetic analysis of the *glmR* null mutant and discovered that either overexpression of the glucosamine 6-phosphate synthase *glmS* or chemical complementation by GlcNAc bypasses essentiality of *glmR*. This study reveals that GlmR plays a regulatory role in channeling carbon into PG metabolism in a carbon source dependent manner, likely by stimulating GlmS activity.

Chapter 3 focuses on the characterization of a suppressor mutation, $pgcA_{G47S}$, obtained from the forward genetic screen described in chapter 2, in a *glmR* deletion mutant. In the process of characterizing $pgcA_{G47S}$, I also discovered that PgcA possesses GlmM-like phosphoglucosamine mutase enzymatic activity in addition to its designated phosphoglucomutase function. This study also shows that the secondary function of PgcA is essential in *glmR* null background.

Chapter 4 focuses on role of c-di-AMP homeostasis in *B. subtilis*. I show that the double deletion of c-di-AMP hydrolase is extremely sensitive to beta-lactam stress likely due to toxic accumulation of c-di-AMP. The mariner transposon mutagenesis was carried out to obtain insight

into the details of the mechanism associated with accumulation of c-di-AMP. My study revealed that the increased expression of multidrug efflux transporter MdtP significantly reduced beta-lactam sensitivity of c-di-AMP double hydrolase mutant, likely due to efflux of excess of c-di-AMP.

B. subtilis has been a very useful model organism for the scientific research due to its nonpathogenic nature, genetic competency and similarities to many pathogenic bacteria. GlmR as well as signaling nucleotide c-di-AMP are important for virulence in many pathogens. GlmR is shown to be essential establishing infection into the host cell by *Mycobacterium tuberculosis* and *Listeria monocytogenes*. Many pathogenic bacteria use c-di-AMP to modulate host immune system to facilitate infection. Hence, the studies described can be applied to get further understanding of bacterial virulence.

1.7 REFERENCES

1. Vollmer W, Blanot D, De Pedro MA. Peptidoglycan structure and architecture. FEMS Microbiology Reviews. 2008;32(2):149-67. doi: 10.1111/j.1574-6976.2007.00094.x.
2. Brown S, Santa Maria JP, Walker S. Wall Teichoic Acids of Gram-Positive Bacteria. Annual review of microbiology. 2013;67:10.1146/annurev-micro-092412-155620. doi: 10.1146/annurev-micro-092412-155620. PubMed PMID: PMC3883102.
3. Sewell EWC, Brown ED. Taking aim at wall teichoic acid synthesis: new biology and new leads for antibiotics. The Journal Of Antibiotics. 2013;67:43. doi: 10.1038/ja.2013.100.
4. Percy MG, Gründling A. Lipoteichoic Acid Synthesis and Function in Gram-Positive Bacteria. Annual Review of Microbiology. 2014;68(1):81-100. doi: 10.1146/annurev-micro-091213-112949. PubMed PMID: 24819367.
5. Beveridge TJ. Structures of Gram-Negative Cell Walls and Their Derived Membrane Vesicles. Journal of Bacteriology. 1999;181(16):4725-33. PubMed PMID: PMC93954.
6. Barreteau H, Kovač A, Boniface A, Sova M, Gobec S, Blanot D. Cytoplasmic steps of peptidoglycan biosynthesis. FEMS Microbiology Reviews. 2008;32(2):168-207. doi: 10.1111/j.1574-6976.2008.00104.x.
7. Winkler WC, Nahvi A, Roth A, Collins JA, Breaker RR. Control of gene expression by a natural metabolite-responsive ribozyme. Nature. 2004;428:281. doi: 10.1038/nature02362.
8. Göpel Y, Khan MA, Görke B. Ménage à trois. RNA Biology. 2014;11(5):433-42. doi: 10.4161/rna.28301.

9. Born TL, Blanchard JS. Structure/function studies on enzymes in the diaminopimelate pathway of bacterial cell wall biosynthesis. Current Opinion in Chemical Biology. 1999;3(5):607-13. doi: https://doi.org/10.1016/S1367-5931(99)00016-2.

10. Bouhss A, Trunkfield AE, Bugg TDH, Mengin-Lecreulx D. The biosynthesis of peptidoglycan lipid-linked intermediates. FEMS Microbiology Reviews. 2008;32(2):208-33. doi: 10.1111/j.1574-6976.2007.00089.x.

11. Ruiz N. Bioinformatics identification of MurJ (MviN) as the peptidoglycan lipid II flippase in *Escherichia coli*. Proceedings of the National Academy of Sciences. 2008;105(40):15553-7. doi: 10.1073/pnas.0808352105.

12. Mohammadi T, van Dam V, Sijbrandi R, Vernet T, Zapun A, Bouhss A, *et al*. Identification of FtsW as a transporter of lipid-linked cell wall precursors across the membrane. The EMBO Journal. 2011;30(8):1425-32. doi: doi:10.1038/emboj.2011.61.

13. Meeske AJ, Sham L-T, Kimsey H, Koo B-M, Gross CA, Bernhardt TG, *et al*. MurJ and a novel lipid II flippase are required for cell wall biogenesis in *Bacillus subtilis*. Proceedings of the National Academy of Sciences. 2015;112(20):6437-42. doi: 10.1073/pnas.1504967112.

14. Sham L-T, Butler EK, Lebar MD, Kahne D, Bernhardt TG, Ruiz N. MurJ is the flippase of lipid-linked precursors for peptidoglycan biogenesis. Science. 2014;345(6193):220-2. doi: 10.1126/science.1254522.

15. Denome SA, Elf PK, Henderson TA, Nelson DE, Young KD. *Escherichia coli* Mutants Lacking All Possible Combinations of Eight Penicillin Binding Proteins: Viability, Characteristics, and Implications for Peptidoglycan Synthesis. Journal of Bacteriology. 1999;181(13):3981-93.

16. McPherson DC, Popham DL. Peptidoglycan Synthesis in the Absence of Class A Penicillin-Binding Proteins in *Bacillus subtilis*. Journal of Bacteriology. 2003;185(4):1423-31. doi: 10.1128/jb.185.4.1423-1431.2003.

17. Meeske AJ, Riley EP, Robins WP, Uehara T, Mekalanos JJ, Kahne D, *et al*. SEDS proteins are a widespread family of bacterial cell wall polymerases. Nature. 2016;537:634. doi: 10.1038/nature19331

18. Emami K, Guyet A, Kawai Y, Devi J, Wu LJ, Allenby N, *et al*. RodA as the missing glycosyltransferase in *Bacillus subtilis* and antibiotic discovery for the peptidoglycan polymerase pathway. Nature Microbiology. 2017;2:16253. doi: 10.1038/nmicrobiol.2016.253

19. Frirdich E, Gaynor EC. Peptidoglycan hydrolases, bacterial shape, and pathogenesis. Current Opinion in Microbiology. 2013;16(6):767-78.

20. Vollmer W, Joris B, Charlier P, Foster S. Bacterial peptidoglycan (murein) hydrolases. FEMS Microbiology Reviews. 2008;32(2):259-86. doi: 10.1111/j.1574-6976.2007.00099.x.

21. Hashimoto M, Ooiwa S, Sekiguchi J. Synthetic Lethality of the lytE cwlO Genotype in *Bacillus subtilis* Is Caused by Lack of Endopeptidase Activity at the Lateral Cell Wall. Journal of Bacteriology. 2012;194(4):796-803. doi: 10.1128/jb.05569-11.

22. Tomasz A. The Mechanism of the Irreversible Antimicrobial Effects of Penicillins: How the Beta-Lactam Antibiotics Kill and Lyse Bacteria. Annual Review of Microbiology. 1979;33(1):113-37. doi: 10.1146/annurev.mi.33.100179.000553. PubMed PMID: 40528.

23. Cho H, Uehara T, Bernhardt Thomas G. Beta-Lactam Antibiotics Induce a Lethal Malfunctioning of the Bacterial Cell Wall Synthesis Machinery. Cell. 2014;159(6):1300-11. doi: 10.1016/j.cell.2014.11.017.

24. Domínguez-Escobar J, Chastanet A, Crevenna AH, Fromion V, Wedlich-Söldner R, Carballido-López R. Processive Movement of MreB-Associated Cell Wall Biosynthetic Complexes in Bacteria. Science. 2011;333(6039):225-8. doi: 10.1126/science.1203466.

25. Garner EC, Bernard R, Wang W, Zhuang X, Rudner DZ, Mitchison T. Coupled, Circumferential Motions of the Cell Wall Synthesis Machinery and MreB Filaments in *B. subtilis*. Science. 2011;333(6039):222-5. doi: 10.1126/science.1203285.

26. Morgenstein RM, Bratton BP, Nguyen JP, Ouzounov N, Shaevitz JW, Gitai Z. RodZ links MreB to cell wall synthesis to mediate MreB rotation and robust morphogenesis. Proceedings of the National Academy of Sciences of the United States of America. 2015;112(40):12510-5. doi: 10.1073/pnas.1509610112. PubMed PMID: PMC4603514.

27. Dion M, Kapoor M, Sun Y, Wilson S, Ryan J, Vigouroux A, *et al*. Cell Diameter in *Bacillus subtilis* is Determined by the Opposing Actions of Two Distinct Cell Wall Synthetic Systems. bioRxiv. 2018. doi: 10.1101/392837.

28. Jones LJF, Carballido-López R, Errington J. Control of Cell Shape in Bacteria. Cell. 2001;104(6):913-22. doi: 10.1016/S0092-8674(01)00287-2.

29. Billaudeau C, Chastanet A, Yao Z, Cornilleau C, Mirouze N, Fromion V, *et al*. Contrasting mechanisms of growth in two model rod-shaped bacteria. Nature Communications. 2017;8:15370. doi: 10.1038/ncomms15370

30. Rueff A-S, Chastanet A, Domínguez-Escobar J, Yao Z, Yates J, Prejean M-V, *et al*. An early cytoplasmic step of peptidoglycan synthesis is associated to MreB in *Bacillus subtilis*. Molecular Microbiology. 2014;91(2):348-62. doi: doi:10.1111/mmi.12467.

31. White CL, Kitich A, Gober JW. Positioning cell wall synthetic complexes by the bacterial morphogenetic proteins MreB and MreD. Molecular Microbiology. 2010;76(3):616-33. doi: doi:10.1111/j.1365-2958.2010.07108.x.

32. Schirner K, Eun Y-J, Dion M, Luo Y, Helmann JD, Garner EC, *et al*. Lipid-linked cell wall precursors regulate membrane association of bacterial actin MreB. Nature Chemical Biology. 2014;11:38. doi: 10.1038/nchembio.1689

33. Divakaruni AV, Baida C, White CL, Gober JW. The cell shape proteins MreB and MreC control cell morphogenesis by positioning cell wall synthetic complexes. Molecular Microbiology. 2007;66(1):174-88. doi: doi:10.1111/j.1365-2958.2007.05910.x.

34. Kearns DB, Losick R. Cell population heterogeneity during growth of *Bacillus subtilis*. Genes & Development. 2005;19(24):3083-94. doi: 10.1101/gad.1373905. PubMed PMID: PMC1315410.

35. Adams DW, Errington J. Bacterial cell division: assembly, maintenance and disassembly of the Z ring. Nature Reviews Microbiology. 2009;7:642. doi: 10.1038/nrmicro2198.

36. Monteiro JM, Pereira AR, Reichmann NT, Saraiva BM, Fernandes PB, Veiga H, *et al*. Peptidoglycan synthesis drives an FtsZ-treadmilling-independent step of cytokinesis. Nature. 2018;554:528. doi: 10.1038/nature25506

37. Fenton AK, Gerdes K. Direct interaction of FtsZ and MreB is required for septum synthesis and cell division in *Escherichia coli*. The EMBO Journal. 2013;32(13):1953-65. doi: 10.1038/emboj.2013.129.

38. Nelson DL, Cox MM, Lehninger AL. Lehninger principles of biochemistry2017.

39. Zhao H, Roistacher DM, Helmann JD. Aspartate deficiency limits peptidoglycan synthesis and sensitizes cells to antibiotics targeting cell wall synthesis in *Bacillus subtilis*. Molecular Microbiology. 0(0). doi: doi:10.1111/mmi.14078.

40. Irnov I, Wang Z, Jannetty ND, Bustamante JA, Rhee KY, Jacobs-Wagner C. Crosstalk between the tricarboxylic acid cycle and peptidoglycan synthesis in *Caulobacter crescentus* through the homeostatic control of α-ketoglutarate. PLOS Genetics. 2017;13(8):e1006978. doi: 10.1371/journal.pgen.1006978.

41. Elbaz M, Ben-Yehuda S. The Metabolic Enzyme ManA Reveals a Link between Cell Wall Integrity and Chromosome Morphology. PLOS Genetics. 2010;6(9):e1001119. doi: 10.1371/journal.pgen.1001119.

42. Kjeldgaard NO, MaalØe O, Schaechter M. The Transition Between Different Physiological States During Balanced Growth of *Salmonella typhimurium*. Microbiology. 1958;19(3):607-16. doi: doi:10.1099/00221287-19-3-607.

43. Westfall CS, Levin PA. Comprehensive analysis of central carbon metabolism illuminates connections between nutrient availability, growth rate, and cell morphology in *Escherichia coli*. PLOS Genetics. 2018;14(2):e1007205. doi: 10.1371/journal.pgen.1007205.

44. Zheng D, Constantinidou C, Hobman JL, Minchin SD. Identification of the CRP regulon using in vitro and in vivo transcriptional profiling. Nucleic Acids Research. 2004;32(19):5874-93. doi: 10.1093/nar/gkh908.

45. Hill NS, Buske PJ, Shi Y, Levin PA. A Moonlighting Enzyme Links *Escherichia coli* Cell Size with Central Metabolism. PLOS Genetics. 2013;9(7):e1003663. doi: 10.1371/journal.pgen.1003663.

46. Monahan LG, Hajduk IV, Blaber SP, Charles IG, Harry EJ. Coordinating Bacterial Cell Division with Nutrient Availability: a Role for Glycolysis. mBio. 2014;5(3). doi: 10.1128/mBio.00935-14.

47. Waxman DJ, Strominger JL. Penicillin-Binding Proteins and the Mechanism of Action of Beta-Lactam Antibiotics1. Annual Review of Biochemistry. 1983;52(1):825-69. doi: 10.1146/annurev.bi.52.070183.004141. PubMed PMID: 6351730.

48. Curtis NA, Orr D, Ross GW, Boulton MG. Affinities of penicillins and cephalosporins for the penicillin-binding proteins of *Escherichia coli* K-12 and their antibacterial activity. Antimicrobial Agents and Chemotherapy. 1979;16(5):533-9. doi: 10.1128/aac.16.5.533.

49. Park JT, Strominger JL. Mode of Action of Penicillin. Biochemical Basis for the Mechanism of Action of Penicillin and for Its Selective Toxicity. 1957;125(3238):99-101. doi: 10.1126/science.125.3238.99.

50. Schwarz U, Asmus A, Frank H. Autolytic enzymes and cell division of *Escherichia coli*. Journal of Molecular Biology. 1969;41(3):419-29.

51. Domínguez-Gil T, Molina R, Alcorlo M, Hermoso JA. Renew or die: The molecular mechanisms of peptidoglycan recycling and antibiotic resistance in Gram-negative pathogens. Drug Resistance Updates. 2016;28:91-104.

52. Fishovitz J, Hermoso JA, Chang M, Mobashery S. Penicillin-Binding Protein 2a of Methicillin-Resistant *Staphylococcus aureus*. IUBMB life. 2014;66(8):572-7. doi: 10.1002/iub.1289. PubMed PMID: PMC4236225.

53. Rolo J, Worning P, Boye Nielsen J, Sobral R, Bowden R, Bouchami O, *et al*. Evidence for the evolutionary steps leading to mecA-mediated β-lactam resistance in *staphylococci*. PLOS Genetics. 2017;13(4):e1006674. doi: 10.1371/journal.pgen.1006674.

54. Poole K. Resistance to β-lactam antibiotics. Cellular and Molecular Life Sciences CMLS. 2004;61(17):2200-23. doi: 10.1007/s00018-004-4060-9.

55. Luo Y, Helmann JD. Analysis of the role of *Bacillus subtilis* σM in β-lactam resistance reveals an essential role for c-di-AMP in peptidoglycan homeostasis. Molecular Microbiology. 2012;83(3):623-39. doi: doi:10.1111/j.1365-2958.2011.07953.x.

56. Eiamphungporn W, Helmann JD. The *Bacillus subtilis* σM regulon and its contribution to cell envelope stress responses. Molecular Microbiology. 2008;67(4):830-48. doi: doi:10.1111/j.1365-2958.2007.06090.x.

57. Horsburgh MJ, Moir A. σM, an ECF RNA polymerase sigma factor of *Bacillus subtilis* 168, is essential for growth and survival in high concentrations of salt. Molecular Microbiology. 1999;32(1):41-50. doi: doi:10.1046/j.1365-2958.1999.01323.x.

58. Thackray PD, Moir A. SigM, an Extracytoplasmic Function Sigma Factor of *Bacillus subtilis*, Is Activated in Response to Cell Wall Antibiotics, Ethanol, Heat, Acid, and Superoxide Stress. Journal of Bacteriology. 2003;185(12):3491-8. doi: 10.1128/jb.185.12.3491-3498.2003.

59. Cázares-Domínguez V, Cruz-Córdova A, Ochoa SA, Escalona G, Arellano-Galindo J, Rodríguez-Leviz A, *et al*. Vancomycin Tolerant, Methicillin-Resistant *Staphylococcus aureus* Reveals the Effects of Vancomycin on Cell Wall Thickening. PLOS ONE. 2015;10(3):e0118791. doi: 10.1371/journal.pone.0118791.

60. Commichau FM, Heidemann JL, Ficner R, Stülke J. Making and breaking of an essential poison: the cyclases and phosphodiesterases that produce and degrade the essential second messenger cyclic di-AMP in bacteria. Journal of Bacteriology. 2018. doi: 10.1128/jb.00462-18.

Chapter 2

A metabolic checkpoint protein GlmR is important for diverting carbon into peptidoglycan biosynthesis in *Bacillus subtilis*[1]

2.1 Abstract

The *Bacillus subtilis* GlmR (formerly YvcK) protein is essential for growth on gluconeogenic carbon sources. Mutants lacking GlmR display a variety of phenotypes suggestive of impaired cell wall synthesis including antibiotic sensitivity, aberrant cell morphology and lysis. To define the role of GlmR, I selected suppressor mutations that ameliorate the sensitivity of a *glmR* null mutant to the beta-lactam antibiotic cefuroxime or restore growth on gluconeogenic carbon sources. Several of the resulting suppressors increase the expression of the GlmS and GlmM proteins that catalyze the first two committed steps in the diversion of carbon from central carbon metabolism into peptidoglycan biosynthesis. Chemical complementation studies indicate that the absence of GlmR can be overcome by provision of cells with N-acetylglucosamine (GlcNAc), even under conditions where GlcNAc cannot re-enter central metabolism and serve as a carbon source for growth. My results indicate that GlmR facilitates the diversion of carbon from the central metabolite fructose-6-phosphate, which is limiting in cells growing on gluconeogenic carbon sources, into peptidoglycan biosynthesis. My data suggest that GlmR stimulates GlmS activity, and I propose that this activation is antagonized by the known GlmR ligand and

[1] This chapter is adapted from Patel V., Wu Q., Chandrangsu P. & Helmann J.D. PLoS Genet. 2018 Sep 24;14(9):e1007689. Wu Q. and Chandrangsu discovered the CEF sensitivity phenotype of *glmR* deletion mutant and carried out the selection of CEF resistant suppressors.

peptidoglycan intermediate UDP-GlcNAc. Thus, GlmR presides over a new mechanism for the regulation of carbon partitioning between central metabolism and peptidoglycan biosynthesis.

2.2 Significance statement

Bacterial cells are surrounded by a peptidoglycan cell wall that is, under most conditions, required for viability. Synthesis of the cell wall requires a considerable diversion of resources from central carbon metabolism into a lipid-linked precursor (lipid II) that is exported from the cell for wall assembly. Here, I propose that GlmR presides over a new mechanism for the regulation of carbon partitioning between central metabolism and peptidoglycan biosynthesis: GlmR activates the GlmS-dependent diversion of carbon from the glycolytic pathway into peptidoglycan synthesis. This effect is particularly important during gluconeogenesis since the GlmS substrate fructose 6-phosphate is present at a reduced level under these conditions

2.3 Introduction

Bacillus subtilis provides a powerful model system for understanding cell wall homeostasis in Gram positive bacteria. Disruption of pathways for the synthesis of peptidoglycan (PG) and other cell envelope components elicits complex adaptive responses often controlled by alternative σ factors or two-component systems [1, 2]. The ECF σ factor σ^M regulates numerous operons involved in PG synthesis and mutants are sensitive to PG synthesis inhibitors [3]. Previously,Yun Luo from my lab found that mutation of *gdpP*, which encodes a cyclic-di-adenosine monophosphate (c-di-AMP) hydrolase, can suppress the sensitivity of *B. subtilis sigM* null mutants towards beta-lactam antibiotics [4]. This suggests that c-di-AMP plays some role in PG homeostasis. Mutations in the *yvcK* gene (herein renamed *glmR*) also exhibit cell envelope defects,

as evidenced by cell bulging and lysis when inoculated into non-glycolytic carbon sources [5]. Moreover, a *yqfF*::*Tn* insertion suppressed the inability of a *glmR* mutant to grow on gluconeogenic media [5]. Although unknown at the time, *yqfF* is now known to encode a second c-di-AMP hydrolase renamed PgpH [6, 7]. These observations encouraged us to investigate possible connections between GlmR, c-di-AMP, and cell envelope homeostasis.

In *B. subtilis*, GlmR (formerly YvcK) is essential for growth on amino acids and intermediates of the tricarboxylic acid cycle and pentose phosphate pathway, but dispensable for growth on glucose and other glycolytic carbon sources [5]. Previous genetic studies revealed that mutations in genes affecting central carbon metabolism (CCM), including *zwf* and *cggR*, allow a *glmR* null mutant to grow on gluconeogenic carbon sources [5]. These observations suggest that GlmR has a yet undefined role in regulating metabolism. In the absence of GlmR, cells display cell envelope defects and lyse under gluconeogenic growth conditions.

The function of GlmR in CCM, and how this relates to cell envelope integrity, is not yet clear. One model suggests that GlmR may function as a cytoskeletal filament protein analogous to MreB to help coordinate cell wall synthesis [8]. MreB, an actin-like cytoskeletal protein, is important for maintaining a rod shape in *B. subtilis* and deletion of *mreB* leads to severe morphological defects and eventual cell lysis, effects attributed to mislocalization of penicillin binding protein 1 (PBP1) [9]. *B. subtilis* GlmR localizes to the membrane in a helical fashion, and overexpression of GlmR rescues the cell defects seen in an *mreB* deletion mutant and restores proper localization of PBP1. Conversely, overexpression of MreB rescues the morphological defects of a *glmR* null mutant when grown on gluconeogenic carbon sources [8].

Recently, GlmR was found to possess a ligand binding site for UDP sugars such as UDP-glucose and UDP-N-acetylglucosamine (UDP-GlcNAc) [10]. Since UDP-GlcNAc is a precursor

of PG synthesis, this suggests that GlmR may sense this intermediate to somehow modulate CCM or cell envelope homeostasis. Mutations altering the UDP-sugar binding site did not affect growth on gluconeogenic media in *B. subtilis*, but did lead to increased sensitivity to bacitracin [10].

Although the biochemical details are unclear, the role of GlmR in metabolism and cell wall homeostasis seems to be widely conserved. Homologs of GlmR are present diverse bacteria and a *glmR* mutant can be complemented by expression of the *Escherichia coli* homolog, YbhK [5]. Mutation of *glmR* homologs in the intracellular pathogens *Mycobacterium tuberculosis* (*cuvA*) and *Listeria monocytogenes* (*yvcK*) leads to alterations in cell morphology and sensitivity to cell wall acting antibiotics, as well as defects in carbon source utilization and establishment of infection in the host cell [11, 12]. Although these diverse phenotypes, biochemical properties and cell localization studies are all intriguing, a unifying model to account for the role of GlmR in the cell has been elusive.

Here, I show that a *B. subtilis* strain lacking *glmR* is susceptible to peptidoglycan (PG) biosynthesis inhibitors such as beta-lactams, vancomycin and moenomycin. Characterization of *glmR* suppressor mutations indicates that increased expression of genes involved in UDP-GlcNAc biosynthesis is sufficient to increase beta-lactam resistance and restore growth on gluconeogenic carbon sources. Moreover, supplementation with GlcNAc can bypass the requirement for GlmR even in strains where GlcNAc cannot enter into CCM. My results support a model in which GlmR functions to help divert carbon to PG biosynthesis, likely through direct interaction with GlmS. I propose that this effect is particularly important during gluconeogenesis since the GlmS substrate fructose 6-phosphate is present at a reduced level under these conditions [13].

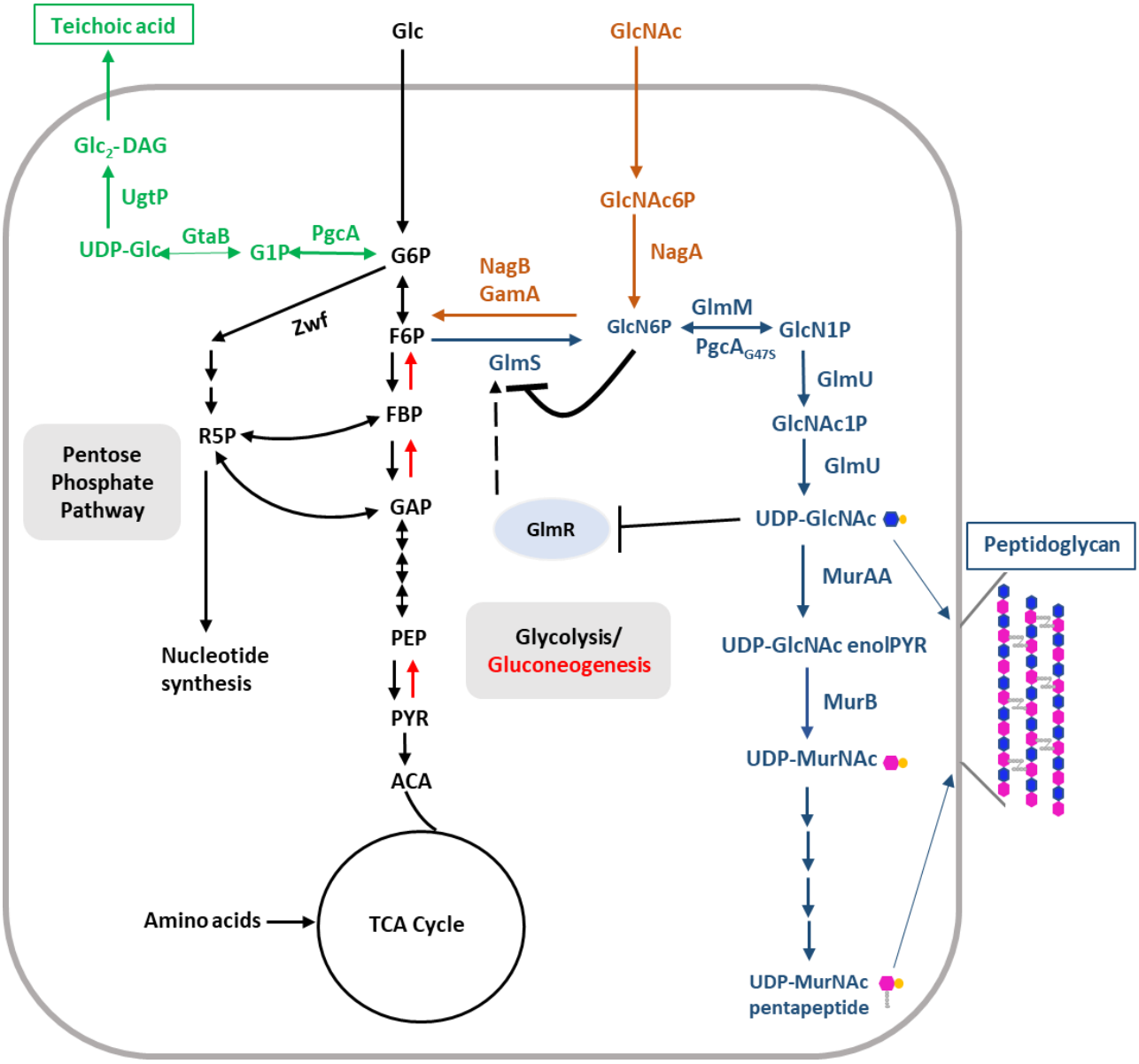
Teichoic acid
Glc
GlcNAc
Glc2-DAG
UgtP
UDP-Glc
GtaB
G1P
PgcA
G6P
GlcNAc6P
NagA
NagB
GamA
Zwf
F6P
GlcN6P
GlmM
PgcAG47S
GlcN1P
GlmS
GlmU
GlcNAc1P
FBP
R5P
Pentose Phosphate Pathway
GlmU
GAP
GlmR
UDP-GlcNAc
Peptidoglycan
MurAA
PEP
Glycolysis/ Gluconeogenesis
UDP-GlcNAc enolPYR
Nucleotide synthesis
MurB
PYR
UDP-MurNAc
ACA
Amino acids
TCA Cycle
UDP-MurNAc pentapeptide

Figure 2.1: Schematic illustration of central carbon, peptidoglycan, UDP-Glc and UDP-GlcNAc metabolism. Central carbon metabolism (CCM; glycolysis/gluconeogenesis, pentose phosphate pathway and TCA cycle) is shown with black colored fonts and arrows. Black double headed arrows represent bidirectional enzyme reactions. Single headed black and red arrows represent glycolysis- and gluconeogenesis-specific enzymatic steps, respectively. UDP-Glc biosynthesis and its incorporation in teichoic acids is depicted in green. Steps of peptidoglycan biosynthesis and GlcNAc feeding into central carbon metabolism are shown in blue and orange, respectively. Black dashed arrow indicates activation.
Abbreviations: Glc=glucose, G6P=glucose-6-phosphate, F6P =fructose-6-phosphate, FBP=fructose-1,6-bisphosphate, GAP=glyceraldehyde-3-phosphate, PEP=phosphoenolpyruvate, PYR=pyruvate, ACA=acetyl-CoA, R5P=ribulose-5-phosphate, G1P=glucose-1-phosphate, UDP-Glc=UDP-glucose, Glc_2-DAG=diglucosyldiacylglycerol, GlcNAc=N-acetylglucosamine, GlcNAc6=N-acetylglucosamine-6-phosphate, GlcN6P = N-Acetylglucosamine-6-phosphate, GlcN1P=N-Acetylglucosamine-1-phosphate, GlcNAc1P=N-acetylglucosamine-1-phosphate, UDP-GlcNAc=UDP-N-acetylglucosamine, UDP-GlcNAc-enolPYR=UDP-N-acetylglucosamine enolpyruvate, UDP-murNAc= UDP-N-acetylmuramic acid.

2.4 Results

2.4.1 Δ*glmR* is sensitive to peptidoglycan synthesis inhibiting antibiotics

To test the role of GlmR in the connection between CCM and PG biosynthesis (Figure 2.1), I generated a *B. subtilis* strain with an in-frame, unmarked deletion of *glmR* (Δ*glmR*) and characterized its growth properties and sensitivity to cell wall antibiotics. Mueller-Hinton (MH) is a gluconeogenic medium containing amino acids as primary carbon source and is commonly used for antibiotic sensitivity experiments. However, Δ*glmR* is unable to grow on MH. This phenotype can be complemented by an ectopic, inducible copy of *glmR* (Figure 2.2A) or addition of glucose (Figure 2.2B and 2.2C), consistent with prior results [5].

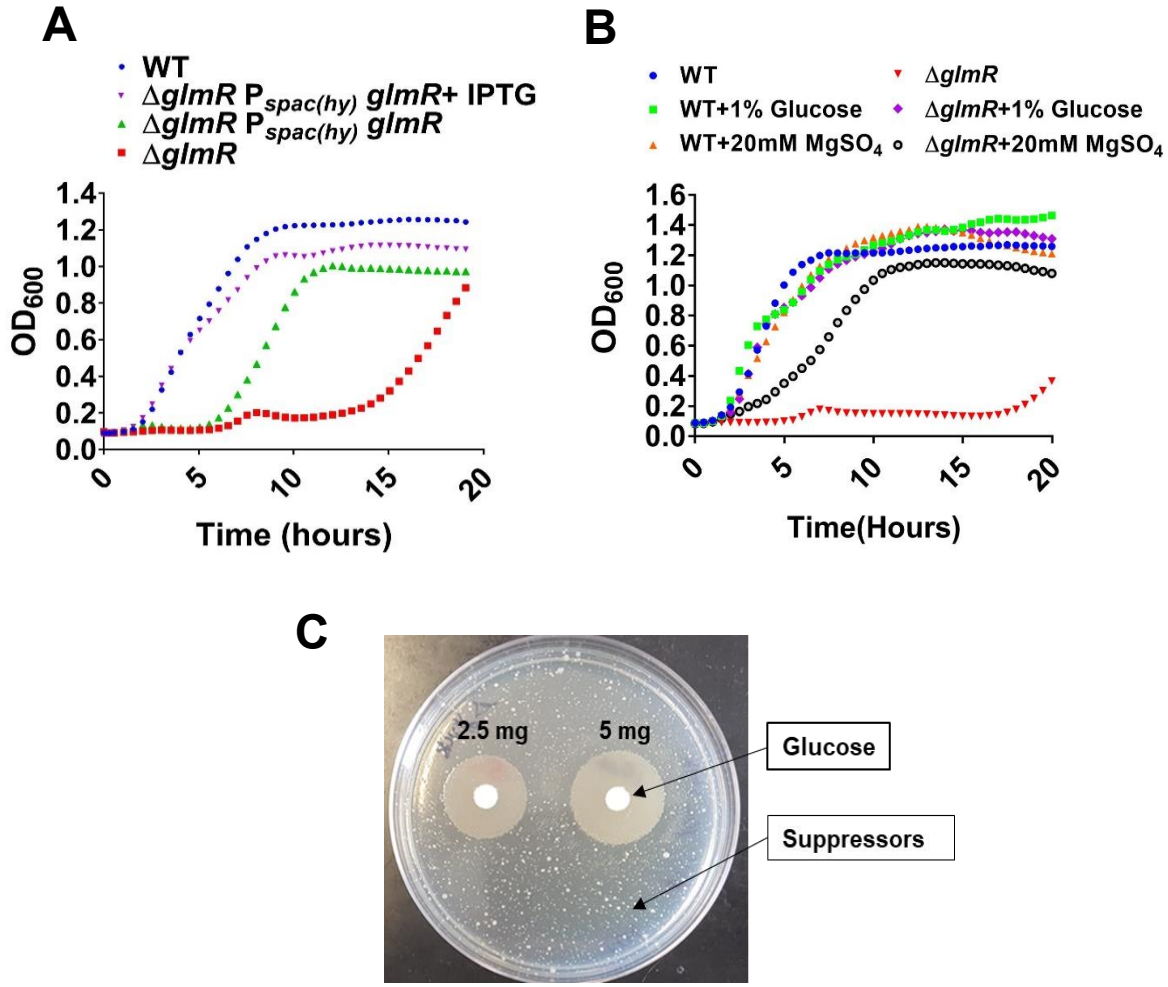

Figure 2.2: Δ*glmR* is unable to grow on MH medium. (A) Growth curves of WT, Δ*glmR* and Δ*glmR amyE*:: P_{spac-} *glmR* on gluconeogenic MH media. **(B)** Growth curves showing the effect of addition of glucose and $MgSO_4$ on growth of Δ*glmR* in MH medium compared to WT. **(C)** Growth stimulation on MH medium by glucose. Top MH agar (4 ml) was plated with 100 µl of Δ*glmR* cells and filter discs containing 2.5 mg and 5 mg of glucose were put on the plate followed by overnight incubation at 37 ^{0}C.

To monitor the impact of the Δ*glmR* mutation on antibiotic sensitivity I performed zone-of-inhibition assays using LB (lysogeny broth) medium, a complex medium containing a variety of mono- and disaccharides (a total carbohydrate concentration of ~0.16%; [14]) and abundant amino

acids. The Δ*glmR* mutant is much more sensitive to the beta-lactam antibiotic cefuroxime (CEF) (Figure 2.3A) as well as to other beta-lactam antibiotics (oxacillin and cefixime), moenomycin, and vancomycin (Figure 2.3B-2.3E), all of which act by affecting the assembly and cross-linking of the peptidoglycan sacculus. However, I did not observe any significant difference in susceptibility between wild-type (WT) and Δ*glmR* to fosfomycin, bacitracin or nisin (Figure 2.3F-2.3H). The lack of significant effect with these compounds may be due to the presence of inducible resistance mechanisms that might mask the effects of the Δ*glmR* mutation [15-18].

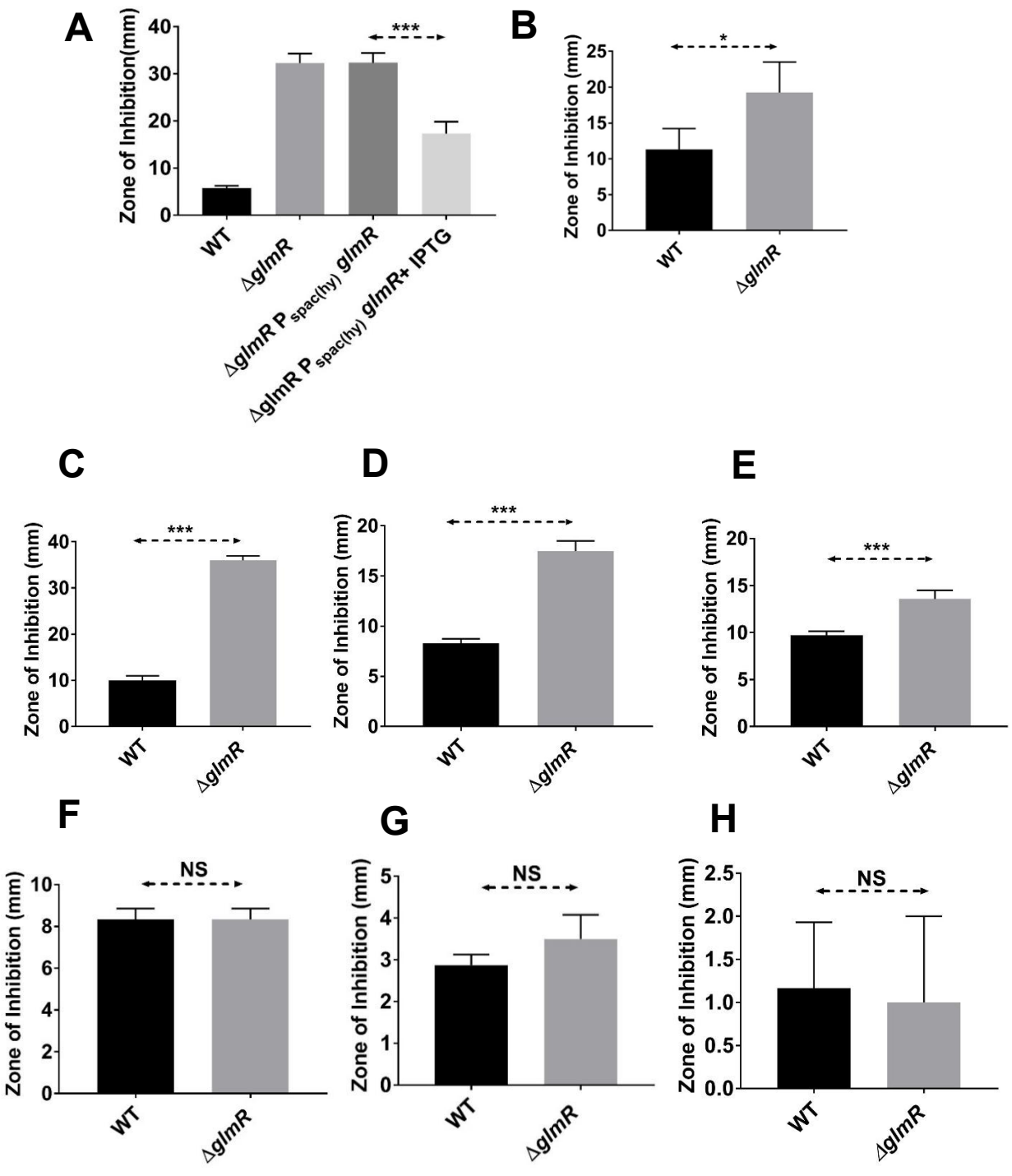
A
Zone of Inhibition(mm)
40
30
20
10
0
***
WT
ΔglmR
ΔglmR P spac(hy) glmR
ΔglmR P spac(hy) glmR+ IPTG
B
Zone of Inhibition (mm)
25
20
15
10
5
0
*
WT
ΔglmR
C
Zone of Inhibition (mm)
40
30
20
10
0
***
WT
ΔglmR
D
Zone of Inhibition (mm)
20
15
10
5
0
***
WT
ΔglmR
E
Zone of Inhibition (mm)
20
15
10
5
0
***
WT
ΔglmR
F
Zone of Inhibition (mm)
10
8
6
4
2
0
NS
WT
ΔglmR
G
Zone of Inhibition (mm)
5
4
3
2
1
0
NS
WT
ΔglmR
H
Zone of Inhibition (mm)
2.5
2.0
1.5
1.0
0.5
0.0
NS
WT
ΔglmR

Figure 2.3: Δ*glmR* is sensitive to CEF and other PG synthesis antibiotics. (A) CEF susceptibility of Δ*glmR* and complementation of the phenotype was tested by disc diffusion assay using 6 µg of antibiotic. IPTG was added to 1 mM to induce expression of ectopic copy of *glmR*. Zone of inhibition (ZOI) was measured after overnight incubation of plates at 37 ^{0}C. ZOI represents the diameter of clear zone surrounding the disc minus the disc (7 mm). Standard deviation (error bars) is based on at least three biological replicates. Three asterisks indicate significant difference with P<0.001 estimated by comparing IPTG treated samples with untreated samples using Tukey test. Disc diffusion assay done with **(B)** oxacillin (1 µg), **(C)** cefixime (40 µg), **(D)** moenomycin (10 µg), **(E)** vancomycin (10 µg), **(F)** fosfomycin (50 µg), **(G)** bacitracin (400 µg) and **(H)** nisin (50 µg). One asterisk and three asterisks represent significance with P <0.05 and P <0.001 respectively. NS indicates that differences were not significant.

I selected CEF for further study due to the significantly higher sensitivity of the Δ*glmR* strain. Induction of an ectopic, IPTG-inducible *glmR* gene partially complements Δ*glmR* cefuroxime sensitivity (Figure 2.3A). Incomplete complementation may indicate that GlmR levels from this construct, while sufficient to restore growth (Figure 2.2A), are insufficient for robust cell wall synthesis. Consistent with this idea, induction of an N-terminally 3X-FLAG-tagged *glmR* allele with an optimized ribosome-binding site (AGGAGG-seven base pairs upstream from start codon), complemented CEF resistance to WT levels (Figure 2.4A). Mutations affecting PG synthesis can often be suppressed by high concentrations of Mg^{2+} [19, 20]. Indeed, Mg^{2+} suppresses the growth defect of a *glmR* deletion mutant on non-glycolytic carbon sources (Figure 2.2B), as shown previously [5], and also partially suppresses CEF sensitivity (Figure 2.4B). These results suggest that a Δ*glmR* strain is impaired in PG synthesis, and therefore more susceptible to antibiotics that interfere directly with PG assembly such as beta-lactams.

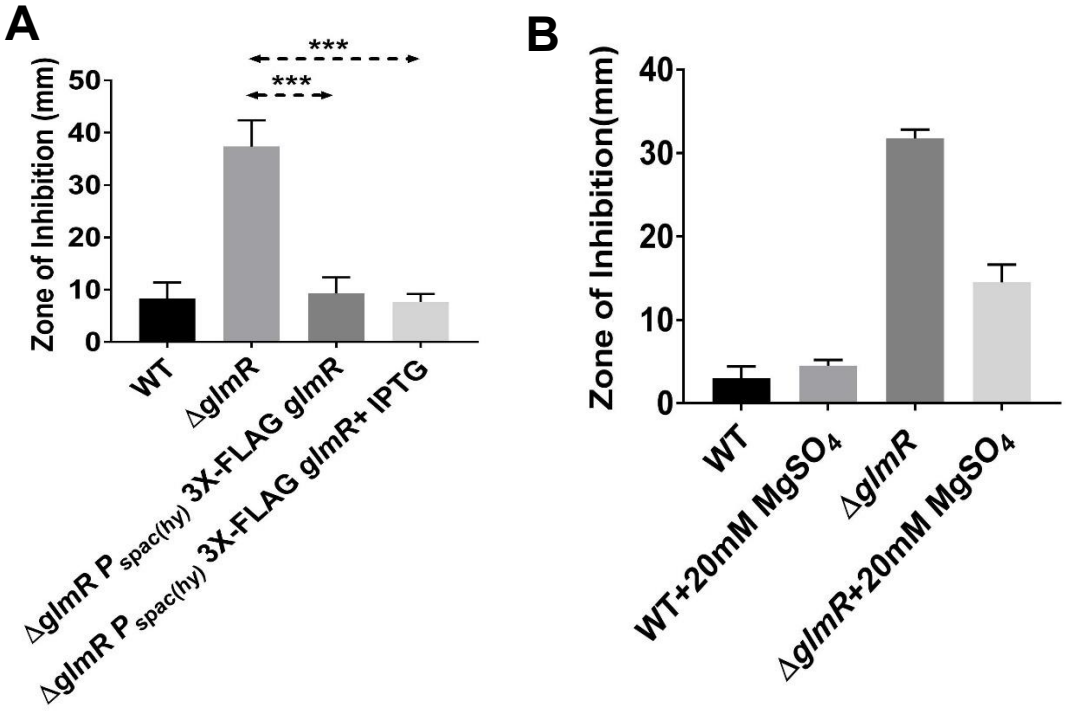

Figure 2.4 Suppression of Δ*glmR* CEF sensitivity by complementation and by Mg^{+2}: (A) CEF susceptibility of Δ*glmR* and complementation of phenotype by IPTG inducible ectopic expression of 3X-FLAG *glmR*. RBS was optimized to AGGAGG that is seven base pair apart from start codon. **(B)** Disc diffusion assay showing suppression of CEF sensitivity of Δ*glmR* by addition of 20 mM $MgSO_4$. In both Figures, statistical significance is indicated by asterisks with P <0.001.

Both the Δ*glmR* and Δ*sigM* mutants are CEF sensitive, and in both cases mutations known to increase c-di-AMP levels suppress this sensitivity (see below). This suggests that GlmR and σ^M may function in the same pathway. However, a Δ*glmR* Δ*sigM* double mutant is much more sensitive than either single mutant (Figure 2.5), suggesting that these are two independent (and additive) pathways for intrinsic CEF resistance.

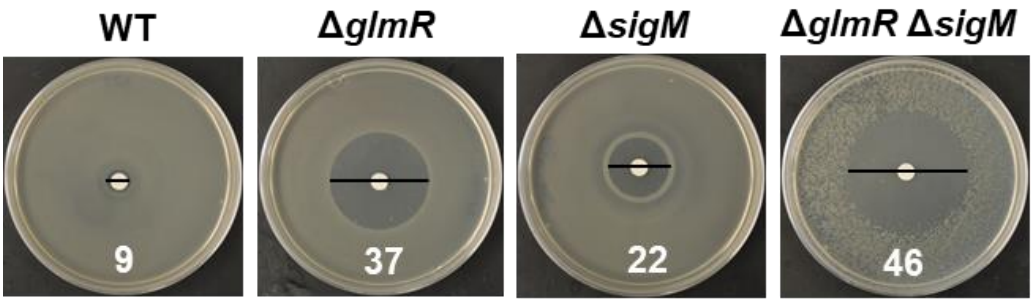

Figure 2.5: ***glmR* functions independently of *sigM*.** Epistasis between *glmR* and *sigM* was determined by disc diffusion assay with 3 µg of CEF on each filter. Numbers at the bottom represent diameter of the zone of inhibition. Above is a representative picture of at least three biological replicates.

2.4.2 The role of GlmR in intrinsic CEF resistance is phosphorylation independent

The CEF sensitivity of the Δ*glmR* strain is suggestive of a defect in PG synthesis. GlmR is also known to be modified on Thr304 by the penicillin binding protein and serine/threonine associated (PASTA) kinase PrkC and phosphatase PrpC [21]. PrkC is activated by muropeptides during spore germination [22] and is regulated by interaction with the cell division protein GpsB during growth [23]. PrkC-dependent phosphorylation of GlmR has been linked to its role in morphogenesis and to resistance to bacitracin, but appears not to be required for growth on gluconeogenic carbon sources [21]. Similarly, this post-translational modification is not required for suppression of CEF sensitivity: both the phosphomimetic $GlmR_{T304E}$ and phosphoablative $GlmR_{T304A}$ mutant proteins complement the null mutant as well as wild-type (Figure 2.6).

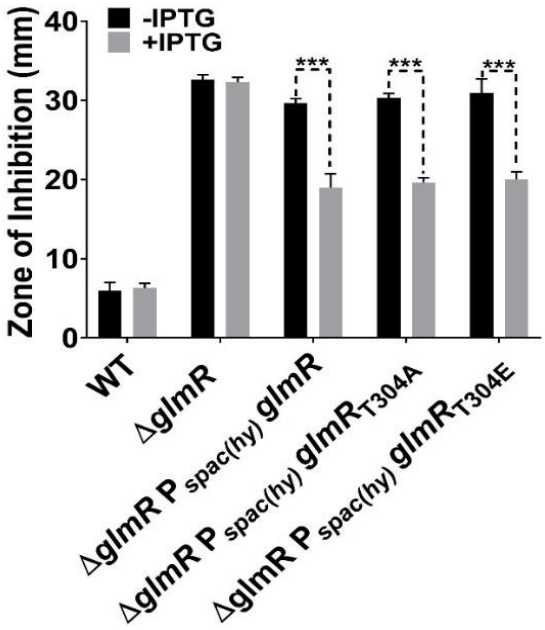

Figure 2.6: The role of GlmR in intrinsic CEF resistance is phosphorylation independent. CEF susceptibility of Δ*glmR* and complementation of the phenotype was tested by disc diffusion assay using 6 µg of antibiotic. IPTG was added to 1 mM to induce expression of ectopic copy of *glmR*. Standard deviation (error bars) is based on at least three biological replicates. Three asterisks indicate significant difference with P<0.001 estimated by comparing IPTG treated samples with untreated samples using Tukey test.

2.4.3 Many Δ*glmR* suppressor mutations affect the *cdaA-cdaR-glmM-glmS* operon

To gain insight into the role of GlmR in *B. subtilis*, I characterized suppressors (both spontaneous and transposon-generated) that either increased CEF resistance or restored the ability of Δ*glmR* to grow on MH medium. The suppressors of Δ*glmR* were isolated either from CEF zone-of-inhibition assays or as colonies on MH medium (Figure 2.2C). The causative mutations were identified by using whole-genome resequencing (spontaneous mutations) or by sequencing of junction fragments (transposon insertions) followed by linkage analysis and/or genetic

reconstruction and complementation (Table 2.1). In general, the selected mutations suppressed both phenotypes associated with Δ*glmR*. Those suppressors selected for increased CEF resistance also recovered an ability to grow on MH medium. Conversely, for those selected for growth on MH medium, nearly all displayed at least a partial increase in CEF resistance relative to the Δ*glmR* starting strain (Table 2.1). In general, in this and previous studies, I find that CEF sensitivity is an excellent reporter for defects in cell wall synthesis. Often, suppressor mutations that fully restore growth may only partially rescue intrinsic CEF resistance. Here, I will focus on those suppressor mutations in the *cdaA-cdaR-glmM-glmS* region of the chromosome, which encodes the two initial enzymes in the peptidoglycan biosynthesis pathway, a major cyclic-di-AMP synthase (CdaA) and a regulator of CdaA (CdaR). I also recovered mutations in other genes in carbon metabolism, including *pgcA* and *zwf*, consistent with prior genetic studies of *glmR* function [5]. The possible mechanisms of suppression for these and other mutations are considered in the Discussion.

Table 2.1 Δ*glmR* suppressor mutations

Selection	Mutant	Genomic region changes	Coding region change	Affected gene or non-coding area	Gene annotation	CEF^R (ZOI, mm)	Growth on MH	Link-age
CEF^R	*glmS1*	200068A>T		Inside *glmS* ribozyme	Senses GlcN6P and controls expression of *glmS*	31	Yes	Yes
	rsiW1	196049G>A	E208E	Penultimate codon of *rsiW* (E208E), affects termination loop stability	Anti-*sigW*	27	Yes	Yes
	rsiW2	196071C>T		Located downstream of *rsiW*. Affects termination loop stability	Non-coding region	27	Yes	Yes
	rsiW3			Tn insertion downstream of rsiW stop codon	Non-coding region	35	ND	Yes
	pgcA$_{G47S}$	1006912G>A	G47A	*pgcA*	Phosphoglucomutase	30	Yes	Yes
	yvcJ$_{L104H}$ *sigA*$_{A197V}$	3572078T>A 2600750G>A	L104H A197V	*yvcJ* *sigA*	GTPase, nucleotide-binding protein; primary σ factor	31	ND	ND
	tufA1::*TnYLB-1*			Tn insertion downstream of *tufA* after stop codon	Elongation factor Tu	29	ND	Yes
MH	*glmS1*	200068A>T		Inside *glmS* ribozyme	Senses GlcN6P and controls expression of *glmS*	31	Yes	Yes
	zwf$_{D405fs}$	2480369delA	D405stop	*zwf*	Glucose 6-phosphate dehydrogenase	31	Yes	Yes
	ispA$_{L140P}$	2526261A>G	L140P	*ispA*	Geranyltransferase	39	Yes	ND
	ispA::*TnYLB-1*			Tn insertion in *ispA*	Geranyltransferase	35	Yes	Yes
	clpX::*TnYLB-1*			Tn insertion in *clpX*	ATP-dependent Clp protease	19	Yes	Yes
	qoxB::*TnYLB-1*			Tn insertion in *qoxB*	Cytochrome aa3 quinol oxidase	26	Yes	Yes

Note: List of Δ*glmR* suppressors obtained using CEF resistance (CEF^R) or growth on MH medium as selection. CEF sensitivity was selected starting with a Δ*glmR* strain (a zone-of-inhibition, ZOI=40 mm) For comparison, WT has a ZOI=12 mm). Genomic region change indicates location of a nucleotide on reference genome of *B. subtilis* subsp. 168 (NCBI reference sequence NC_000964.3). Coding region changes show predicted amino acid substitutions.

Many of the Δ*glmR* suppressors (Table 2.1) contained changes in a chromosomal region around two neighboring operons: *sigW-rsiW* and *cdaA-cdaR-glmM-glmS* (Figure 2.7A). These included a transposon insertion immediately after the *rsiW* stop codon (*rsiW3*) and point mutations in the *glmS* ribozyme (*glmS1*; 200068A>T), in the penultimate codon of *rsiW* (*rsiW1*; 196049G>A), and downstream of *rsiW* (*rsiW2*; 196071C>T). Note that the identical *glmS* mutation (*glmS1*) was recovered independently in both selection conditions.

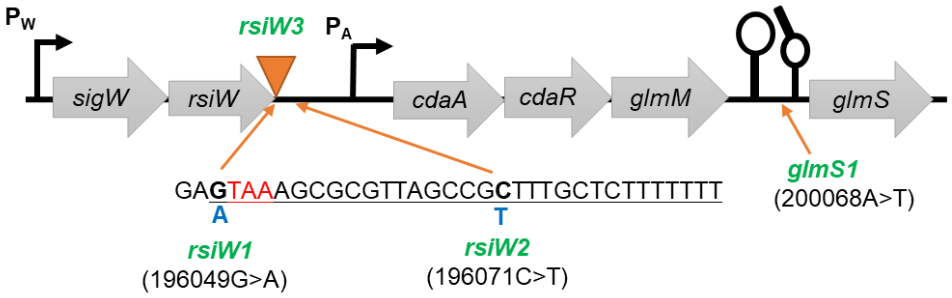

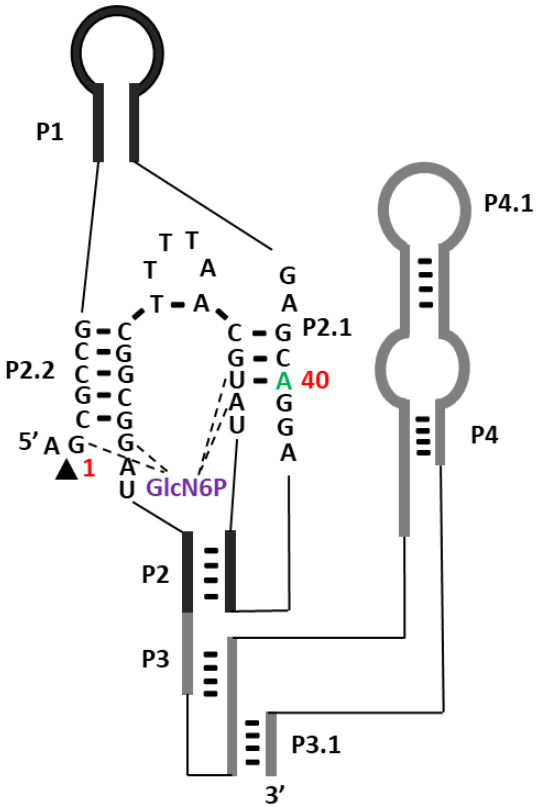

Figure 2.7: Location of *glmR* suppressor mutations in the *sigW-rsiW* and *cdaA-cdaR-glmM-glmS* operons. (A) The *sigW-rsiW* transcription termination loop (underlined) is shown with the *rsiW* stop codon (red). Suppressor mutations included single nucleotide changes (*rsiW1* and *rsiW2*; blue) and a transposon insertion (*rsiW3*; orange triangle). **(B)** Secondary structure of *glmS* ribozyme catalytic domain in *B. subtilis*. The arrowhead indicates the site of self-cleavage. The guanine at the cleavage site is considered the first residue (G1). The green letter (40A) identifies the site of the *glmS1* mutation (40A>T).

Since most of the suppressor mutations did not fully restore CEF resistance to WT levels (Table 2.1), we[1] selected several with intermediate levels of resistance as a starting point for selection of further increased CEF resistance. The most frequent secondary mutations were in *rho* (Table 2.2). A *rho* deletion mutant has been associated with beta-lactam resistance in *B. subtilis* previously [24]. Interestingly, a Δ*glmR* Δ*rho* double mutant is actually more sensitive to CEF than Δ*glmR* (Figure 2.4), and it is only when a primary suppressor mutation (such as *glmS1*) is present in Δ*glmR* that *rho* mutations confers significant CEF resistance (Figure 2.4 and Table 2.2).

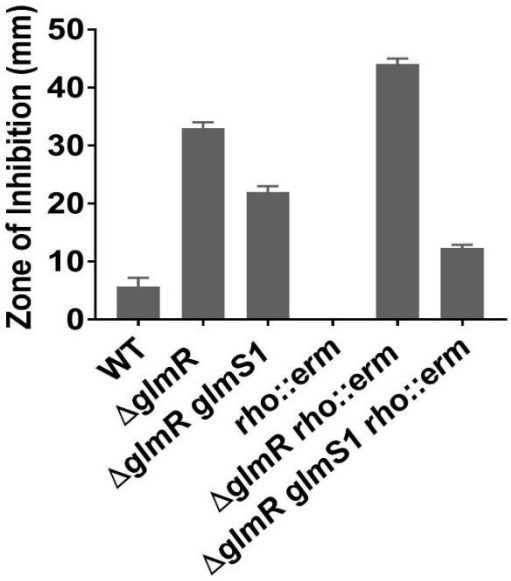

Figure 2.8: *rho* deletion suppresses Δ*glmR* cefuroxime sensitivity phenotype only if a primary suppressor mutation (*glmS1*) is present. CEF disc diffusion assay showing effect of *rho* mutation. Statistical significance with P <0.001 is indicated with three asterisks.

Table 2.1 Secondary suppressors of CEF resistance

Primary CEF^R suppressor of Δ*glmR*	ZOI (mm) of Δ*glmR* with primary suppressor	Secondary mutation	Coding region change	ZOI (mm) with primary and secondary suppressors
glmS1	*30*	rho_{E36fS}	105delA	16
rsiW1	*27*	rho_{R282I}	845G>T	16
rsiW2	*27*	rho_{T337K}	1010C>A	17
$pgcA_{G47S}$	*29*	rho_{I288fs}	861_862insG	17
$pgcA_{G47S}$	*29*	rho_{E59K}	175G>A	17

2.4.4 The *glmS1* ribozyme mutation abolishes negative feedback regulation of *glmS*

GlmS is an amidotransferase that catalyzes the first step in PG synthesis (Figure 2.1) by conversion of the glycolysis intermediate fructose-6-phosphate into glucosamine-6-phosphate (GlcN6P) using glutamine as an amino group donor [25]. Expression of GlmS is under negative feedback control mediated by a ribozyme structure encoded in the 5'-untranslated region (5'-UTR) of the *glmS* mRNA. Upon binding to the GlmS product, GlcN6P, the ribozyme promotes site specific self-cleavage of *glmS* mRNA and consequently reduces *glmS* expression [26].

The *glmS1* suppressor mutation is a base change in the catalytic domain of the *glmS* ribozyme (Figure 2.7B) [27]. After moving the *glms1* mutation into a Δ*glmR* strain, the reconstructed Δ*glmRglmS1* strain regains the ability to grow on gluconeogenic carbon sources (Figure 2.9A) and has increased resistance to CEF (Figure 2.9B). I hypothesized that *glmS1* might interfere with the catalytic activity of the *glmS* ribozyme. Consistent with this idea, the *glmS1* mutation caused a >50-fold increase in *glmS* mRNA compared to WT (Figure 2.9C) and a corresponding increase in GlmS protein levels (Figure 2.9D). I did not see any significant difference in *glmS* mRNA level between WT and Δ*glmR*.

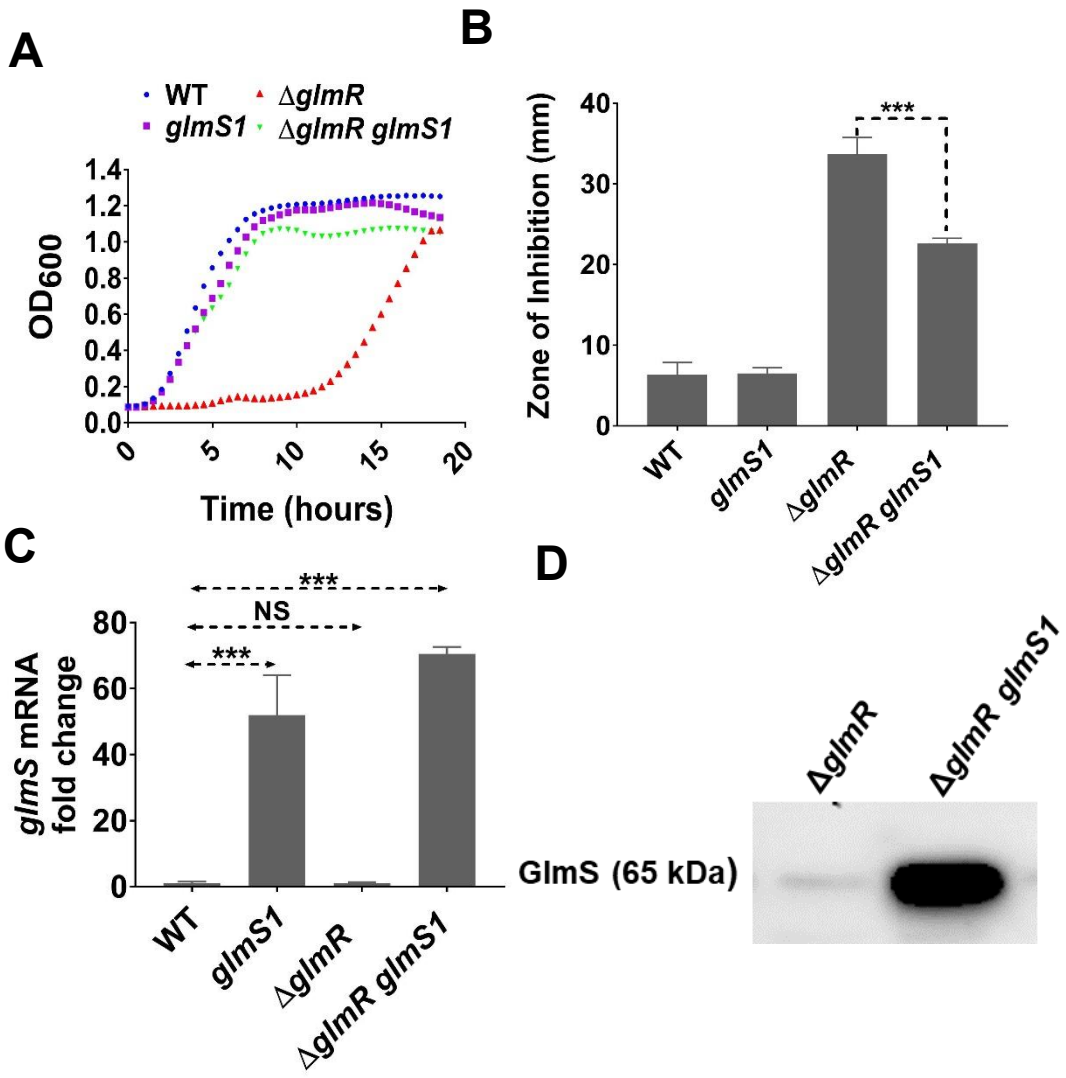

Figure 2.9: *glmS1* suppresses Δ*glmR* by abolishing negative feedback regulation of *glmS* expression. (A) Representative growth curves in MH medium (n>3) showing the effect of point mutation *glmS1* in Δ*glmR* compared to WT, *glmS1* and Δ*glmR*. **(B)** Disc diffusion assay showing the effect of *glmS1* on CEF sensitivity phenotype of Δ*glmR*. 6 µg CEF was used in the assay. Standard deviation (error bars) is based on at least three biological replicates. Three asterisks indicate significant difference with P <0.001 using Tukey test. **(C)** qRT-PCR results showing *glmS* RNA level in *glmS1*, Δ*glmR* and Δ*glmR glmS1* relative to WT from cells harvested at OD_{600} of 0.5 grown in LB. Standard deviation (error bars) is based on at least three biological replicates. Statistical significance is determined by Tukey test where three asterisks indicate P <0.001 and NS is non-significant (P >0.05). **(D)** Western blot analysis of GlmS protein in Δ*glmR* and Δ*glmR glmS1* using anti-GlmS antibodies. 5 µg of total protein was loaded in each lane.

2.4.5 Point mutations in the *sigW-rsiW* transcription termination loop suppress Δ*glmR*

Reconstruction of Δ*glmR* strains with mutations *rsiW1* or *rsiW2* confirmed that these changes allow growth of Δ*glmR* on gluconeogenic growth medium (Figure 2.10A) as well as increased resistance to CEF (Figure 2.10B). The *rsiW1* mutation is silent with respect to the sequence of RsiW and *rsiW2* is downstream of the *rsiW* coding region (Figure 2.7A). I hypothesized that these point mutations might affect the intrinsic transcription terminator of the *sigW-rsiW* operon. *In silico* analysis indicated that each mutation generates a mismatch in the stem of the transcription terminator that is predicted to decrease stability and therefore increase readthrough from the *sigW-rsiW* operon into the downstream *cdaA-cdaR-glmS-glmM* operon (Figure 2.10E). Indeed, the *rsiW1* or *rsiW2* suppressor mutations led to a >10-fold increase in the mRNA level for the first gene of this operon, *cdaA* (Figure 2.10D).

Expression of the *sigW-rsiW* operon is dependent on an autoregulatory σ^W-dependent promoter. An in-frame deletion mutation of *sigW* abolished the ability of the *rsiW1* and *rsiW2* mutations to suppress the Δ*glmR* phenotype (Figure 2.10B). However, in a strain with a *sigW*::*erm* disruption mutation the *rsiW1* and *rsiW2* mutations still conferred increased CEF resistance since the *erm* σ^A promoter now reads into the *cdaA* operon (Figure 2.10C). These observations support my hypothesis that *rsiW1* and *rsiW2* increase expression of *cdaA-cdaR-glmM-glmS*. A similar increase in transcription may explain the phenotype of the *rsiW3* Tn insertion (Table 2.1).

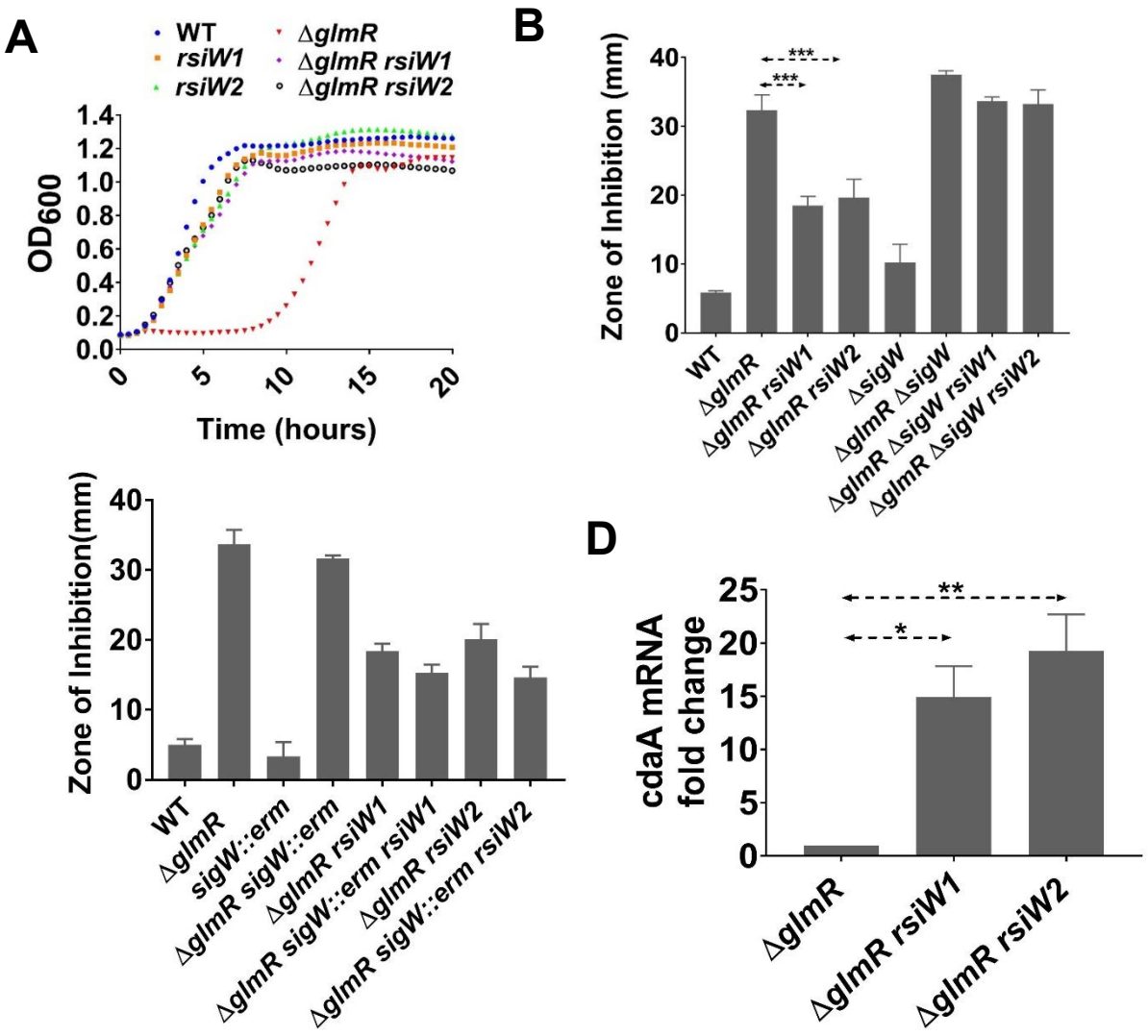

ΔG(Kcal/mol)	-9.70	-6.50	-7.20

Figure 2.10: Point mutations in the *sigW-rsiW* operon transcription termination loop suppress Δ*glmR* phenotypes. (A) Growth curves showing the effect of *rsiW1* and *rsiW2* on the ability of Δ*glmR* to grow on gluconeogenic MH medium. (**B) and (C)** Disc diffusion assays carried out with 6 µg CEF. Standard deviation (error bars) is based on at least three biological replicates. Three asterisks represent statistical significance with P <0.001 with the Tukey test. **(D)** qRT-PCR analysis of *cdaA* mRNA fold change relative to *glmR*. One and two asterisks represent statistical significance with P value less than 0.05 and 0.01 respectively. **(E)** Transcription termination loop secondary structure prediction for WT and with point mutations (*rsiW1* and *rsiW2*) are shown with their relative free energy value prediction.

2.4.6 Increased expression of genes from the *cdaA-cdaR-glmM-glmS* operon suppresses Δ*glmR* growth phenotypes

I reasoned that the *rsiW1, rsiW2* and *rsiW3* mutations likely lead to elevated expression of the *cdaA-cdaR-glmM-glmS* operon. The first two genes encode the major synthase (CdaA) for c-di-AMP and an activator protein (CdaR) [6, 7]. The final two genes encode enzymes for the initial steps of PG biosynthesis that (together with GlmU; also known as GcaD; [28]) convert F6P to UDP-GlcNAc (Figure 2.1). To determine which gene(s) in this operon are involved in suppression of the Δ*glmR* phenotypes I integrated IPTG-inducible copies of various portions of this operon (including *cdaA, cdaA-cdaR, cdaA-cdaR-glmM, cdaA-cdaR-glmM-glmS, glmM-glmS*) at the *amyE* locus in the Δ*glmR* strain. These strains were tested for CEF sensitivity and growth on MH medium. Overexpression of *cdaA* or *cdaA-cdaR* was not sufficient to increase CEF resistance of Δ*glmR* (Figure 2.11A), although I did note an increased frequency of spontaneous suppressors. Overexpression of *cdaA-cdaR-glmM* or *glmM-glmS* partially restored CEF resistance (Figure 2.11A). However, when the whole operon (*cdaA-cdaR-glmM-glmS*) was induced CEF resistance was restored to essentially WT levels (Figure 2.11A). Increased expression of *cdaA-cdaR-glmM* or *cdaA-cdaR-glmM-glmS* also suppressed the essentiality of Δ*glmR* on gluconeogenic MH medium (Figure 2.11B). In contrast, induction of *cdaA-cdaR* alone has a comparatively weak and variable effect on growth, which may reflect the rapid emergence of suppressors in this strain

(Figure 2.11B). From these results I conclude that the key factor in increased fitness of the Δ*glmR* strain is elevated expression of GlmS and/or GlmM, but that c-di-AMP may also play a role.

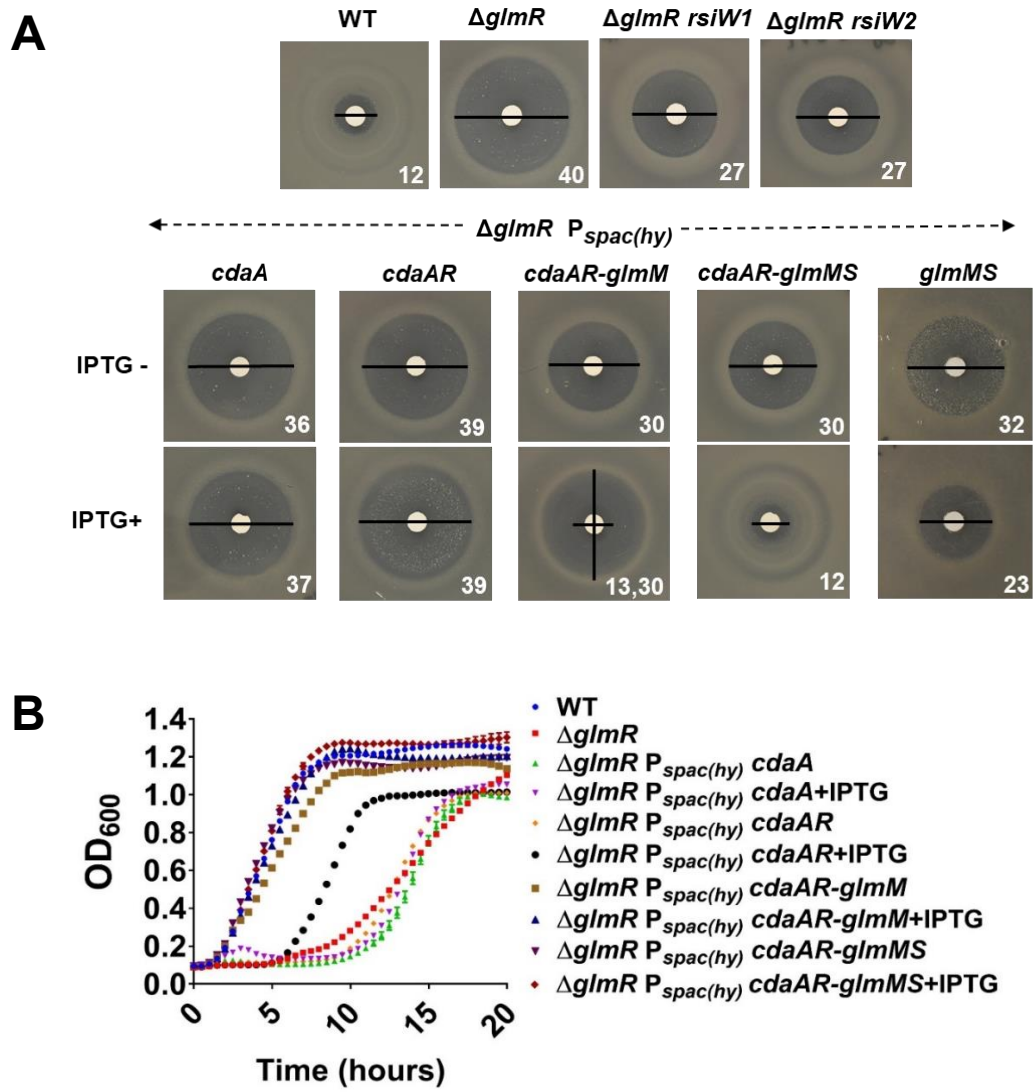

Figure 2.11: Suppression of *glmR* by overexpression of *glmS* and *glmM*. (A) Disc diffusion assays (representative images; n>3) illustrating effects of overexpression of *cdaA*, *cdaA-cdaR (cdaAR)*, *glmM-glmS*, *cdaAR-glmM* or *cdaAR-glmM-glmS* on the CEF sensitivity of the Δ*glmR* strain. Numbers represents diameter of ZOI (mm). Note that for *cdaAR-glmM* there is a small clear inner zone (13 mm), and a larger zone of greatly reduced growth (30 mm). **(B)** Growth curves in MH media for the strains shown in panel (A).

An increase of c-di-AMP has been previously associated with CEF resistance since mutations in *gdpP*, encoding the major c-di-AMP hydrolase, suppress the CEF sensitivity of a *sigM* mutant [4]. Moreover, a *yqfF*::*Tn* insertion, affecting a second c-di-AMP hydrolase renamed PgpH [6, 7], suppresses the inability of a *glmR* (*yvcK*) mutant to grow on gluconeogenic media [5]. I have confirmed these findings and here demonstrate that inactivation of *gdpP* increases CEF resistance of Δ*glmR*, although *pgpH* does not have a significant effect under my conditions (Figure 2.12A and 2.12B). It is interesting to note that a *gdpP pgpH* double mutant, which has greatly elevated c-di-AMP levels and is growth impaired [7], is also highly sensitive to CEF. This effect is not additive with Δ*glmR*, suggesting that excess c-di-AMP may affect the same pathway as GlmR (Figure 2.12A and 2.12B). Consistently, the ability of CdaA and CdaR to increase CEF resistance in a Δ*glmR* mutant seems to be contingent on the additional expression of GlmM and GlmS, as noted above (Figure 2.11A). CdaA forms a complex with both CdaR and GlmM [7, 29], suggesting that c-di-AMP may modulate GlmM activity.

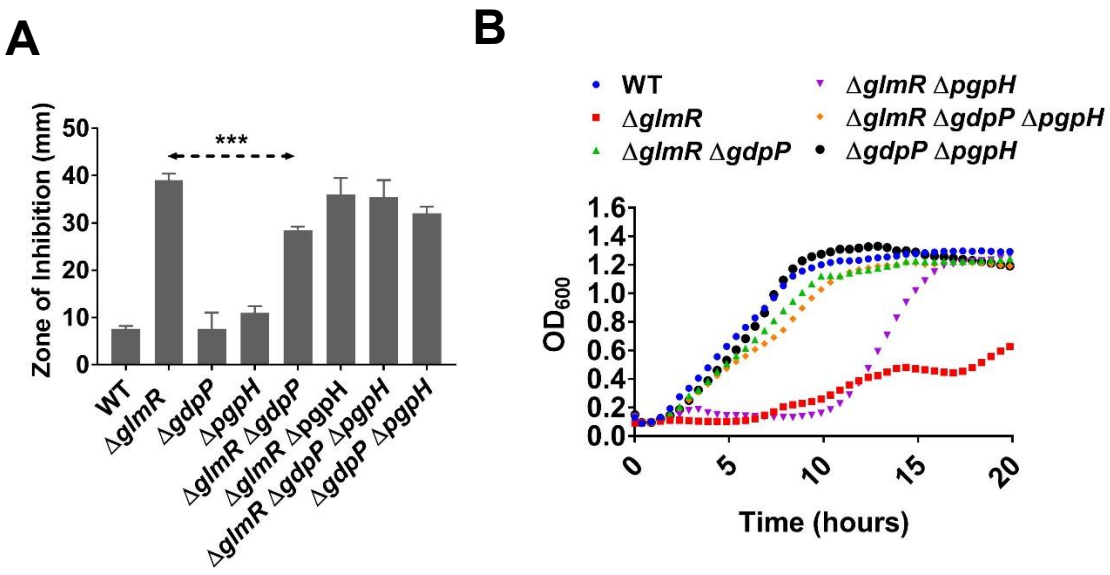

Figure 2.12: Effects of c-di-AMP hydrolase deletion mutations on CEF sensitivity and growth on MH medium for the Δ*glmR* strain. (A) CEF susceptibility and **(B)** growth on MH medium for Δ*glmR* in combination with *gdpP* and *pgpH* deletions and the *gdpP pgpH* double deletion.

2.4.7 Increasing expression of UDP-GlcNAc biosynthetic enzymes suppresses Δ*glmR* phenotypes

I next considered whether a Δ*glmR* strain might be phenotypically suppressed by over-expression of other individual enzymes upstream and downstream of UDP-GlcNAc. Induction of *glmS, glmM* or *glmU* (Figure 2.1), partially restored CEF resistance (Figure 2.13A) and restored the ability of Δ*glmR* to grow on gluconeogenic medium (Figure 2.13B). I suggest that these enzymes increase the forward reaction catalyzed by GlmS by consumption of the product, GlcN6P. GlcN6P is potent inhibitor of GlmS (product inhibition) [30], a property shared with the human ortholog [31].

A portion of cellular UDP-GlcNAc is converted to UDP-MurNAc, the second building block of PG, by MurA and MurB (Figure 2.1). *B. subtilis* has two MurA paralogs, MurAA and MurAB, but only MurA is essential. UDP-MurNAc is then modified by addition of a pentapeptide

side-chain and transferred to the undecaprenylphosphate carrier lipid to ultimately generate lipid II (Figure 2.1), a lipid-linked GlcNAc-MurNAc-pentapeptide that is the substrate for extracellular PG synthesis [32]. Overexpression of *murAA* or *murB* increased the sensitivity of the Δ*glmR* strain to CEF (Figure 2.13C), and neither rescued the growth defect of Δ*glmR* on MH medium (Figure 2.13D).

I reasoned that the effects of MurAA and MurB overproduction might be relieved in cells that have increased capacity to synthesize UDP-GlcNAc. To test this hypothesis, I introduced the *glmS1* mutation (which abolishes negative feedback regulation of *glmS*) into the Δ*glmR amyE*::$P_{spac(hy)}$ *murAA* and Δ*glmR amyE*::$P_{spac(hy)}$ *murB* strains. In these *glmS1* strains, induction of *murAA* or *murB* no longer increases sensitivity to CEF (Figure 2.13C). Based on these observations I hypothesize that *B. subtilis* lacking GlmR is impaired specifically in UDP-GlcNAc biosynthesis. The resulting inability to efficiently synthesize PG is a likely reason for the essentiality of *glmR* on gluconeogenic media.

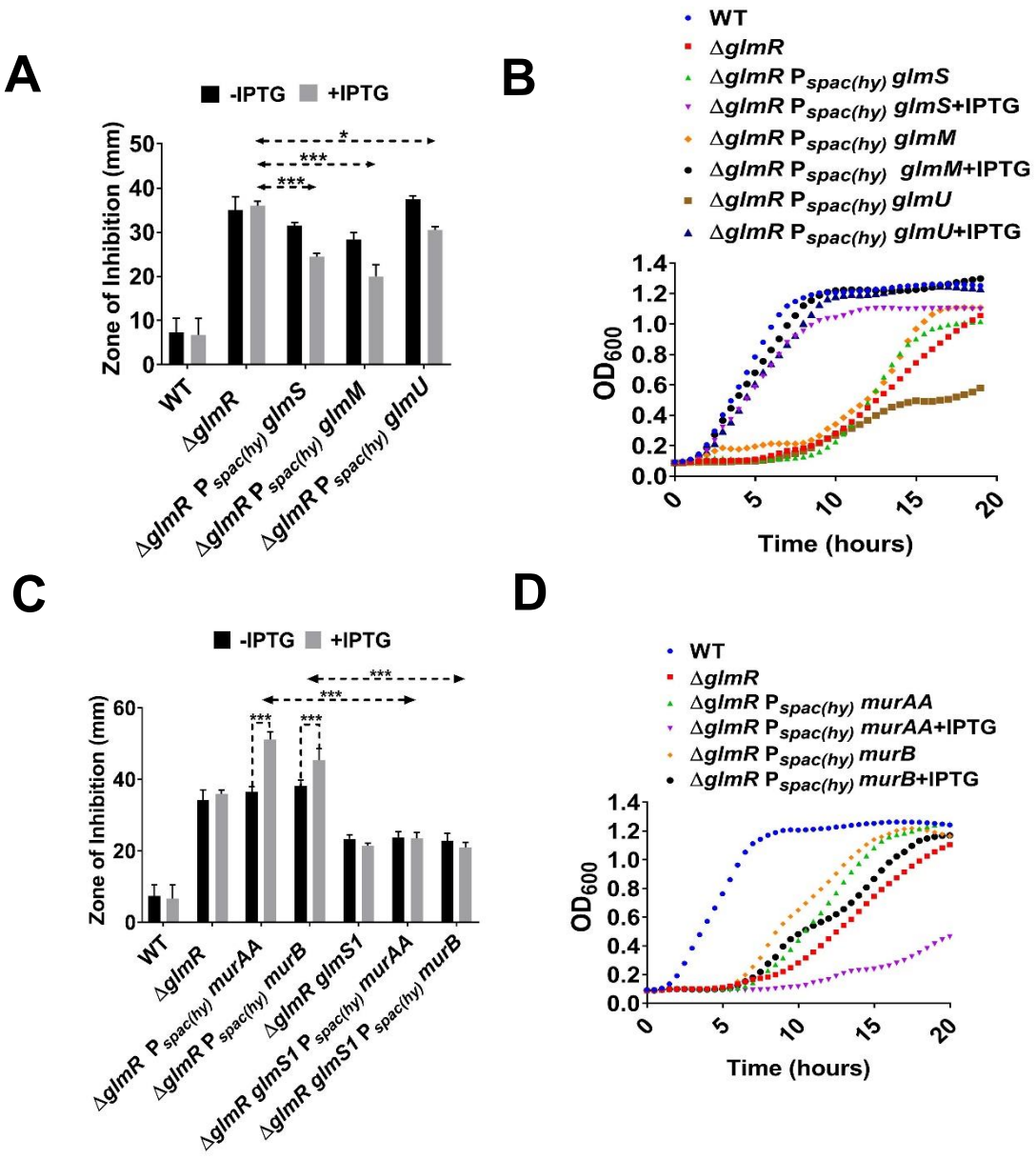

Figure 2.13: Increasing UDP-GlcNAc suppresses Δ*glmR*. (A) Disc diffusion showing the change in CEF susceptibility of Δ*glmR* when *glmM*, *glmS* and *glmU* were overexpressed. Standard deviation (error bars) is based on at least three biological replicates. One and three asterisks indicate significant value with P <0.05 and P <0.001 respectively as determined by Tukey test. **(B)** Growth curves in MH media with Δ*glmR* overexpressing *glmM, glmS and glmU* in comparison to WT and Δ*glmR*. **(C)** Disc diffusion assay showing CEF susceptibility of Δ*glmR* when *murAA* and *murB* are overexpressed. The figure also shows the effect on CEF sensitivity when *glmS1* is introduced in Δ*glmR amyE*:: $P_{spac(hy)}$ *murAA* and Δ*glmR amyE*::$P_{spac(hy)}$ *murB* respectively. Three asterisks indicate significance (P <0.001) as determined by Tukey test. **(D)** Growth curve experiment done in MH medium showing the consequence of *murAA* and *murB* overexpression on Δ*glmR*.

2.4.8 Mutations of the GlmR UDP-GlcNAc binding site do not significantly affect CEF resistance

GlmR was recently found to bind UDP-sugars such as UDP-glucose and UDP-GlcNAc [10]. UDP-GlcNAc bound with five times higher affinity that UDP-Glc, suggesting that the former may be a regulatory ligand for GlmR. I used CRISPR-gene editing to introduce single amino acid substitutions in the UDP-GlcNAc binding site of GlmR that were previously shown to abolish ligand binding (Y265A, R301A and R301E). Consistent with prior results [10], none of these three mutations affected the ability of GlmR to support growth on gluconeogenic MH medium (Figure 2.14A), nor did they have a significant impact on CEF resistance (Figure 2.14B). I therefore suggest that ligand binding serves as a feedback mechanism to down-regulate GlmR activity when UDP-GlcNAc levels are high. Under gluconeogenic conditions, when GlmR is required for redirecting carbon from CCM into PG synthesis, this binding site would be vacant, and therefore these mutations would not affect the stimulatory function of GlmR (Figure 2.1).

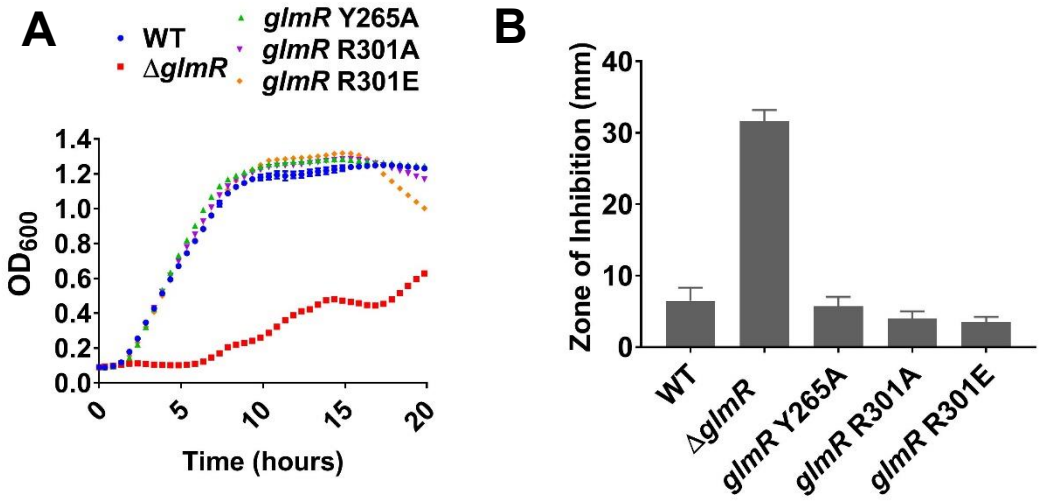

Figure 2.14: Mutations of the GlmR UDP-GlcNAc binding site do not affect gluconeogenic growth. (A) Growth curve with UDP-GlcNAc binding site mutants of GlmR in gluconeogenic MH medium and **(B)** CEF sensitivity of GlcNAc binding site mutants of GlmR tested on LB medium with 6 µg of antibiotic.

2.4.9 Addition of GlcNAc bypasses the essentiality of *glmR* on gluconeogenic media

Since Δ*glmR* suppressor mutations lead to increased *glmS* expression (Figure 2.9C and 2.9D), I reasoned that the Δ*glmR* strain may be specifically defective in GlmS activity. If this is the case, I hypothesized that provision of cells with GlcNAc would chemically complement the Δ*glmR* growth defect. Indeed, when a disc containing GlcNAc was placed on a MH medium plate strong growth of the Δ*glmR* strain was observed (Figure 2.15A).

GlcNAc is taken up by the GlcNAc-specific phosphoenolpyruvate phosphotransferase system (PTS) protein NagP and enters the cell as GlcNAc-6-phosphate [33]. Deacetylation by NagA then generates GlcN6P (Figure 2.1), which is also the product generated by GlmS [34]. GlcN6P can either feed into peptidoglycan biosynthesis (GlmM and GlmU) or feed CCM by conversion to F6P by either of two inducible deaminases (NagB and GamA) [33, 35] (Figure 2.1). The ability of GlcNAc to support growth of the Δ*glmR* strain requires NagA, but is independent of the GamA and NagB deaminases (Figure 2.15B). This indicates that the limiting step in metabolism during growth of the Δ*glmR* strain on largely gluconeogenic carbon sources is the GlmS-catalyzed conversion of F6P to GlcN6P. This limitation can be by-passed by up-regulation of GlmS (e.g. by overexpression, Figure 2.13B, or in the *glmS1* mutant strain, Figure 2.9) or by provision of cells with GlcNAc. The ability of overproduced GlmM or GlmU to support growth (Figure 2.13B) may therefore seem surprising, but may be explained by more rapid consumption of GlcN6P, which would prevent product inhibition of GlmS and also increase translation of GlmS by inhibiting *glmS* ribozyme cleavage.

To test if GlcNAc addition also suppresses the increased CEF sensitivity, I tested WT and Δ*glmR* strains on LB agar supplemented with 0.5% and 1% GlcNAc. Addition of GlcNAc partially suppressed the CEF sensitivity of Δ*glmR*, but had no significant effect on a strain in which GlmS was up-regulated by the *glmS1* suppressor mutation (Figure 2.15C). In a Δ*glmR* Δ*nagB* Δ*gamA* strain in which added GlcNAc cannot re-enter CCM, CEF resistance is restored to near WT levels (Figure 2.15D). The greater suppression seen in this strain may result from the inability of this strain to catabolize incoming GlcNAc, which thereby further increases the flux into PG synthesis. This supports the notion that a major contributor to CEF sensitivity is a metabolic defect that limits the ability of the cell to synthesize PG, apparently due to a limitation in the ability of GlmS to redirect carbon from CCM to cell wall synthesis. I hypothesize that GlmR may directly stimulate GlmS enzyme activity. This is supported by evidence of a GlmR-GlmS protein interaction in bacterial two-hybrid assays (Figure 2.16). The observed interaction is robust, as compared to the positive control, and is not observed with other proteins tested including CdaA, GlmM, or CdaR (Figure 2.16).

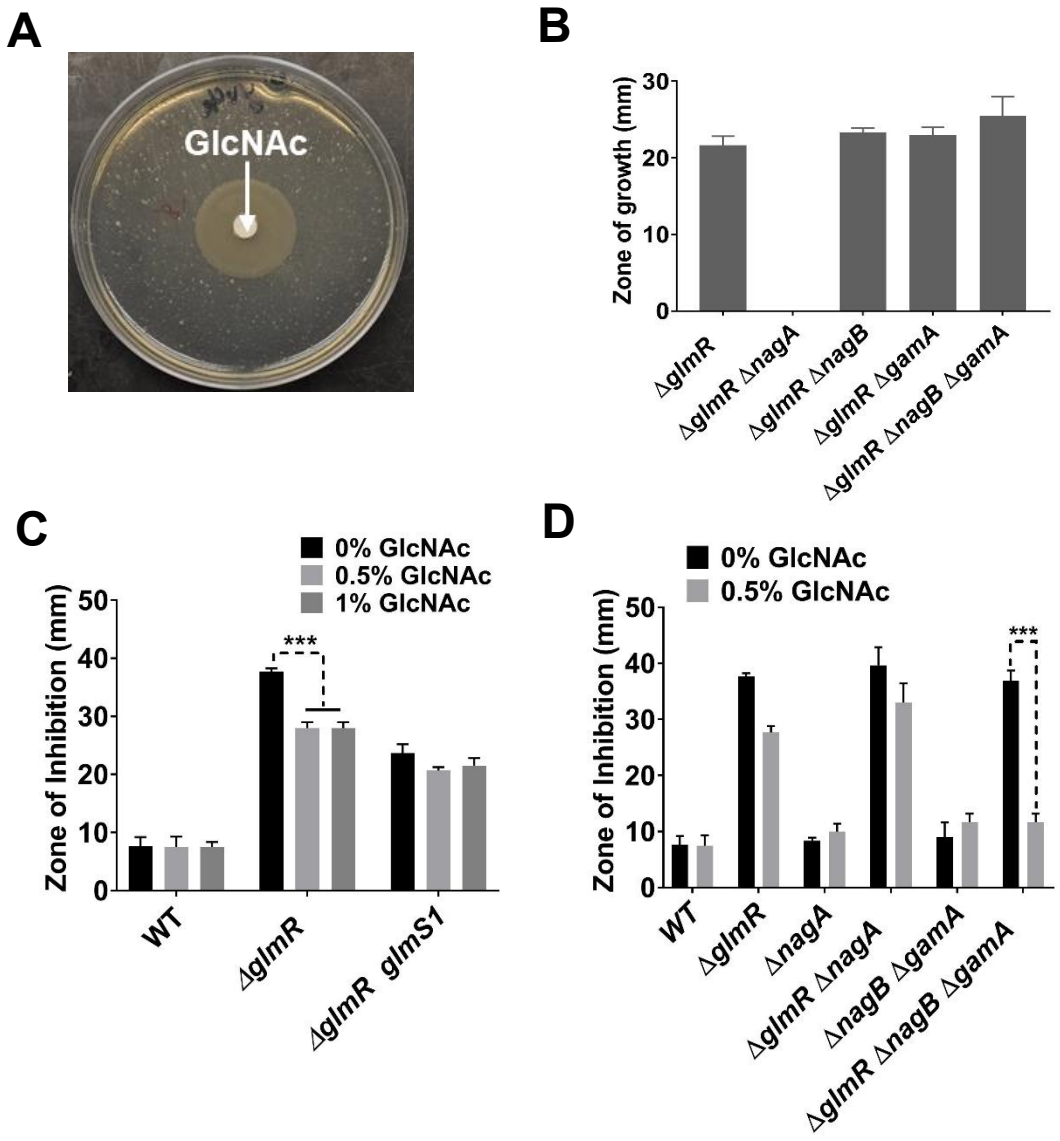

Figure 2.15: Addition of GlcNAc bypasses the essentiality of *glmR* on gluconeogenic media. **(A)** An MH agar plate with Δ*glmR* showing the zone of growth around a GlcNAc disc. **(B)** Bar graphs representing the zone of growth for Δ*glmR*, Δ*glmR* Δ*nagA*, Δ*glmR* Δ*nagB*, Δ*glmR* Δ*gamA* and Δ*glmR* Δ*nagB* Δ*gamA*. **(C)** Disc diffusion assay showing the effect of GlcNAc (0.5 or 1%) on CEF sensitivity of WT, Δ*glmR* and Δ*glmR glmS1* and **(D)** Disc diffusion assay comparing the effect of 0.5% GlcNAc on CEF sensitivity of WT, Δ*glmR*, Δ*nagA*, Δ*glmR* Δ*nagA*, Δ*gamA* Δ*nagB* and Δ*glmR* Δ*gamA* Δ*nagA*. Three asterisks indicate significance with P <0.001 as determined by Tukey test.

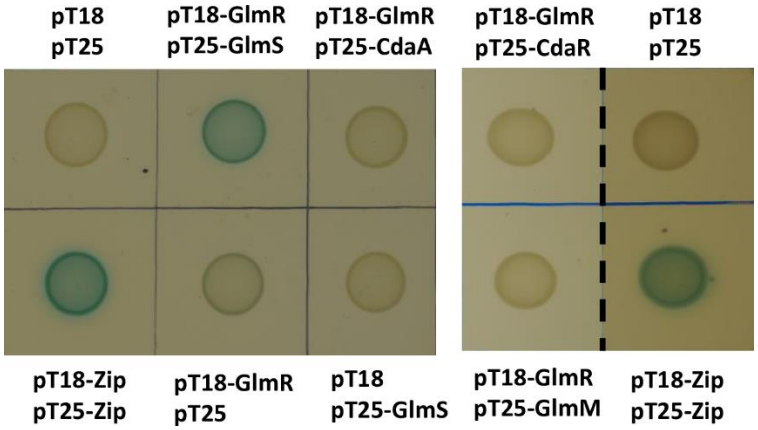

Figure 2.16: Bacterial two hybrid assay. pT18-containing *glmR* and the compatible plasmid pT25 containing *glmS* or *cdaA* were transformed into *E. coli* strain BTH101. When co-expressed protein fusions interact, the *Bordetella pertussis* adenylate cyclase is active as assessed by blue color in the presence of X-gal.

2.5 Discussion

Here I present a forward genetic analysis that indicates that GlmR regulates the redirection of carbon from CCM into PG biosynthesis, likely by stimulation of GlmS activity. The regulation of CCM as cells adapt to nutrient availability is exceptionally complex and involves numerous transcriptional regulators and post-transcriptional regulatory mechanisms [36, 37]. The carbon catabolite control protein CcpA plays a central role in this process and represses genes for the utilization of non-preferred carbon sources when glucose is available [38], as well as the operon encoding *glmR*: *yvcI-yvcJ-glmR-yvcL-crh-yvcN* [39]. As a result, GlmR should be most abundant when CcpA activity is low. CcpA repressor activity is indirectly stimulated by elevated levels of fructose-1,6-bisphosphate present during growth on preferred carbon sources [40-42]. During growth on non-preferred, gluconeogenic carbon sources GlmR will be more abundant, consistent with its role in diverting carbon to PG synthesis under these conditions.

The GlmR (formerly YvcK) protein is conditionally essential and plays a poorly defined role in cell morphology and antibiotic resistance [10-12, 21]. Homologs in *M. tuberculosis* (CuvA) and *L. monocytogenes* (YvcK) appear to also play a role in helping maintain cell shape [11, 12]. GlmR was suggested to lead to a dysregulation of carbon metabolism since mutations affecting metabolic enzymes (e.g. Zwf) and CCM regulatory proteins (e.g. CggR) suppress the *glmR* null mutant and allow growth on gluconeogenic carbon sources [5]. Cytological evidence suggests that GlmR and CuvA localize to membrane sites associated with PG synthesis, and it has been noted that GlmR and MreB appear to functionally substitute for one another, perhaps in coordinating the assembly of PG biosynthetic complexes [8, 11]. Despite intensive study, the connection between these disparate phenotypes has been elusive. Here, I propose that several of the phenotypes can be explained by stimulation of the key branchpoint enzyme, GlmS.

It remains possible that, in addition to stimulation of GlmS activity, GlmR may have other functions. This is suggested by the observation that the role of GlmR in intrinsic CEF resistance is independent of protein phosphorylation as judged by the analysis of phosphomimetic and phosphablative mutants (Figure 2.6). In contrast, phosphorylation of GlmR was shown to affect bacitracin sensitivity and cell morphogenesis in an *mreB* mutant background [21]. Although the *M. tuberculosis* GlmR ortholog CuvA is also modified by phosphorylation by Ser/Thr PASTA kinases, this modification is not important for complementation of carbon source specific growth defects or for localization to sites of PG synthesis [11, 12], and perhaps regulates other functions. Analysis of phosphosite mutants of the *L. monocytogenes* GlmR ortholog suggests that a phosphomimetic variant is unaffected in metabolism and cell wall homeostasis, but is impaired in virulence [11, 12]. Further studies are needed to clarify how GlmR phosphorylation affects some, but not all, activities of this protein.

2.5.1 *A model for GlmR as a feedback inhibited activator of GlmS*

My genetic analysis supports a model in which GlmR activates GlmS, and I suggest that this activity is inhibited when GlmR is bound to the downstream metabolite, UDP-GlcNAc (Figure 2.1). This model is supported by several key observations. First, overproduction of GlmS, in either the *glmS1* mutant or by induction from an ectopic *glmS* gene, is sufficient to restore growth of the *glmR* null mutant on MH medium (Figure 2.9,2.13). Second, a *glmR* mutant can be chemically complemented by GlcNAc, even under conditions where GlcNAc cannot be routed into CCM (Figure 2.15). Since metabolism of GlcNAc generates GlcN6P, this addition specifically bypasses the GlmS reaction (Figure 2.1). Therefore, I suggest that GlmS (rather than GlmM or GlmU) is limiting the flux of carbon into PG in the Δ*glmR* strain. Third, previous metabolomics measurements indicate that F6P levels are ~16-fold lower during growth on gluconeogenic carbon sources when compared to glucose [13], consistent with the requirement for GlmR under these conditions (Figure 2.1). Fourth, GlmR was recently found to bind UDP-GlcNAc [10]. However, mutations that abolish binding do not affect the ability of GlmR to stimulate growth under gluconeogenic conditions [10] or to provide intrinsic CEF resistance (Figure 2.14), as predicted by the hypothesis that UDP-GlcNAc antagonizes GlmR function (Figure 2.1).

GlmS is recognized as the key branch-point enzyme in bacteria for diverting carbon from CCM into PG synthesis, and in eukaryotes the GlmS ortholog diverts carbon into hexosamine synthesis. Both classes of enzyme are in some cases feedback regulated by UDP-GlcNAc [43-47]. Here, UDP-GlcNAc binding is proposed to antagonize GlmR function [10], and therefore reduce stimulation of GlmS. Although I have not yet demonstrated that GlmR can directly activate GlmS activity, the two proteins interact *in vivo* as judged by a bacterial two-hybrid assay (Figure 2.16).

In addition to GlmS, I also demonstrate that overproduction of either GlmM or GlmU, but not by enzymes downstream of the key intermediate UDP-GlcNAc, can suppress the *glmR* growth defect under gluconeogenic conditions. GlmS catalyzes a reversible reaction, and its product (GlcN6P) is a potent inhibitor of the forward reaction [30]. Moreover, GlcN6P binds to the *glmS* ribozyme to cleave the mRNA and suppress translation [26]. Therefore, I suggest that increasing the level of GlmM and/or GlmU likely helps pull the reaction in the forward direction and may also stimulate GlmS translation.

2.5.2 *GlmR activation of GlmS as a framework for understanding other suppressor mutations*

With a defined model in hand, I can revisit the other suppressor mutations recovered both in my selection conditions (Table 2.1) and the studies of Görke *et al.* [5]. As noted previously, many of the mutations that suppress *glmR* affect CCM. I recovered a frameshift mutation in *zwf*, a gene also recovered in the previous transposon-based selection for *glmR* suppressors [5]. Normally, Zwf diverts a substantial fraction of glucose-6-phosphate from glycolysis into the pentose phosphate pathway [48]. I speculate that in the absence of Zwf there is increased flux leading to F6P, the GlmS substrate. I also recovered a mutation in *pgcA*, which encodes another branch point enzyme that uses glucose-6-phosphate. Previously, it was reported that a mutation in *cggR*, encoding the central glycolytic genes regulator, also suppresses *glmR* [5]. Since a *cggR* null mutant will have increased levels of several key enzymes that function in both glycolysis and gluconeogenesis [49], I speculate that this mutation alleviates the metabolic restriction in the *glmR* strain by increasing gluconeogenesis and therefore F6P levels.

A second class of mutations that increase the fitness of the Δ*glmR* strain are those that lead to elevated c-di-AMP levels. This was foreshadowed by the finding that a *pgpH* (formerly *yqfF*)

mutation suppresses *glmR* [5]. In my studies, I find that *gdpP* suppresses *glmR* both for growth on MH medium and for CEF resistance, whereas *pgpH* has a lesser effect (Figure 2.12). CdaA is regulated by interaction with the CdaR protein and also forms a complex with GlmM [7, 29]. Indeed, the *cdaA-cdaR-glmM* genes are co-transcribed in a wide variety of species, suggesting a functional connection. This has led to the suggestion that GlmM may regulate c-di-AMP synthesis [7, 29]. Conversely, CdaA may regulate GlmM. In this scenario, conditions that lead to elevated c-di-AMP may alter the CdaA-CdaR complex to favor a stimulatory interaction of CdaA with GlmM. Indeed, it is striking that induction of the entire *cdaAR-glmMS* operon fully restores CEF resistance to a *glmR* mutant (Figure 2.11), whereas this is not the case for the *glmR glmS1* strain (Figure 2.9) or for induction of *glmS* alone (Figure 2.13). Alternatively, c-di-AMP is also known to regulate potassium homeostasis by interaction with both protein and RNA (riboswitch) targets [50-53]. This c-di-AMP dependent osmolyte transport is important for maintaining turgor pressure in the cell and it has been proposed that perturbations of c-di-AMP metabolism can affect cell envelope integrity by increasing resistance against osmotic stresses [54].

A third class of suppressor mutations is in genes important for energy generation by the electron transport chain. These include mutations in *qoxB*, encoding cytochrome aa3 quinol oxidase, and *yqiD(ispA),* encoding a geranyltransferase that is involved in synthesis of isoprenoid compounds including menaquinone, an electron carrier important for respiration (Table 2.1). Mutations in both of these loci have been previously associated with an increased ability of cells to survive the transition to L-forms that lack a peptidoglycan cell wall [55]. This observation led to a model in which a lethal consequence of cell wall defects is oxidative damage triggered by increased flux through the electron transport chain when carbon flux into peptidoglycan is

eliminated [55]. Regardless of the precise mechanism, it is intriguing that mutations in these same genes were recovered as suppressors of Δ*glmR*.

Finally, I recovered one strain containing a missense mutation in *yvcJ* (Table 2.1), the gene immediately upstream of *glmR*. The role of YvcJ is unknown, but it has GTPase activity, affects phosphorylation of an uncharacterized cell component, and has an apparent role in natural competence [56, 57]. Since this strain contained an additional mutation in *sigA* (Table 2.1), further work is needed to determine the effect of the *yvcJ* mutation on CEF resistance. Curiously, mutants of the *E. coli* YvcJ homolog (RapZ; formerly YhbJ) lead to overproduction of GlmS [58]. RapZ appears to sense GlcN6P and regulates the processing and stability of a small RNA, GlmZ, that activates GlmS synthesis [46, 58, 59]. It is presently unknown whether YvcJ plays a related role in *B. subtilis*, perhaps by interacting either with GlmR or the *glmS* ribozyme.

In conclusion, the results presented here highlight the importance of the GlmS branch point in regulating the flow of carbon from CCM into PG synthesis. In eukaryotes, GlmS orthologs serve as the initiating enzyme for hexosamine biosynthesis, and are sensitive to both GlcN6P product inhibition [31] and feedback regulation by UDP-GlcNAc, which binds to the isomerase domain [43, 44]. In bacteria, GlmS is also subject to complex regulation at the level of both synthesis and activity [45-47]. In *B. subtilis*, GlmS is feedback inhibited by its immediate product, GlcN6P [30], which also activates the *glmS* ribozyme [26]. GlmR provides another layer of regulation. My results support a model in which GlmR stimulates GlmS activity, and I propose that binding of UDP-GlcNAc may attenuate this stimulation.

2.6 Methods

2.6.1 Bacterial strains and growth conditions:

B. subtilis strains used are derived from strain 168 (*trpC2*) (S2 Table). *E. coli* strain DH5α was used for cloning and strain BTH101 [60] for bacterial two hybrid experiments. Bacteria were cultured in LB broth. Strains with a *glmR* deletion mutation were cultured on LB with 20 mM $MgSO_4$ unless specified otherwise. Antibiotics were added to growth media when required at the following concentrations: 100 μg/ml ampicillin, 30 μg/ml chloramphenicol for *E. coli*, 10 μg/ml kanamycin, 10 μg/ml chloramphenicol, 5 μg/ml tetracycline, 100 μg/ml spectinomycin and 1 μg/ml erythromycin with 25 μg/ml lincomycin (erm; macrolide-lincomycin-streptogramin B resistance).

2.6.2 Cloning, transformation and strain construction:

For cloning procedures, restriction digestion and ligation with T4 ligase was done as per manufacturer's instructions (NEB, USA). Plasmids were then transformed into competent DH5α cells [61]. Cloning was confirmed by polymerase chain reaction (PCR) followed by Sanger sequencing. *B. subtilis* transformation was carried out in minimal competence media with 12 mM $MgSO_4$. DNA was added when cells reached OD_{600} of ~0.7-0.8. Generation of *B. subtilis* strains overexpressing gene(s) at *amyE* was achieved using pPL82 [62] carrying gene(s) of interest followed by transformation into the indicated *B. subtilis* recipient strain.

Bacillus knockout erythromycin (BKE) strains with various gene deletion mutations of *B. subtilis* were obtained from the *Bacillus* Genetic Stock Center (BGSC) [63]. Chromosomal DNA from each BKE strain was transformed into the lab strain *B. subtilis* 168. The erythromycin resistance cassette was removed using pDR244 [63], which produces Cre recombinase at the

permissive temperature of 30^0 C, to generate in-frame deletions. pDR244 was transformed into *B. subtilis* strain at 30^0 C and plated on LB plates with spectinomycin. Colonies were picked after two overnight incubations and patched three successive times on LB plates incubated at the non-permissive temperature 42^0 C overnight. Strains were then patched on spectinomycin- and erythromycin-containing plates to confirm the absence of both markers. All the deletion mutants used in study are markerless deletions except Δ*rho* (*rho*::*erm*).

Single nucleotide mutations *glmS1*, *rsiW1* and *rsiW2* were reconstructed using the integration vector pMutin4 that has an *erm* resistance marker and *lacZ* [64]. A fragment of DNA with the mutation of interest was cloned into pMutin4 and confirmed with PCR and Sanger sequencing. The vector was transformed into *B. subtilis* where it integrated at locus by single crossover homologous recombination. Transformants were selected on plates with Erm and 40 μg/ml X-gal. After overnight incubation, a few blue color colonies were picked. Since pMutin4 integration is unstable, cells were grown without antibiotic selection three consecutive times with each time adding 1:100 dilution of cells from previous culture. Cells were then plated on LB plates with X-gal and white colonies were picked and sequenced to find those strains that retained the single nucleotide mutation of interest.

2.6.3 Mariner transposon mutagenesis:

Mariner transposon mutagenesis procedure was carried out in Δ*glmR* as described previously [65]. In brief, Δ*glmR* was transformed with the pMarA vector. The strain with pMarA was grown in 5 ml LB broth until mid-exponential phase and various dilutions of cells were plated on selection medium. In independent experiments CEF resistance and ability to grow on MH media were used as a selection.

2.6.4 Spontaneous suppressor analysis:

Spontaneous suppressors of Δ*glmR* were picked from the clear zone of CEF disc diffusion plates and independently from MH plates after overnight incubation at 37^0 C. Chromosomal DNA was extracted from these suppressors was sequenced using an Illumina machine. The sequencing data were analyzed using CLC genomics workbench.

2.6.5 Antibiotic sensitivity assays:

Antibiotic sensitivity was tested using disc diffusion assays, which were carried out on LB medium. Strains to be tested were grown in 5 ml LB broth at 37^0 C with vigorous shaking to an OD_{600} of ~0.4. 100 µl of cells were added to 4 ml top LB agar (0.7% agar) kept at 50^0 C. 1 mM IPTG was added to top agar when indicated. Top agar with cells was poured over 15 ml LB bottom agar (1.5%) plate. A Whatman paper disc (7mm dia) with 6 µg CEF was put on the plate unless specified otherwise. Plates were incubated at 37^0 C overnight and the clear zone of inhibition was measured the next day. Values for CEF resistance (Table 2.1) report the diameter of the zone of growth inhibition. For all histograms, the values shown have the diameter of the filter disk (7 mm) subtracted from the average diameter.

2.6.6 Growth Assay on MH:

To test the ability of *B. subtilis* mutants to grow under gluconeogenic conditions MH medium (Sigma-Aldrich, USA) was used, prepared per the manufacturer's instruction. Growth was monitored using a Bioscreen growth analyzer with 200 µl of MH broth in 100 well Bioscreen plates inoculated with 2 µl of *B. subtilis* strains pre-grown in LB broth at 37^0 C to an OD_{600} of

~0.4. When required, glucose, $MgSO_4$ and IPTG were added to the final concentrations of 1%, 20 mM and 1 mM respectively.

2.6.7 qRT-PCR:

Strains of interest were grown to an OD_{600} of ~0.5. 1.5 ml of culture was used for RNA extraction. RNA isolation (Qiagen, USA) and cDNA preparation (Thermofisher, USA) was carried out as suggested by the manufacturer. qRT-PCR was carried out using a Bio-Rad iTaq universal SYBR green super mix. 23S rRNA was used to normalize the cycle threshold (Ct) value.

2.6.8 Cell lysate preparation and western blot:

For GlmS measurements, Δ*glmR* and Δ*glmR glmS1* strains were grown in LB medium to an OD_{600} of ~0.3 at 37^{o} C with shaking. 30 ml of culture was withdrawn and centrifuged at 5000 rpm for 10 minutes. Cell pellets were frozen at -20^{o} C. Pellets were washed once with 1X phosphate buffer saline (pH 7.4). 150 µl of lysis buffer (20 mM tris-HCl, 100 mM NaCl, 1 mM EDTA, 1 mM DTT, 10% glycerol and protease inhibitor cocktail) was used to re-suspend the cell pellets. One tablet of protease inhibitor cocktail from Roche diagnostics was added to 10 ml of lysis buffer. Cells were lysed by sonication. After centrifugation cell lysates were transferred to fresh tubes. Protein concentration was measured by Bradford assay (Bio-Rad). 5 µg of protein was run on a 4-15% gradient gel from Bio-Rad. Protein was transferred onto a PVDF membrane using a Bio-Rad transblot turbo transfer system. The membrane was blocked with 5% milk powder for one hour followed by overnight incubation with primary anti-GlmS polyclonal antibodies [66] added to 1:3000 dilution in 1X tris buffer saline with 0.1% tween 20 and 0.5% milk powder. After three

washes, the membrane was incubated with a 1:3000 dilution of HRP conjugated anti-Rabbit antibodies (Sigma). Bands were visualized on a Bio-Rad Chemidoc MP imaging system.

2.6.9 GlcNAc disc diffusion assay:

Strains of interest were grown in 5 ml LB medium to an OD_{600} of ~0.4. 100 µl of cells were added to 4 ml top MH agar (0.7% agar) preheated at 50^0 C and was laid on a 15 ml MH agar (1.5%) plate. A disc with 0.5 mg GlcNAc (Sigma, USA) was put on the plate. After overnight incubation at 37^0 C, the zone of growth surrounding the disc was measured.

2.6.10 CRISPR editing:

DNA changed encoding single amino acid substitutions ($GlmR_{Y255A,}$ $GlmR_{R301A}$ and $GlmR_{R301E}$) were generated at the native *glmR* locus using CRISPR editing as described [67]. In brief, oligonucleotides encoding a 20 nucleotide gRNA with flanking BsaI sites and a repair fragment carrying mutations of interest with flanking SfiI restrictions sites were cloned sequentially into vector pJOE8999 followed by transformation into *E. coli* DH5α cells. The resultant plasmid was transformed into recipient *B. subtilis* strain and cells were plated on 15 µg/ml kanamycin plates with 0.2% mannose. Transformation was carried out at 30^o C as pJOE8999 cannot replicate at higher temperatures. The transformants were patched on LB agar plates and incubated at the non-permissive temperature of 42^0 C. The loss of vector was confirmed by the inability of selected isolates on kanamycin plates. The presence of the desired mutations was confirmed by Sanger sequencing.

2.6.11 Bacterial two hybrid:

Vectors pT18 and pT25 and strains for bacterial two hybrid were prepared as described [60]. *E. coli* BTH101 strains carrying pT18 and pT25 with genes of interest were grown in LB broth overnight at 30 ^{0}C with 100 µg/ml ampicillin, 50 µg/ml chloramphenicol and 0.5 mM IPTG. 10 µl of cells were spotted on LB plate with 100 µg/ml ampicillin, 50 µg/ml chloramphenicol, 0.5 mM IPTG and 40 µg/ml X-gal. Plates were incubated overnight at 30^0 C.

2.6.12 RNA structure analysis:

In silico analysis was carried out using NUPACK web application [68].

Table 2.3 *B. subtilis* strains used in this study

Strain	Genotype	Source/ ref
168	*trpC2*	Lab stock
HB16822	*trpC2 rho::erm*	This work
HB16825	*trpC2 glmR rho::erm*	This work
HB16848	*trpC2 glmR*	This work
HB16849	*trpC2 sigW*	This work
HB16850	*trpC2 glmR sigW*	This work
HB16858	*trpC2* 200068A>T (*glmS1*)	This work
HB16868	*trpC2 glmR glmS1*	This work
HB16905	*trpC2 glmR amyE*::$P_{spac(hy)}$-*cdaA-cdaR*	This work
HB16910	*trpC2 glmR amyE*::$P_{spac(hy)}$-*glmM*	This work
HB16913	*trpC2 glmR amyE*::$P_{spac(hy)}$-*cdaA*	This work
HB16942	*trpC2* 196071C>T (*rsiW2*)	This work
HB16943	*trpC2 glmR glmS1 rho::erm*	This work
HB16950	*trpC2 glmR rsiW2*	This work
HB16951	*trpC2 glmR amyE*::$P_{spac(hy)}$ -*glmR*	This work
HB16954	*trpC2 glmR amyE*::$P_{spac(hy)}$-*glmR*$_{T304A}$	This work
HB16955	*trpC2 glmR amyE*::$P_{spac(hy)}$-*glmR*$_{T304E}$	This work
HB16960	*trpC2* 196049G>A (*rsiW1*)	This work
HB16963	*trpC2 glmR amyE*::$P_{spac(hy)}$-*cdaA-cdaR-glmM*	This work

HB16964	*trpC2 glmR amyE*::$P_{spac(hy)}$-*murAA*	This work
HB16965	*trpC2 glmR rsiW1*	This work
HB16979	*trpC2 glmR glmS1 amyE::*$P_{spac(hy)}$ *murAA*	This work
HB16994	*trpC2 glmR nagB*	This work
HB20901	*trpC2 nagA*	This work
HB20902	*trpC2 glmR nagA*	This work
HB20917	*trpC2 glmR nagB gamA*	This work
HB21902	*trpC glmR zwf*	This work
HB21906	*trpC2 glmR amyE::*$P_{spac(hy)}$ *zwf*	This work
HB21915	*trpC2 glmR sigW::erm rsiW1*	This work
HB21916	*trpC2 glmR sigW rsiW2*	This work
HB21920	*trpC2 glmR sigW rsiW1*	This work
HB21921	*trpC2 glmR sigW rsiW2*	This work
HB21922	*trpC2 glmR amyE*::$P_{spac(hy)}$-*glmU*	This work
HB21923	*trpC2 glmR amyE*::$P_{spac(hy)}$-*murB*	This work
HB21926	*trpC2 glmR amyE*::$P_{spac(hy)}$-*cdaA-cdaR-glmM-glmS*	This work
HB21929	*trpC2 glmR glmS1 amyE*::$P_{spac(hy)}$-*murB*	This work
HB21932	*trpC2 glmR*$_{Y265A}$	This work
HB21942	*trpC glmR amyE*::$P_{spac(hy)}$-*glmS*	This work
HB21947	*trpC2 nagB gamA*	This work
HB21957	*trpC2 glmR*$_{R301A}$	This work
HB21958	*trpC2 glmR*$_{R301E}$	This work

2.7 REFERENCES

1. Helmann JD. *Bacillus subtilis* extracytoplasmic function (ECF) sigma factors and defense of the cell envelope. Current Opinion in Microbiology. 2016;30:122-32.
2. Mascher T, Helmann JD, Unden G. Stimulus Perception in Bacterial Signal-Transducing Histidine Kinases. Microbiology and Molecular Biology Reviews. 2006;70(4):910-38. doi: 10.1128/mmbr.00020-06.
3. Eiamphungporn W, Helmann JD. The *Bacillus subtilis* σ^M Regulon and its Contribution to Cell Envelope Stress Responses. Molecular microbiology. 2008;67(4):830-48. doi: 10.1111/j.1365-2958.2007.06090.x. PubMed PMID: PMC3025603.
4. Luo Y, Helmann JD. Analysis of the role of *Bacillus subtilis* σ^M in β-lactam resistance reveals an essential role for c-di-AMP in peptidoglycan homeostasis. Molecular Microbiology. 2012;83(3):623-39. doi: 10.1111/j.1365-2958.2011.07953.x.
5. Görke B, Foulquier E, Galinier A. YvcK of *Bacillus subtilis* is required for a normal cell shape and for growth on Krebs cycle intermediates and substrates of the pentose phosphate pathway. Microbiology. 2005;151(11):3777-91. doi: doi:10.1099/mic.0.28172-0.
6. Huynh TN, Luo S, Pensinger D, Sauer J-D, Tong L, Woodward JJ. An HD-domain phosphodiesterase mediates cooperative hydrolysis of c-di-AMP to affect bacterial growth and virulence. Proceedings of the National Academy of Sciences. 2015;112(7):E747-E56. doi: 10.1073/pnas.1416485112.
7. Gundlach J, Mehne FMP, Herzberg C, Kampf J, Valerius O, Kaever V, *et al*. An Essential Poison: Synthesis and Degradation of Cyclic Di-AMP in *Bacillus subtilis*. Journal of Bacteriology. 2015;197(20):3265-74. doi: 10.1128/jb.00564-15.

8. Foulquier E, Pompeo F, Bernadac A, Espinosa L, Galinier A. The YvcK protein is required for morphogenesis via localization of PBP1 under gluconeogenic growth conditions in *Bacillus subtilis*. Molecular Microbiology. 2011;80(2):309-18. doi: 10.1111/j.1365-2958.2011.07587.x.

9. Kawai Y, Daniel RA, Errington J. Regulation of cell wall morphogenesis in *Bacillus subtilis* by recruitment of PBP1 to the MreB helix. Molecular Microbiology. 2009;71(5):1131-44. doi: 10.1111/j.1365-2958.2009.06601.x.

10. Foulquier E, Galinier A. YvcK, a protein required for cell wall integrity and optimal carbon source utilization, binds uridine diphosphate-sugars. Scientific Reports. 2017;7(1):4139. doi: 10.1038/s41598-017-04064-2.

11. Mir M, Prisic S, Kang C-M, Lun S, Guo H, Murry JP, *et al*. Mycobacterial Gene *cuvA* Is Required for Optimal Nutrient Utilization and Virulence. Infection and Immunity. 2014;82(10):4104-17. doi: 10.1128/iai.02207-14.

12. Pensinger DA, Boldon KM, Chen GY, Vincent WJB, Sherman K, Xiong M, *et al*. The *Listeria monocytogenes* PASTA Kinase PrkA and Its Substrate YvcK Are Required for Cell Wall Homeostasis, Metabolism, and Virulence. PLOS Pathogens. 2016;12(11):e1006001. doi: 10.1371/journal.ppat.1006001.

13. Kleijn RJ, Buescher JM, Le Chat L, Jules M, Aymerich S, Sauer U. Metabolic Fluxes during Strong Carbon Catabolite Repression by Malate in *Bacillus subtilis*. Journal of Biological Chemistry. 2010;285(3):1587-96. doi: 10.1074/jbc.M109.061747.

14. Baev MV, Baev D, Radek AJ, Campbell JW. Growth of *Escherichia coli* MG1655 on LB medium: monitoring utilization of sugars, alcohols, and organic acids with transcriptional

microarrays. Applied Microbiology and Biotechnology. 2006;71(3):310-6. doi: 10.1007/s00253-006-0317-6.

15. Cao M, Bernat BA, Wang Z, Armstrong RN, Helmann JD. FosB, a cysteine-dependent fosfomycin resistance protein under the control of sigma(W), an extracytoplasmic-function sigma factor in *Bacillus subtilis*. J Bacteriol. 2001;183(7):2380-3. doi: 10.1128/JB.183.7.2380-2383.2001. PubMed PMID: 11244082; PubMed Central PMCID: PMCPMC95149.

16. Kingston AW, Liao X, Helmann JD. Contributions of the sigma(W), sigma(M) and sigma(X) regulons to the lantibiotic resistome of *Bacillus subtilis*. Mol Microbiol. 2013;90(3):502-18. doi: 10.1111/mmi.12380. PubMed PMID: 23980836; PubMed Central PMCID: PMCPMC4067139.

17. Radeck J, Gebhard S, Orchard PS, Kirchner M, Bauer S, Mascher T, *et al*. Anatomy of the bacitracin resistance network in *Bacillus subtilis*. Mol Microbiol. 2016;100(4):607-20. doi: 10.1111/mmi.13336. PubMed PMID: 26815905.

18. Thompson MK, Keithly ME, Harp J, Cook PD, Jagessar KL, Sulikowski GA, *et al*. Structural and chemical aspects of resistance to the antibiotic fosfomycin conferred by FosB from *Bacillus cereus*. Biochemistry. 2013;52(41):7350-62. doi: 10.1021/bi4009648. PubMed PMID: 24004181; PubMed Central PMCID: PMCPMC4108214.

19. Formstone A, Errington J. A magnesium-dependent *mreB* null mutant: implications for the role of *mreB* in *Bacillus subtilis*. Molecular Microbiology. 2005;55(6):1646-57. doi: 10.1111/j.1365-2958.2005.04506.x.

20. Chastanet A1 C-LR. The actin-like MreB proteins in *Bacillus subtilis*: a new turn. Front Biosci (Schol Ed). 2012:1582-606.

21. Foulquier E, Pompeo F, Freton C, Cordier B, Grangeasse C, Galinier A. PrkC-mediated Phosphorylation of Overexpressed YvcK Protein Regulates PBP1 Protein Localization in *Bacillus subtilis mre*B Mutant Cells. Journal of Biological Chemistry. 2014;289(34):23662-9. doi: 10.1074/jbc.M114.562496.

22. Shah IM, Laaberki M-H, Popham DL, Dworkin J. A Eukaryotic-like Ser/Thr Kinase Signals Bacteria to Exit Dormancy in Response to Peptidoglycan Fragments. Cell. 2008;135(3):486-96.

23. Pompeo F, Foulquier E, Serrano B, Grangeasse C, Galinier A. Phosphorylation of the cell division protein GpsB regulates PrkC kinase activity through a negative feedback loop in *Bacillus subtilis*. Molecular Microbiology. 2015;97(1):139-50. doi: 10.1111/mmi.13015.

24. Lee YH, Helmann JD. Mutations in the Primary Sigma Factor σ^A and Termination Factor Rho That Reduce Susceptibility to Cell Wall Antibiotics. Journal of Bacteriology. 2014;196(21):3700-11. doi: 10.1128/jb.02022-14.

25. Milewski S. Glucosamine-6-phosphate synthase—the multi-facets enzyme. Biochimica et Biophysica Acta (BBA) - Protein Structure and Molecular Enzymology. 2002;1597(2):173-92.

26. Winkler WC, Nahvi A, Roth A, Collins JA, Breaker RR. Control of gene expression by a natural metabolite-responsive ribozyme. Nature. 2004;428:281. doi: 10.1038/nature02362.

27. Cochrane JC, Lipchock SV, Strobel SA. Structural Investigation of the GlmS Ribozyme Bound to Its Catalytic Cofactor. Chemistry & Biology. 2007;14(1):97-105.

28. Hove-Jensen B. Identification of *tms*-26 as an allele of the *gcaD* gene, which encodes N-acetylglucosamine 1-phosphate uridyltransferase in *Bacillus subtilis*. J Bacteriol.

1992;174(21):6852-6. PubMed PMID: 1328164; PubMed Central PMCID: PMCPMC207362.

29. Zhu Y, Pham TH, Nhiep THN, Vu NMT, Marcellin E, Chakrabortti A, *et al*. Cyclic-di-AMP synthesis by the diadenylate cyclase CdaA is modulated by the peptidoglycan biosynthesis enzyme GlmM in *Lactococcus lactis*. Molecular Microbiology. 2016;99(6):1015-27. doi: 10.1111/mmi.13281.

30. Deng MD, Grund AD, Wassink SL, Peng SS, Nielsen KL, Huckins BD, *et al*. Directed evolution and characterization of *Escherichia coli* glucosamine synthase. Biochimie. 2006;88(5):419-29. PubMed PMID: 16871653.

31. Broschat KO, Gorka C, Page JD, Martin-Berger CL, Davies MS, Huang Hc HC, *et al*. Kinetic characterization of human glutamine-fructose-6-phosphate amidotransferase I: potent feedback inhibition by glucosamine 6-phosphate. J Biol Chem. 2002;277(17):14764-70. doi: 10.1074/jbc.M201056200. PubMed PMID: 11842094.

32. van Heijenoort J. Lipid Intermediates in the Biosynthesis of Bacterial Peptidoglycan. Microbiology and Molecular Biology Reviews. 2007;71(4):620-35. doi: 10.1128/mmbr.00016-07.

33. Gaugué I, Oberto J, Putzer H, Plumbridge J. The Use of Amino Sugars by *Bacillus subtilis*: Presence of a Unique Operon for the Catabolism of Glucosamine. PLOS ONE. 2013;8(5):e63025. doi: 10.1371/journal.pone.0063025.

34. Souza JM, Plumbridge JA, Calcagno ML. N-Acetylglucosamine-6-phosphate Deacetylase from *Escherichia coli*: Purification and Molecular and Kinetic Characterization. Archives of Biochemistry and Biophysics. 1997;340(2):338-46. doi: https://doi.org/10.1006/abbi.1997.9780.

35. Vincent F, Yates D, Garman E, Davies GJ, Brannigan JA. The Three-dimensional Structure of the N-Acetylglucosamine-6-phosphate Deacetylase, NagA, from *Bacillus subtilis*: A MEMBER OF THE UREASE SUPERFAMILY. Journal of Biological Chemistry. 2004;279(4):2809-16. doi: 10.1074/jbc.M310165200.

36. Chubukov V, Gerosa L, Kochanowski K, Sauer U. Coordination of microbial metabolism. Nature Reviews Microbiology. 2014;12:327. doi: 10.1038/nrmicro3238.

37. Fujita Y. Carbon Catabolite Control of the Metabolic Network in *Bacillus subtilis*. Bioscience, Biotechnology, and Biochemistry. 2009;73(2):245-59. doi: 10.1271/bbb.80479.

38. Warner JB, Lolkema JS. CcpA-Dependent Carbon Catabolite Repression in Bacteria. Microbiology and Molecular Biology Reviews. 2003;67(4):475-90. doi: 10.1128/mmbr.67.4.475-490.2003.

39. Blencke H-M, Homuth G, Ludwig H, Mäder U, Hecker M, Stülke J. Transcriptional profiling of gene expression in response to glucose in *Bacillus subtilis*: regulation of the central metabolic pathways. Metabolic Engineering. 2003;5(2):133-49. doi: https://doi.org/10.1016/S1096-7176(03)00009-0.

40. Meyer FM, Jules M, Mehne FM, Le Coq D, Landmann JJ, Gorke B, *et al*. Malate-mediated carbon catabolite repression in *Bacillus subtilis* involves the HPrK/CcpA pathway. J Bacteriol. 2011;193(24):6939-49. doi: 10.1128/JB.06197-11. PubMed PMID: 22001508; PubMed Central PMCID: PMCPMC3232832.

41. Schumacher MA, Sprehe M, Bartholomae M, Hillen W, Brennan RG. Structures of carbon catabolite protein A-(HPr-Ser46-P) bound to diverse catabolite response element sites reveal the basis for high-affinity binding to degenerate DNA operators. Nucleic Acids Res.

2011;39(7):2931-42. doi: 10.1093/nar/gkq1177. PubMed PMID: 21106498; PubMed Central PMCID: PMCPMC3074128.

42. Fujita Y. Carbon catabolite control of the metabolic network in *Bacillus subtilis*. Biosci Biotechnol Biochem. 2009;73(2):245-59. doi: 10.1271/bbb.80479. PubMed PMID: 19202299.

43. Kornfeld R. Studies on L-glutamine D-fructose 6-phosphate amidotransferase. I. Feedback inhibition by uridine diphosphate-N-acetylglucosamine. J Biol Chem. 1967;242(13):3135-41. PubMed PMID: 4961641.

44. Assrir N, Richez C, Durand P, Guittet E, Badet B, Lescop E, *et al*. Mapping the UDP-N-acetylglucosamine regulatory site of human glucosamine-6P synthase by saturation-transfer difference NMR and site-directed mutagenesis. Biochimie. 2014;97:39-48. doi: 10.1016/j.biochi.2013.09.011. PubMed PMID: 24075873.

45. Ferre-D'Amare AR. The *glmS* ribozyme: use of a small molecule coenzyme by a gene-regulatory RNA. Q Rev Biophys. 2010;43(4):423-47. doi: 10.1017/S0033583510000144. PubMed PMID: 20822574; PubMed Central PMCID: PMCPMC3409577.

46. Gopel Y, Khan MA, Gorke B. Menage a trois: post-transcriptional control of the key enzyme for cell envelope synthesis by a base-pairing small RNA, an RNase adaptor protein, and a small RNA mimic. RNA Biol. 2014;11(5):433-42. doi: 10.4161/rna.28301. PubMed PMID: 24667238; PubMed Central PMCID: PMCPMC4152352.

47. Kawada-Matsuo M, Oogai Y, Komatsuzawa H. Sugar Allocation to Metabolic Pathways is Tightly Regulated and Affects the Virulence of *Streptococcus mutans*. Genes (Basel). 2016;8(1). doi: 10.3390/genes8010011. PubMed PMID: 28036052; PubMed Central PMCID: PMCPMC5295006.

48. Opheim D, Bernlohr RW. Purification and Regulation of Glucose-6-Phosphate Dehydrogenase from *Bacillus licheniformis*. Journal of Bacteriology. 1973;116(3):1150-9.

49. Ludwig H, Homuth G, Schmalisch M, Dyka FM, Hecker M, Stülke J. Transcription of glycolytic genes and operons in *Bacillus subtilis*: evidence for the presence of multiple levels of control of the *gapA* operon. Molecular Microbiology. 2001;41(2):409-22. doi: 10.1046/j.1365-2958.2001.02523.x.

50. Commichau FM, Dickmanns A, Gundlach J, Ficner R, Stülke J. A jack of all trades: the multiple roles of the unique essential second messenger cyclic di-AMP. Molecular Microbiology. 2015;97(2):189-204. doi: 10.1111/mmi.13026.

51. Corrigan RM, Campeotto I, Jeganathan T, Roelofs KG, Lee VT, Gründling A. Systematic identification of conserved bacterial c-di-AMP receptor proteins. Proceedings of the National Academy of Sciences. 2013;110(22):9084-9. doi: 10.1073/pnas.1300595110.

52. Nelson JW, Sudarsan N, Furukawa K, Weinberg Z, Wang JX, Breaker RR. Riboswitches in eubacteria sense the second messenger c-di-AMP. Nature Chemical Biology. 2013;9:834. doi: 10.1038/nchembio.1363.

53. Gundlach J, Herzberg C, Kaever V, Gunka K, Hoffmann T, Weiß M, *et al*. Control of potassium homeostasis is an essential function of the second messenger cyclic di-AMP in *Bacillus subtilis*. Science Signaling. 2017;10(475). doi: 10.1126/scisignal.aal3011.

54. Commichau FM, Gibhardt J, Halbedel S, Gundlach J, Stülke J. A Delicate Connection: c-di-AMP Affects Cell Integrity by Controlling Osmolyte Transport. Trends in Microbiology. 26(3):175-85. doi: 10.1016/j.tim.2017.09.003.

55. Kawai Y, Mercier R, Wu Ling J, Domínguez-Cuevas P, Oshima T, Errington J. Cell Growth of Wall-Free L-Form Bacteria Is Limited by Oxidative Damage. Current Biology. 2015;25(12):1613-8. doi: https://doi.org/10.1016/j.cub.2015.04.031.

56. Luciano J, Foulquier E, Fantino J-R, Galinier A, Pompeo F. Characterization of YvcJ, a Conserved P-Loop-Containing Protein, and Its Implication in Competence in *Bacillus subtilis*. Journal of Bacteriology. 2009;191(5):1556-64. doi: 10.1128/jb.01493-08.

57. Pompeo F, Luciano J, Brochier-Armanet C, Galinier A. The GTPase Function of YvcJ and Its Subcellular Relocalization Are Dependent on Growth Conditions in *Bacillus subtilis.* Journal of Molecular Microbiology and Biotechnology. 2011;20(3):156-67.

58. Kalamorz F, Reichenbach B, März W, Rak B, Görke B. Feedback control of glucosamine-6-phosphate synthase GlmS expression depends on the small RNA GlmZ and involves the novel protein YhbJ in *Escherichia coli*. Molecular Microbiology. 2007;65(6):1518-33. doi: 10.1111/j.1365-2958.2007.05888.x.

59. Gopel Y, Papenfort K, Reichenbach B, Vogel J, Gorke B. Targeted decay of a regulatory small RNA by an adaptor protein for RNase E and counteraction by an anti-adaptor RNA. Genes Dev. 2013;27(5):552-64. doi: 10.1101/gad.210112.112. PubMed PMID: 23475961; PubMed Central PMCID: PMCPMC3605468.

60. Karimova G, Pidoux J, Ullmann A, Ladant D. A bacterial two-hybrid system based on a reconstituted signal transduction pathway. Proceedings of the National Academy of Sciences. 1998;95(10):5752-6.

61. Cohen SN, Chang ACY, Hsu L. Nonchromosomal Antibiotic Resistance in Bacteria: Genetic Transformation of Escherichia coli by R-Factor DNA. Proceedings of the National

Academy of Sciences of the United States of America. 1972;69(8):2110-4. PubMed PMID: PMC426879.

62. Quisel JD, Burkholder WF, Grossman AD. In Vivo Effects of Sporulation Kinases on Mutant Spo0A Proteins in *Bacillus subtilis*. Journal of Bacteriology. 2001;183(22):6573-8. doi: 10.1128/jb.183.22.6573-6578.2001.

63. Koo B-M, Kritikos G, Farelli JD, Todor H, Tong K, Kimsey H, *et al*. Construction and Analysis of Two Genome-Scale Deletion Libraries for *Bacillus subtilis*. Cell Systems. 2017;4(3):291-305.e7. doi: https://doi.org/10.1016/j.cels.2016.12.013.

64. Vagner V, Dervyn E, Ehrlich SD. A vector for systematic gene inactivation in *Bacillus subtilis*. Microbiology. 1998;144(11):3097-104. doi: doi:10.1099/00221287-144-11-3097.

65. Le Breton Y, Mohapatra NP, Haldenwang WG. In Vivo Random Mutagenesis of *Bacillus subtilis* by Use of TnYLB-1, a mariner-Based Transposon. Applied and Environmental Microbiology. 2006;72(1):327-33. doi: 10.1128/aem.72.1.327-333.2006.

66. Gerth U, Kock H, Kusters I, Michalik S, Switzer RL, Hecker M. Clp-Dependent Proteolysis Down-Regulates Central Metabolic Pathways in Glucose-Starved *Bacillus subtilis*. Journal of Bacteriology. 2008;190(1):321-31. doi: 10.1128/jb.01233-07.

67. Altenbuchner J. Editing of the *Bacillus subtilis* Genome by the CRISPR-Cas9 System. Applied and Environmental Microbiology. 2016;82(17):5421-7. doi: 10.1128/aem.01453-16.

68. Zadeh JN, Steenberg CD, Bois JS, Wolfe BR, Pierce MB, Khan AR, *et al*. NUPACK: Analysis and design of nucleic acid systems. Journal of Computational Chemistry. 2011;32(1):170-3. doi: 10.1002/jcc.21596.

Chapter 3

Phosphoglucomutase PgcA plays an essential role in peptidoglycan biosynthesis in Δ*glmR* mutant in *Bacillus subtilis*

3.1 Abstract

Phosphoglucomutase (PgcA) interconverts glucose 6-phosphate and glucose 1-phosphate by intramolecular transfer of the phosphoryl moiety. Glucose 1-phosphate is a precursor for UDP-glucose (UDP-Glc) biosynthesis. UDP-Glc serves as a glucosyl donor for phosphate containing anionic polymers known as teichoic acids in *Bacillus subtilis*. I discovered from a suppressor screen that a *pgcA*$_{G47S}$ allele of *pgcA* suppresses essentiality of *glmR* on gluconeogenic carbon source. In this study, I provide evidence that PgcA may have phosphoglucosamine mutase activity that can contribute to peptidoglycan biosynthesis pathway in *B. subtilis*. This moonlighting activity of PgcA is essential in *glmR* deletion mutant. PgcA can only be deleted from Δ*glmR* if the designated phosphoglucosamine mutase GlmM is overexpressed. Additionally, I show that *pgcA*$_{G47S}$ is a gain of function mutation and propose that PgcA$_{G47S}$ allele has increased phosphohexosamine mutase enzymatic activity.

3.2 Introduction

Bacillus subtilis is a gram-positive spore forming soil bacterium that has been used as a model organism to study various aspect of bacterial physiology. *B. subtilis* has a thick peptidoglycan (PG) polymer covering the cytoplasmic membrane to provide protection against internal turgor pressure and various extracellular stresses. PG comprises of long glycan chains with

alternating subunits of N-acetylglucosamine (GlcNAc) and N-acetylmuramic acid (MurNAc) that are crosslinked to adjacent glycan chains with short peptide chains. Another characteristic component of the gram-positive cell wall is anionic polymers called teichoic acids. The teichoic acids are either covalently attached to the PG layer (wall teichoic acid or WTA) or connected to the membrane via a lipid anchor (lipoteichoic acid or LTA). Bacterial cell wall synthesis and morphogenesis is strictly governed by nutrient availability.

I have previously shown that gluconeogenesis factor GlmR (previously known as YvcK) plays an essential role in diverting carbon from central carbon metabolism (CCM) to PG precursor biosynthesis [1]. A *glmR* deletion mutant is unable to grow on any gluconeogenic carbon source due to severe impairment in PG precursor biosynthesis, and this also results in increased sensitization of Δ*glmR* to various PG synthesis inhibiting antibiotics. Essentiality of *glmR* can be bypassed by exogenously added GlcNAc. Additionally, the mutations that overexpress enzymes catalyzing the first two steps of UDP-GlcNAc biosynthesis also bypass carbon source dependent *glmR* essentiality as characterized from a suppressor screen. GlmS (glucosamine 6-phosphate synthase) and GlmM (Phosphoglucosamine mutase) catalyze the first two steps of UDP-GlcNAc biosynthesis [2]. In the same forward genetic study, I also picked up $pgcA_{G47S}$ as one of the suppressors that rescues growth defect phenotype Δ*glmR* on gluconeogenic medium.

The phosphoglucomutase enzyme PgcA catalyzes the first step in UDP-glucose (UDP-Glc) biosynthesis, the conversion of glucose 6-phosphate (G6P) to glucose 1-phosphate (G1P). The second step in the pathway is catalyzed by GtaB (Fig 3.1). UDP-Glc is used for glucosylation of teichoic acids in *B. subtilis*. Enzyme UgtP carries out glucosylation of the lipoteichoic acid (LTA) anchor. A deletion mutant of *pgcA* displays aberrant morphology due to a lack of glucolipids [3]. The glucolipid metabolic pathway is also a determinant of nutrition based regulation of cell size

[4]. This pathway relays a signal of nutritional availability to cell division apparatus, where a downstream enzyme of the PgcA pathway, UgtP, antagonizes FtsZ ring assembly at the division plane when UDP-Glc levels are high in the cell [4].

In this study, I characterized the effect of *pgcA*$_{G47S}$ in a *glmR* deletion mutant. I show that PgcA$_{G47S}$ is a gain of function mutation and the functional gain is independent of the glucolipid biosynthesis pathway. These findings lead me to hypothesize that PgcA moonlights as phosphoglucosamine mutase enzyme in *B. subtilis* in addition to its designated function. PgcA thus, is also important for PG biosynthesis especially in a *glmR* deletion mutant.

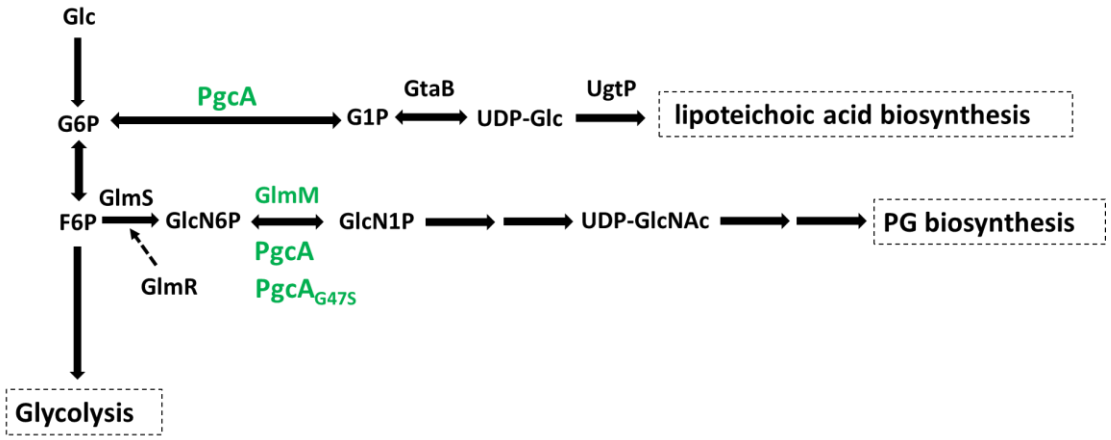

Fig 3.1: Schematic depicting a brief over view of glucolipid biosynthesis and PG biosynthesis pathway in *B. subtilis*. Phosphoglucomutase, PgcA and its mutant allele PgcA$_{G47S}$ and phosphoglucosamine mutase GlmM are shown in green letters. Activation of GlmS by GlmR is depicted by broken arrow.

Abbreviations: Glc=Glucose, G6P=glucose 6-phosphate, F6P=fructose 6-phosphate, G1P=glucose 1-phosphate, UDP-glc=UDP-glucose, GlcN6P=glucosamine 6-phosphate, GlcN1P=glucosamine 1-phosphate, UDP-GlcNAc=UDP-glucosamine 6-phosphate

3.3 Results

3.3.1 *glmR* and *pgcA* double deletion is synthetic lethal

To get insight into a role of GlmR in *B. subtilis*, I have previously carried out suppressor analysis. In my screen I discovered that a single amino acid change G47S in PgcA allowed a *glmR* deletion mutant to grow on gluconeogenic carbon sources. To find out if $pgcA_{G47S}$ behaves as null allele, I tried constructing Δ*glmR* Δ*pgcA* double mutant. Recipient Δ*glmR* and wild type (WT) strains were transformed by chromosomal DNA with *pgcA::mls* mutation. I got over 1500 colonies of *pgcA* mutants with the WT recipient, however I only got 1-10 colonies of candidate Δ*pgcA* Δ*glmR* cells (Fig 3.2, Table 3.1). PCR screening was carried out for the putative Δ*glmR* Δ*pgcA* transformants, and I found that they all had a WT copy of *glmR* crossed back into the strain, likely through genetic congression.

It is known that high magnesium as well as addition of glucose supports the growth of *glmR* deletion mutant [5]. Therefore, I tried constructing Δ*glmR* Δ*pgcA* with either high Mg^{+2} or 1% glucose in the medium. When high magnesium was added I did see some microcolonies, however they could not be sub-cultured. The few healthy-looking colonies obtained from the transformation plates had WT copy of *glmR* crossed back (Table 3.1). I was not able to construct Δ*glmR* Δ*pgcA* double mutant in all the growth conditions I tried. Therefore, to achieve a conditional Δ*glmR* Δ*pgcA* mutant, an IPTG-inducible copy of *pgcA* was introduced to ectopic locus in *glmR* deletion mutant and *pgcA* was deleted from this strain in presence of 1 mM IPTG.

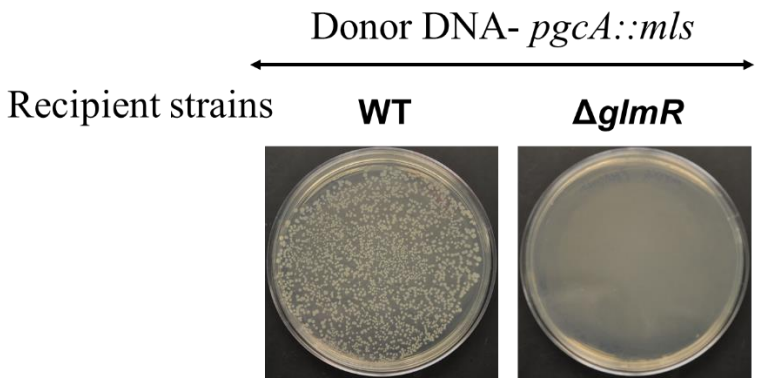

Fig 3.2: *glmR* and *pgcA* double deletion is synthetic lethal.
Recipient strains, WT and Δ*glmR* were transformed with *pgcA:mls* chromosomal DNA and the transformants were selected on LB plate with mls antibiotic and 20 mM $MgSO_4$. Pictures of the plate show transformation plates with overnight incubation at 37^0 C.

Table 3.1 *glmR* and *pgcA* double deletion is surmised to be synthetic lethal.

Growth condition	WT			Δ*glmR*		
	Replicate 1	Replicate 2	Replicate 3	Replicate 1	Replicate 2	Replicate 3
LB	>1200	>1330	>1500	2*	5*	8*
LB+1% Glucose	>1500	>1000	>1400	10*	3*	7*
LB+20 mM $MgSO_4$	>1000	>1500	>1200	9*	1*	5*

Note: Number of colony forming units (CFUs) obtained deletion attempt of *pgcA* from WT and Δ*glmR* mutant strains. Note that the numbers of transformants shown in Δ*glmR* columns had WT copy of *glmR* crossed backed and they only has *pgcA::mls* mutation. All the numbers with asterisks indicate that the WT copy for *glmR* was crossed back in the strain in this and all following tables.

3.3.2 *pgcA*$_{G47A}$ is a gain of function mutation

To characterize *pgcA*$_{G47S}$ allele, I introduced an IPTG-inducible copy of *pgcA* and *pgcA*$_{G47S}$ in a *glmR* deletion mutant. The resulting strain was tested for the growth on gluconeogenic Muller Hinton medium (MH) [1] and for CEF sensitivity (Fig 3.3A-3.3B). WT copy of *pgcA* when induced, fully suppresses growth defect of Δ*glmR* on gluconeogenic medium and reduces CEF

sensitivity. When PgcA$_{G47S}$ was overexpressed in Δ*glmR* completely suppresses the growth and CEF sensitivity phenotypes in Δ*glmR* (Fig 3.3A-3.3B). Even the low-level basal expression of PgcA$_{G47S}$ from the P$_{spac(hy)}$ promoter in the absence of the inducer completely restored the growth phenotype on MH medium and significantly reduced CEF susceptibility. These findings suggest that *pgcA*$_{G47S}$ is a dominant mutation. Overproduction of native PgcA suppresses Δ*glmR* associated phenotypes, but PgcA$_{G47S}$ suppresses even when not induced (low level expression) in the presence of native PgcA.

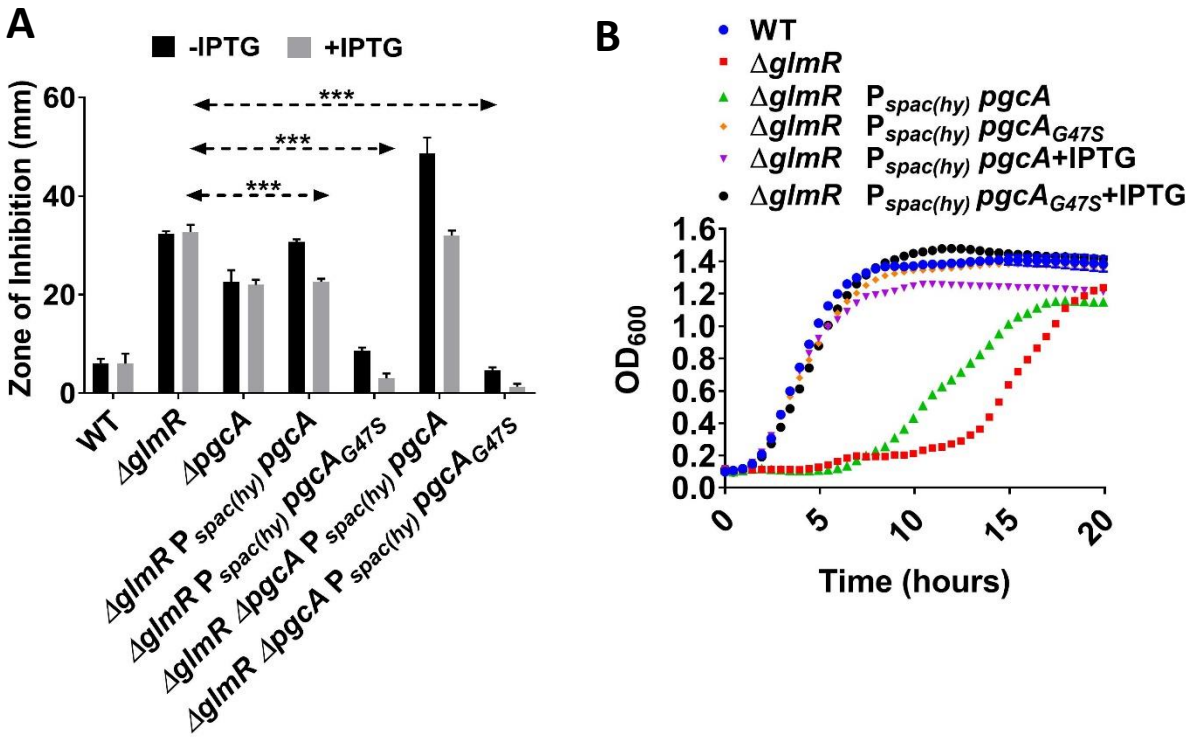

Fig 3.3: *pgcA*$_{G47A}$ is a gain of function mutation.

pgcA and *pgcA*$_{G47S}$ were ectopically expressed at *amyE* locus in Δ*glmR* and Δ*glmR* Δ*pgcA* and tested for **(A)** CEF sensitivity by disc diffusion assay and **(B)** representative growth curve on MH (N>3). 1 mM IPTG was added when required. 6 µg CEF was used for disc diffusion assay. Standard deviation (error bars) is based on at least three biological replicates. Three asterisks represent statistical significance with P <0.001 with Tukey test.

3.3.3 *pgcA*$_{G47S}$ suppresses *glmR* deletion mutation associated phenotypes independent of UDP-Glc biosynthesis pathway.

I first considered the possibility that PgcA$_{G47S}$ has higher catalytic activity that increases the flux of glucose-6-phosphate to UDP-glucose. This possibility was ruled out, however, by epistasis studies. The elevated CEF resistance and ability to grow on MH medium of the Δ*glmR* *pgcA*$_{G47S}$ cells is retained even in the absence of the subsequent enzyme in the UDP-glucose pathway, GtaB and a downstream glucosyltransferase enzyme UgtP (Fig 3.4A and 3.4B). Additionally, I was able to delete *gtaB* as well as *ugtP* in Δ*glmR*, whereas all attempts to generate Δ*glmR* Δ*pgcA* were unsuccessful and led to microcolonies that could not be further cultivated (Table 3.2). Taken together, these observations suggest that PgcA$_{G47S}$ suppresses *glmR* null mutant phenotype due to a function independent of the UDP-Glc biosynthesis pathway.

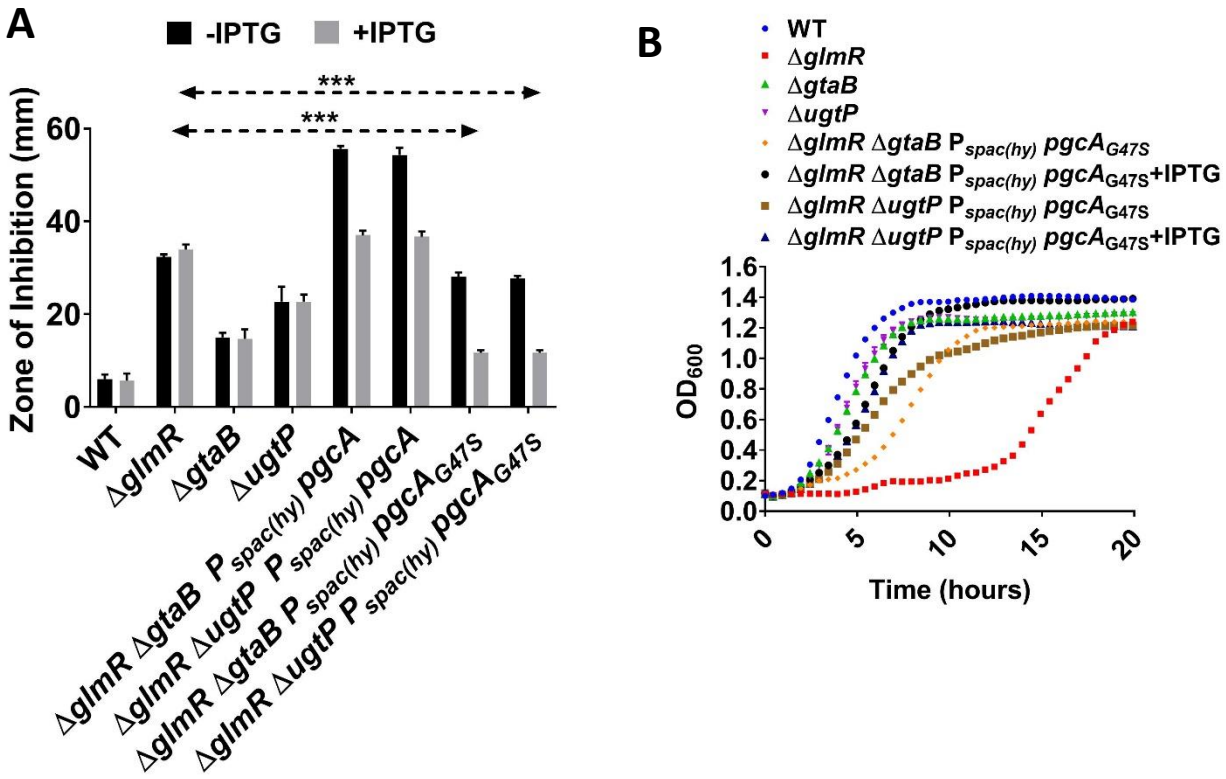

Fig 3.4: *pgcA*$_{G47S}$ suppresses *glmR* deletion mutation associated phenotypes independent of UDP-Glc biosynthesis pathway. (C) CEF susceptibility assay done with 6 µg antibiotic and **(D)** representative growth curve on MH medium.1mM IPTG was added when required. Standard deviation (error bars) is based on at least three biological replicates. Three asterisks represent statistical significance with P <0.001 with Tukey test.

Table 3.2: Δ*glmR* Δ*gtaB* and Δ*glmR* Δ*ugtP* double deletions are viable.

		Number of transformants		
Recipient	Donor DNA	Replicate 1	Replicate 2	Replicate 3
Δ*glmR*	*pgcA::mls*	9*	3*	2*
	gtaB::mls	>600	>800	>500
	ugtP::mls	>700	>900	>950

Note: Chromosomal DNA of *pgcA::mls*, *gtaB::mls* and *ugtP::mls* was transformed into recipient Δ*glmR* strain. Expected transformants genotypes were Δ*glmR pgcA::mls*, Δ*glmR gtaB::mls* and Δ*glmR ugtP::mls*.

3.3.4 PgcA has GlmM-like activity in *B. subtilis*

PgcA and GlmM are both enzymes from phosphohexose mutase family and have the same catalytic mechanism with different substrate specificity. However, there are examples of individual phosphohexose mutases acting on multiple, related substrates [6, 7]. Interestingly, G47S mutation of *pgcA* affects the putative glucose 6-phosphate binding site. I therefore hypothesized that PgcA may also function *in vivo* like GlmM, using glucosamine-6-phosphate to make glucosamine-1-phosphate. By this model, PgcA plays a role in PG synthesis, and the $PgcA_{G47S}$ variant may increase this activity and thereby increase the flux of carbon from CCM towards peptidoglycan. This idea is supported by the observation that *pgcA* and *glmR* are a synthetic lethal pair.

To further test this hypothesis, I tried deleting *pgcA* from a *glmR* deletion strain overexpressing *glmM*. Transformants were selected on LB medium containing 20 mM Mg^{2+} to support the growth of cells with compromised cell wall function. Healthy Δ*glmR* Δ*pgcA* *amyE*::$P_{spac(hy)}$ *glmM* transformants were only obtained at high frequency on plates containing 1mM IPTG, and therefore overexpressing GlmM protein. A few colonies that grew in absence of IPTG had a WT copy of *glmR* crossed back into the strain (Fig 3.5). I also tried deleting *pgcA* from *glmR* null mutant in a control experiment overexpressing either *glmS* or *glmU* without any success (Table 3.3).

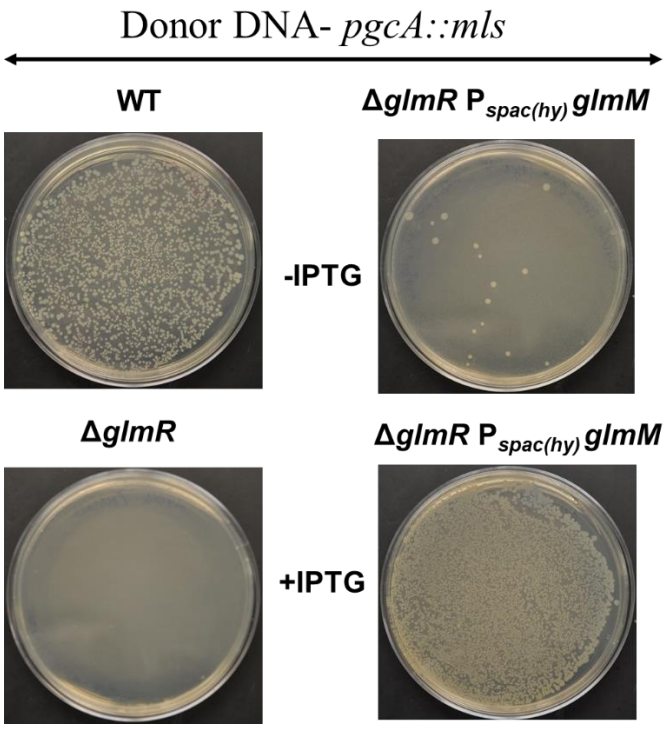

Fig 3.5: PgcA has GlmM-like activity *B. subtilis.* WT, Δ*glmR and* Δ*glmR* $P_{spac(hy)}$ *glmM* transformation carried out with *pgcA::mls* strain chromosomal DNA. Transformants were selected on LB agar containing mls antibiotic and 20 mM $MgSO_4$. 1mM IPTG was added to the medium when necessary.

Table 3.3 *pgcA* can be deleted from Δ*glmR* if GlmM is overexpressed

Recipient Strains	Replicate 1	Replicate 2	Replicate 3
Δ*glmR* $P_{sapc(hy)}$ *glmM*	>1000	>1400	>1500
Δ*glmR* $P_{sapc(hy)}$ *glmS*	5*	2*	7*
Δ*glmR* $P_{sapc(hy)}$ *glmU*	3*	4*	8*

Note: In an attempt to delete *pgcA*, transformation of above listed recipient strains was carried out with *pgcA::mls* DNA in presence of 1 mM IPTG.

3.4 Discussion and future directions

In this study I obtain genetic evidence suggesting that PgcA possesses GlmM like phosphoglucosamine mutase activity in addition to its designated phosphoglucomutase activity. GlmM is involved in UDP-GlcNAc biosynthesis, an essential precursor of bacterial cell-wall. My genetic analysis suggests that in *B. subtilis* PgcA plays role in glucolipid biosynthesis pathway as well as in PG biosynthesis pathway. All phosphohexomutase family enzymes catalyze a reversible intramolecular phosphoryl transfer reaction on the sugar substrate. Amino acid residues from their unique substrate binding site determines substrate specificity to carry out catalytically similar reaction. It is interesting that PgcA can also act on GlcN 6-P nonspecifically. This moonlighting function of PgcA is important for *B. subtilis* especially in the PG precursors deprived *glmR* null mutant as *pgcA* is essential in that strain background. This suggests that in *B. subtilis* GlmM as well as to some extent PgcA catalyze the second step of UDP-GlcNAc biosynthesis. In fact, there are examples of phosphohexomutase family enzyme promiscuity in different organisms as well. It has been noted previously that in *Escherichia coli* GlmM can interconvert glucose-phosphate isomers at low levels which can be enhanced 20-folds by a single mutation in a substrate binding site [7, 8]. Moreover, in *Trypanosoma brucei*, a dedicated phosphoglucomutase is absent and is substituted by the promiscuous activity of phosphomannose mutase and a phospho-N-acetylglucosamine mutase [6]. However, to my knowledge the ability of PgcA (or a mutant form of PgcA) to catalyze the GlmM reaction has not previously been suggested.

$PgcA_{G47S}$ has supposedly increased GlmM-like activity and that bypasses the requirement of Δ*glmR* on gluconeogenic carbon source. GlmM when over expressed also facilitates the growth of Δ*glmR* on gluconeogenic carbon source. I show that despite deleting any gene functioning

downstream of *pgcA* in glucolipid biosynthesis pathway (Table 2), Δ*glmR pgcA*$_{G47S}$ is still able to grow on gluconeogenic carbon source. I attempted to delete *glmM* from WT strain overexpressing PgcA$_{G47S}$ without success. This suggest that even with enhanced GlmM-like activity PgcA$_{G47S}$ is still not enough by itself to carry out catalysis for PG biosynthesis as well as glucolipid biosynthesis pathway. In an alternate explanation, GlmM can be a part of essential multiprotein complex designated to carry out PG biosynthesis. In PG biosynthesis pathway there are examples of early steps of PG biosynthesis communicating with later steps and protein-protein interactions for catalytic process [9]. Moreover, cytoplasmic protein GlmM localizes at the membrane using c-di-AMP synthase CdaA as an anchor protein [10]. It is possible that GlmM communicates with PG elongation machinery and plays a significant role in connecting PG polymerization with earlier steps of PG precursors biosynthesis. Therefore, deletion of GlmM may not be viable. It would be interesting to test, if catalytically inactive *glmM* can replace WT copy in *pgcA*$_{G47S}$ strain background.

In conclusion, my genetic analysis suggests that PgcA has GlmM like activity that can be enhanced by the G47S mutation in PgcA. Further investigation needs to be carried out to biochemically measure phosphoglucosamine mutase activity of PgcA and PgcA$_{G47S}$.

3.5 Material and Methods

3.5.1 Bacterial strains and growth conditions:

B. subtilis strains used are derived from strain 168 (*trpC2*). *E. coli* strain DH5α was used for cloning. Bacteria were cultured in LB broth. Strains with a *glmR* deletion mutation were cultured on LB with 20 mM $MgSO_4$ unless specified otherwise. Antibiotics were added to growth

media when required at the following concentrations: 100 µg/ml ampicillin, 30 µg/ml chloramphenicol for *E. coli*, 10 µg/ml kanamycin, 10 µg/ml chloramphenicol, 5 µg/ml tetracycline, 100 µg/ml spectinomycin and 1 µg/ml erythromycin with 25 µg/ml lincomycin (erm; macrolide-lincomycin-streptogramin B resistance).

3.5.2 Cloning, transformation and strain construction:

For cloning procedures, restriction digestion and T4 ligation was carried out as per NEB protocols. The *E. coli* DH5α strain was used for cloned vector transformation and amplification. Cloning was confirmed by polymerase chain reaction (PCR) followed by Sanger's sequencing. *B. subtilis* transformation was carried out in minimal competence media with 12 mM of $MgSO_4$. DNA was added when OD_{600} of competent strain reached 0.7-0.8. After one hour of incubation at 37^0 C, cells were plated on LB agar plate with the necessary antibiotic for selection. IPTG was added to final concentration of 1 mM in transformation medium and transformant selection plate when required. Vector pPL82 was used for all the gene overexpression constructs at *amyE* locus.

All *B. subtilis* bacillus knock out erythromycin (BKE) deletion mutants were obtained from Bacillus genomic stock center (BGSC). *Erm(mls)* cassette from these strains were removed using pDR244 [11] as described previously [1].

3.5.3 Antibiotic susceptibility assay

Antibiotic sensitivity was tested using disc diffusion assays, which were carried out on LB medium. Strains to be tested were grown in 5 ml LB broth at 37^0 C with vigorous shaking to an OD_{600} of ~0.4. 100 µl of cells were added to 4 ml top LB agar (0.7% agar) kept at 50^0 C. 1 mM IPTG was added to the top agar when indicated. Top agar with cells was poured over 15 ml LB

bottom agar (1.5%) plate. A Whatman paper disc (7mm diameter) with 6 µg CEF was put on the plate unless specified otherwise. Plates were incubated at 37^0 C overnight and the clear zone of inhibition was measured the next day.

3.5.4 Growth Assay on MH:

To test the ability of *B. subtilis* mutants to grow on gluconeogenic medium I used MH medium (Sigma-Aldrich, USA) prepared per the manufacturer's instruction. Growth was monitored using a bioscreen growth analyzer with 200 µl of MH broth in 100 well Bioscreen plates inoculated with 2 µl of *B. subtilis* strains pre-grown in LB broth at 37^0 C to an OD_{600} of ~0.4. When required, glucose, $MgSO_4$ and IPTG was added to the final concentrations of 1%, 20 mM and 1 mM respectively.

Table 3.4 *B. subtilis* strains used in this study.

Strain	Genotype	Source/ ref
168	*trpC2*	Lab stock
HB16820	*trpC2 pgcA::mls*	This work
HB16848	*trpC2 glmR*	This work
HB16910	*trpC2 glmR amyE*::$P_{spac(hy)}$-*glmM*	This work
HB16945	*trpC2 glmR amyE::*$P_{spac(hy)}$ *pgcA*	This work
HB16946	*trpC2 glmR amyE::*$P_{spac(hy)}$ $pgcA_{G47S}$	This work
HB16948	*trpC2 glmR pgcA::mls amyE::*$P_{spac(hy)}$ *pgcA*	This work
HB16849	*trpC2 glmR pgcA::mls amyE::*$P_{spac(hy)}$ $pgcA_{G47S}$	This work
HB21922	*trpC2 glmR amyE*::$P_{spac(hy)}$-*glmU*	This work
HB21942	*trpC glmR amyE*::$P_{spac(hy)}$-*glmS*	This work
HB21981	*trpC2 glmR gtaB::mls amyE::*$P_{spac(hy)}$ *pgcA*	This work
HB21982	*trpC2 glmR ugtP::mls amyE::*$P_{spac(hy)}$ *pgcA*	This work
HB21983	*trpC2 glmR gtaB::mls amyE::*$P_{spac(hy)}$ $pgcA_{G47S}$	This work
HB21984	*trpC2 glmR ugtP::mls amyE::*$P_{spac(hy)}$ $pgcA_{G47S}$	This work

3.6 REFERENCES

1. Patel V, Wu Q, Chandrangsu P, Helmann JD. A metabolic checkpoint protein GlmR is important for diverting carbon into peptidoglycan biosynthesis in *Bacillus subtilis*. PLOS Genetics. 2018;14(9):e1007689. doi: 10.1371/journal.pgen.1007689.
2. Barreteau H, Kovač A, Boniface A, Sova M, Gobec S, Blanot D. Cytoplasmic steps of peptidoglycan biosynthesis. FEMS Microbiology Reviews. 2008;32(2):168-207. doi: 10.1111/j.1574-6976.2008.00104.x.
3. Matsuoka S, Seki T, Matsumoto K, Hara H. Suppression of abnormal morphology and extracytoplasmic function sigma activity in Bacillus subtilis ugtP mutant cells by expression of heterologous glucolipid synthases from *Acholeplasma laidlawii*. Bioscience, Biotechnology, and Biochemistry. 2016;80(12):2325-33. doi: 10.1080/09168451.2016.1217147.
4. Weart RB, Lee AH, Chien A-C, Haeusser DP, Hill NS, Levin PA. A Metabolic Sensor Governing Cell Size in Bacteria. Cell. 2007;130(2):335-47. doi: 10.1016/j.cell.2007.05.043.
5. Görke B, Foulquier E, Galinier A. YvcK of *Bacillus subtilis* is required for a normal cell shape and for growth on Krebs cycle intermediates and substrates of the pentose phosphate pathway. Microbiology. 2005;151(11):3777-91. doi: doi:10.1099/mic.0.28172-0.
6. Bandini G, Mariño K, Güther MLS, Wernimont AK, Kuettel S, Qiu W, *et al*. Phosphoglucomutase is absent in *Trypanosoma brucei* and redundantly substituted by phosphomannomutase and phospho-N-acetylglucosamine mutase. Molecular microbiology. 2012;85(3):513-34. doi: 10.1111/j.1365-2958.2012.08124.x. PubMed PMID: 22676716.

7. Jolly L, Ferrari P, Blanot D, van Heijenoort J, Fassy F, Mengin-Lecreulx D. Reaction mechanism of phosphoglucosamine mutase from *Escherichia coli*. European Journal of Biochemistry. 1999;262(1):202-10. doi: doi:10.1046/j.1432-1327.1999.00373.x.

8. Mengin-Lecreulx D, van Heijenoort J. Characterization of the Essential Gene glmM Encoding Phosphoglucosamine Mutase in *Escherichia coli*. Journal of Biological Chemistry. 1996;271(1):32-9. doi: 10.1074/jbc.271.1.32.

9. Mohammadi T, Karczmarek A, Crouvoisier M, Bouhss A, Mengin-Lecreulx D, den Blaauwen T. The essential peptidoglycan glycosyltransferase MurG forms a complex with proteins involved in lateral envelope growth as well as with proteins involved in cell division in *Escherichia coli*. Molecular Microbiology. 2007;65(4):1106-21. doi: 10.1111/j.1365-2958.2007.05851.x. PubMed PMID: PMC2170320.

10. Gundlach J, Mehne FMP, Herzberg C, Kampf J, Valerius O, Kaever V, *et al*. An Essential Poison: Synthesis and Degradation of Cyclic Di-AMP in *Bacillus subtilis*. Journal of Bacteriology. 2015;197(20):3265-74. doi: 10.1128/jb.00564-15.

11. Koo B-M, Kritikos G, Farelli JD, Todor H, Tong K, Kimsey H, *et al*. Construction and Analysis of Two Genome-Scale Deletion Libraries for *Bacillus subtilis*. Cell Systems. 2017;4(3):291-305.e7. doi: 10.1016/j.cels.2016.12.013.

Chapter 4

Over expression of multidrug efflux pump (MdtP) restores cefuroxime sensitivity of c-di-AMP double hydrolase mutant in *Bacillus subtilis*

4.1 Abstract

The signaling nucleotide cyclic diadenosine monophosphate (c-di-AMP) is present in a wide variety of bacteria. This essential molecule is important for controlling many cellular activities including cell wall homeostasis. Previous studies shown have that moderately high concentration of c-di-AMP confer resistance to beta-lactam antibiotics in *Bacillus subtilis* as well as in other organisms. In this study I show that a *B. subtilis* strain lacking both c-di-AMP phosphodiesterases (Δ*gdpP* Δ*pgpH*) is very sensitive to beta-lactam antibiotic cefuroxime due to accumulation of high c-di-AMP. To understand why high c-di-AMP is toxic I carried out a mariner transposon mutagenesis to obtain cefuroxime resistant suppressors of Δ*gdpP* Δ*pgpH*. I found frequent mutations in a gene encoding a transcription repressor of the multidrug resistant *mdtR-mdtP* operon, *mdtR* and the major autolysin for lateral peptidoglycan biosynthesis *cwlO*. In this study I show that the increased expression of the multidrug efflux transporter MdtP, either by deletion of the repressor *mdtR* or by ectopic overexpression, can relieve cefuroxime sensitivity of Δ*gdpP* Δ*pgpH.* This is likely caused by excreting excess c-di-AMP. Additionally, I observed that c-di-AMP accumulation does not induce *mdtP* expression. There is evidence of c-di-AMP being exported outside of the cell by multidrug efflux pumps in the model organisms *B. subtilis* and

Listeria monocytogenes. In this study I show that MdtP is a putative transporter of c-di-AMP in *B. subtilis*.

4.2 Introduction

Organisms sense changes in environment and respond accordingly through signal transduction pathways. In many organisms, various nucleotides serve as secondary messengers that relay cues from the environment to modulate appropriate cellular pathways. C-di-AMP is a signaling molecule found mostly in gram-positive bacteria. C-di-AMP is the only known signaling molecule that is essential in all organisms in which it is found [1]. Recent studies have shown that c-di-AMP is essential in standard complex growth medium used in the lab, however it is dispensable in defined medium [2]. Studies have shown that c-di-AMP plays an important role in cell-wall homeostasis, potassium homeostasis, DNA repair, central carbon metabolism, biofilm formation and virulence in various model organism [3]. C-di-AMP transduces signal by first binding to the receptor molecules to subsequently regulate the downstream process. While c-di-AMP binds to specific protein receptor to regulate the pathways in bacteria, in *B. subtilis* c-di-AMP also binds to the riboswitch to regulate potassium homeostasis [3].

C-di-AMP is synthesized from two molecules of ATPs by specialized enzymes called deadenylate cyclases (DAC) and degraded by phosphodiesterases (PDE). In *B. subtilis* there are three DACs and two known PDEs. DAC enzyme CdaA is a major cyclase in a vegetative cell and important for cell-wall homeostasis. CdaA is a membrane associated protein that is broadly conserved across other phyla [4]. DisA (DNA integrity scanning protein) is a DNA binding check point protein that scans chromosome for the chromosomal damage before a cell commits to

sporulation [5]. The third DAC enzyme CdaS is expressed exclusively during sporulation and is required for spore germination [6]. PDE enzymes GdpP and PgpH possess DHH/DHH1 and HD catalytic domains, respectively. These enzymes break down c-di-AMP in to the linear molecule 5'-pApA [7, 8]. Both GdpP and PgpH are membrane proteins and their catalytic activity is allosterically inhibited by another signaling molecule ppGpp as measured by *in vitro* analysis [7, 8].

Studies have shown that a moderate increase in c-di-AMP concentration can be conditionally beneficial. Moderately high c-di-AMP levels ameliorates susceptibility to antibiotics that inhibit cell-wall biosynthesis [9,10]. In *B. subtilis* elevated c-di-AMP concentrations confer resistance to the beta-lactam antibiotic cefuroxime (CEF) in the otherwise very susceptible *sigM* deletion mutant strain [9]. *sigM* encodes an extra cytoplasmic function (ECF) sigma factor σ^M which is important for resistance against various cell wall acting compounds including CEF [11]. Although moderate increase in c-di-AMP can be advantageous, very high concentration of c-di-AMP in double PDE Δ*gdpP* Δ*pgpH* mutant is toxic [4]. In *B. subtilis* toxic accumulation of c-di-AMP leads to severe morphological defects and early cell lysis. This suggest that c-di-AMP levels need to be maintained at appropriate levels by coordinated DAC and PDE enzyme activities. Either too much or too little c-di-AMP is detrimental to the bacterium.

I show in this study that Δ*gdpP* Δ*pgpH* mutant is highly susceptible to CEF. To understand why high c-di-AMP confers CEF susceptibility, I carried out mariner transposon mutagenesis. Transposon insertions were mapped in genes for the major peptidoglycan (PG) biosynthesis autolysin *cwlO*, the multi drug efflux pump repressor (*mdtR*) and the DAC enzyme *cdaA*. I showed that deletion of L, D-endopeptidases *cwlO* or *lytE* significantly reduces CEF susceptibility in

double PDE mutant strains. My genetic analysis suggests that a mutation in *mdtR* causes de-repression of the multidrug efflux transporter MdtP and overexpression of MdtP likely secretes c-di-AMP outside of the cell. Efflux of excess of c-di-AMP restores CEF resistance in the Δ*gdpP* Δ*pgpH* mutant. I also note that accumulation of c-di-AMP does not induce *mdtP* expression. Although constitutive expression of *mdtP* does seems to transport some c-di-AMP out of the cell, either ectopic overproduction or de-repression of *mdtP* in Δ*mdtR* exhibit notable reduction in CEF sensitivity in the Δ*gdpP* Δ*pgpH* mutant.

4.3 Results

4.3.1 C-di-AMP double PDE (Δ*gdpP* Δ*pgpH*) mutant is highly susceptible to beta-lactam antibiotic cefuroxime (CEF)

In *B. subtilis* the Δ*sigM* deletion mutant is very sensitive to the beta-lactam antibiotic CEF and this sensitivity can be ameliorated by disruption of the c-di-AMP hydrolase *gdpP* [9]. This observation suggested that increased concentration of c-di-AMP reduces CEF sensitivity. In this study, I show that deletion of the second PDE enzyme *pgpH* did not decrease CEF sensitivity of *sigM* (Figure 4.1A). This suggests that GdpP is a primary c-di-AMP hydrolase important for CEF resistance in *B. subtilis* in the experimental condition used in this study. When both PDE enzymes coding genes *gdpP* and *pgpH* were deleted in either the *sigM* or WT background, both strains became significantly more sensitive CEF, likely due to accumulation of excess c-di-AMP (Figure 4.1A).

Increased susceptibility to beta-lactam antibiotic indicates impairment of the cell wall metabolism. Many phenotypes due to mutation in cell wall biosynthesis genes can be suppressed by high concentration of Mg^{+2} in the medium [12-14]. A previous study has suggested that high Mg^{+2} helps keep the balance between PG biosynthesis and degradation when the balance is shifted towards increased PG degradation [15]. Therefore, I tested if CEF sensitivity of Δ*gdpP* Δ*pgpH* double deletion mutant can be suppressed by 10 mM or 20 mM of $MgSO_4$. No change in CEF sensitivity of Δ*gdpP* Δ*pgpH* was observed when high Mg^{+2} was added to the medium (Figure 4.1B).

Deletion mutants Δ*gdpP* Δ*pgpH* and Δ*sigM* Δ*gdpP* Δ*pgpH* can be complemented by an IPTG inducible ectopic copy of *pgpH* (Figure 4.1C). Leaky expression from the uninduced copy of *pgpH* is sufficient to reduce CEF susceptibility of the Δ*gdpP* Δ*pgpH* double mutant. Interestingly, in a Δ*sigM* Δ*gdpP* Δ*pgpH* strain, even the uninduced copy of *pgpH* reduces CEF sensitivity significantly; however, addition, of 1mM IPTG increases CEF susceptibility relative to the uninduced counterpart (Figure. 4.1C). This evidence reiterates that c-di-AMP is beneficial only at the appropriate concentration.

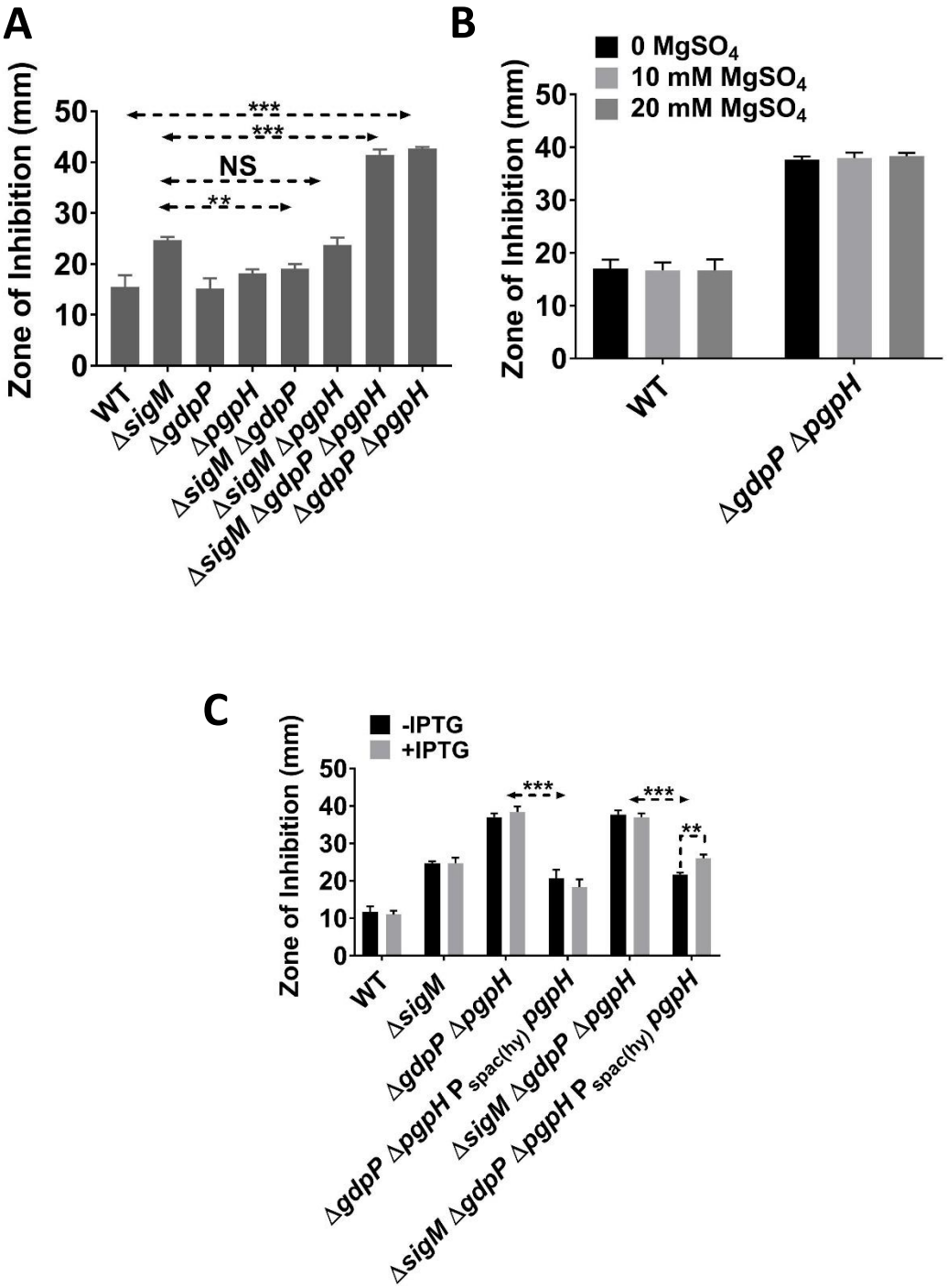
A
Zone of Inhibition (mm)
50
40
30
20
10
0
***
***
NS
**
WT
ΔsigM
ΔgdpP
ΔpgpH
ΔsigM ΔgdpP
ΔsigM ΔpgpH
ΔgdpP ΔpgpH
ΔsigM ΔgdpP ΔpgpH
B
0 MgSO4
10 mM MgSO4
20 mM MgSO4
Zone of Inhibition (mm)
WT
ΔgdpP ΔpgpH
C
-IPTG
+IPTG
Zone of Inhibition (mm)
***
***
**
WT
ΔsigM
ΔgdpP ΔpgpH
ΔgdpP ΔpgpH Pspac(hy) pgpH
ΔsigM ΔgdpP ΔpgpH
ΔsigM ΔgdpP ΔpgpH Pspac(hy) pgpH

Figure 4.1: C-di-AMP double PDE (Δ*gdpP* Δ*pgpH*) mutant is highly susceptible to beta-lactam antibiotic Cefuroxime (CEF)

(A) CEF susceptibility of designated strains was tested in the disc diffusion assay using 6 µg of CEF containing disc. Bars represent diameter of clear zone surrounding the disc. Standard deviation (error bars) are based on at least three biological replicates in all bar graphs. NS represents non-significant (P >0.05) and three asterisks indicate significant difference with P<0.001 estimated using Tukey test. (B) Disc diffusion assay done with 6 µg of CEF. In the 4 ml top agar $MgSO_4$ was added to 10 mM or 20 mM final concentration. (C) *pgpH* complementation study done with disc diffusion assay. IPTG was added to top agar to final concentration of 1 mM. Three asterisks indicate significant difference with P<0.001 estimated using Sidak's multiple comparison test.

4.3.2 High CEF susceptibility of Δ*gdpP* Δ*pgpH* can be suppressed by inactivation of *mdtR*, *cwlO* or *cdaA*.

To understand why c-di-AMP accumulation leads to high CEF sensitivity, I carried out mariner transposon mutagenesis in a Δ*gdpP* Δ*pgpH* strain. Two independent experiments were carried out in the presence of CEF as selection. In both the screens, transposon insertions in *mdtR*, encoding the repressor MdtR for the *mdtR-mdtP* operon, and in *cwlO*, encoding the primary autolysin for PG elongation, were recovered. In addition, transposon insertions in the major DAC gene *cdaA* and unknown function gene *yesJ* were recovered once (Table 4.1). Strain reconstruction showed that deletion of *yesJ* in Δ*gdpP* Δ*pgpH* conferred resistance to CEF, therefore I ruled this insertion out as a false positive.

Table 4.1 Mariner transposon mutagenesis suppressors

Gene affected	Function	Frequency
mdtR	Transcription repressor of multi drug efflux pump *mdtP*	2
cwlO	Major autolysin	2
cdaA	Diadenylate cyclase	1
yesJ	Unknown	1

The major vegetative DAC enzyme CdaA is important for the cell wall homeostasis [9]. *cdaA* is a part of a four gene operon that also includes *cdaR*, *glmM* and *glmS*. CdaA localizes at the cell membrane with regulatory protein CdaR and the essential enzyme phosphoglucosamine mutase GlmM, which catalyzes one of the earlier steps in PG biosynthesis [16]. It has been suggested that CdaR and GlmM both modulate CdaA enzymatic activity; however, how this might occur is not known [4, 17]. GlmS catalyzes the first and the rate limiting step in PG precursor biosynthesis by converting the central carbon metabolite fructose 6-phosphate into glucosamine 6-phosphate [18]. Since CdaA and GlmM physically interact, and their genes are part of the same operon with *glmS*, this suggests that c-di-AMP may affect PG homeostasis by somehow affecting GlmM or GlmS activity. Here I show that CEF susceptibility of Δ*gdpP* Δ*pgpH* is suppressed by inactivation of *cdaA* (Figure 4.2A). Whereas deletion of second vegetative DAC enzyme encoding gene *disA* does not have a significant effect (Figure 4.2A). This observation reiterates that CdaA is the primary DAC for PG homeostasis.

A mariner insertion in *cwlO*, encoding a D, L-endopeptidase, significantly reduced the Δ*gdpP* Δ*pgpH* CEF susceptibility. I constructed Δ*cwlO* Δ*gdpP* Δ*pgpH* strain and tested for CEF sensitivity to confirm the mariner mutagenesis result (Figure 4.2B). *B. subtilis* has two D, L-endopeptidases; CwlO and LytE. Their activity is essential for PG biosynthesis during the cell elongation. I also tested effect the *lytE* deletion in Δ*gdpP* Δ*pgpH* for CEF sensitivity. I observe that deletion of either one of the major autolysins can significantly reduce CEF susceptibility of the double PDE mutant strain indicating skewed balance of PG synthesis to the PG lysis.

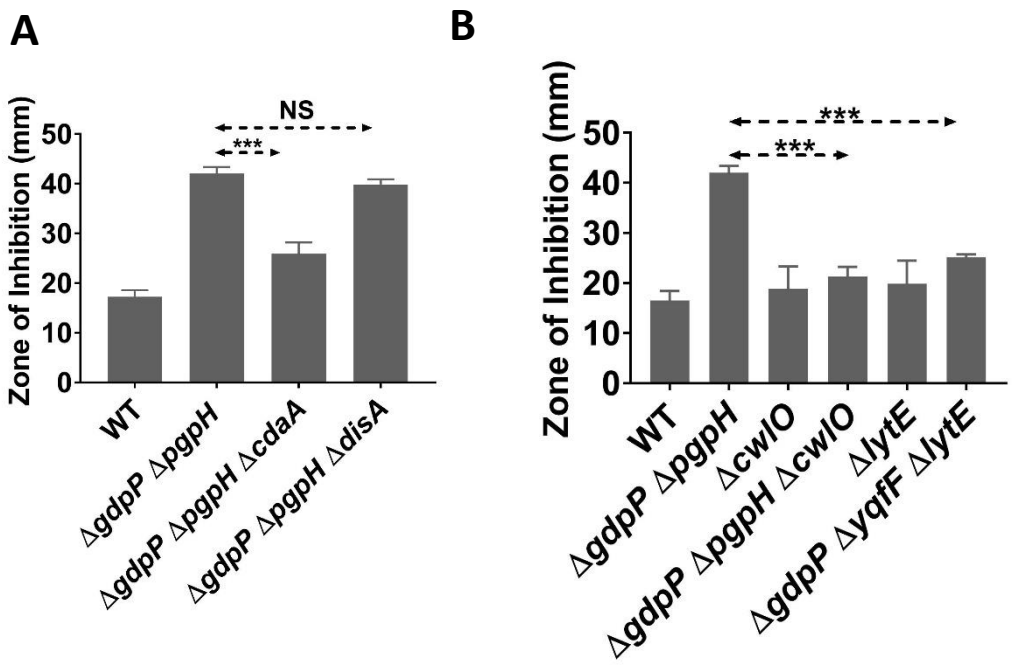

Figure 4.2: High CEF susceptibility of Δ*gdpP* Δ*pgpH* can be suppressed by inactivation of *cwlO* and *cdaA*. (A) and (B) show disc diffusion assay bar graph of CEF sensitivity. 6 µg of CEF was used in this assay. NS represent non-significant with P value less than 0.05. Three asterisks indicate significant difference with P<0.001 estimated using Tukey test.

4.3.3 Increased expression of the multidrug efflux transporter MdtP reduces CEF susceptibility of Δ*gdpP* Δ*pgpH* possibly by excreting excess of c-di-AMP

The two gene operon *mdtR-mdtP* is regulated by the transcription repressor MdtR [19]. MdtP confers low level resistance to antibiotics such as fusidic acid, novobiocin, streptomycin and actinomycin D [19]. A markerless clean deletion of *mdtR* in the double PDE mutant strain (Δ*gdpP* Δ*pgpH*) suppressed the CEF sensitivity, confirming my observation from the mariner transposon mutagenesis studies (Table 4.1, Figure 4.3A). An ectopic copy of *mdtP* at the *thrC* locus, expressed by its native promoter complements the *mdtR* deletion in Δ*gdpP* Δ*pgpH.* The resulting strain is now as sensitive to CEF sensitive as Δ*gdpP* Δ*pgpH* (Figure 4.3A). Deletion of *mdtP* in Δ*mdtR*

Δ*gdpP* Δ*pgpH* returns the sensitivity back to Δ*gdpP* Δ*pgpH* levels, suggesting that the *mdtP* over expression leads to suppression of CEF sensitivity in the Δ*gdpP* Δ*pgpH* strain in the absence of the transcription repressor MdtR (Figure 4.3A). I also observed that when *mdtP* was deleted from Δ*gdpP* Δ*pgpH,* the resulting strain was sicker and had an early cell lysis phenotype (data not shown). I then overexpressed *mdtP* ectopically under the IPTG inducible promoter in WT and the Δ*gdpP* Δ*pgpH* double mutant. WT becomes slightly more sensitive upon IPTG inducible *mdtP* overexpression. In Δ*gdpP* Δ*pgpH,* overexpression of *mdtP* significantly reduced CEF sensitivity. Even leaky expression from uninduced copy is enough to restore CEF resistance of Δ*gdpP* Δ*pgpH* to almost WT levels (Figure 4.3B).

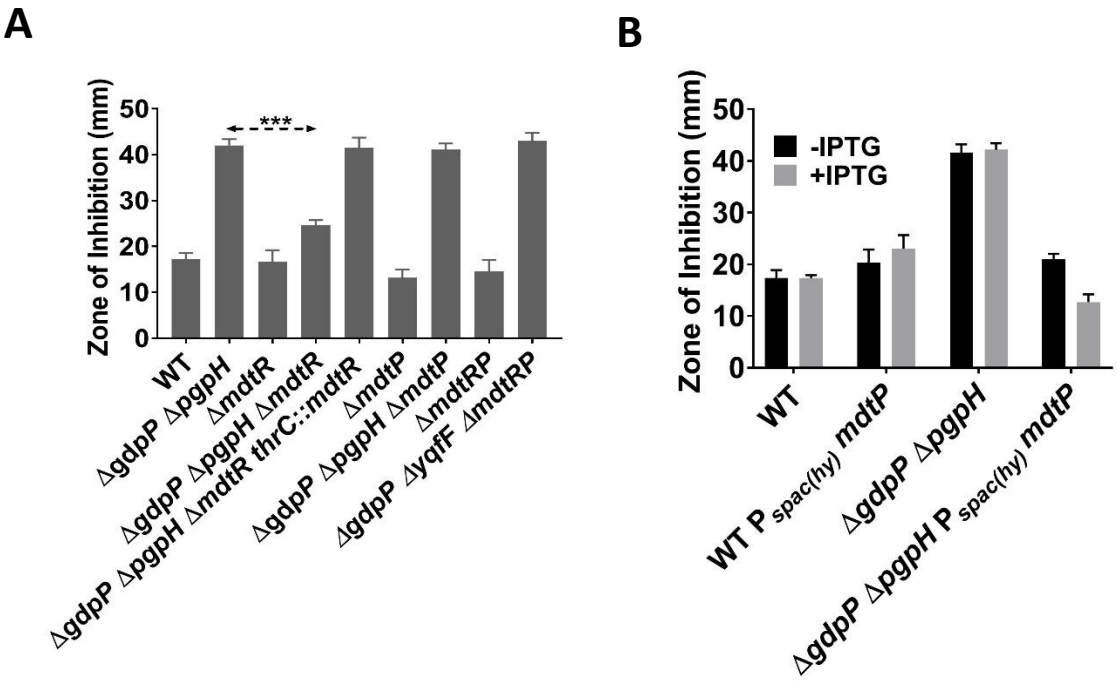

Figure 4.3: Increased expression of the multidrug efflux transporter MdtP reduces CEF susceptibility of Δ*gdpP* Δ*pgpH*, possibly by excreting excess of c-di-AMP

(A) and (B) Disc diffusion assay done with 6 µg CEF. IPTG was added to 1mM final concentration when needed. Statistical analysis was carried out by Tukey's test and three asterisks represent P<0.001.

I did not see differences in the zone of inhibition between Δ*gdpP* Δ*pgpH* and Δ*mdtRP* Δ*gdpP* Δ*pgpH*, although the latter strain is relatively sick. I carried out a growth curve study to see if there is a difference in CEF sensitivity between these two strains. Indeed, I observed that the Δ*gdpP* Δ*pgpH* Δ*mdtRP* strain is more sensitive to CEF that Δ*gdpP* Δ*pgpH* (Figure 4.4B,4.4D). This observation indicates that basal expression of MdtP protects cells against the deleterious effects of elevated c-di-AMP, likely by exporting CEF out of the cells.

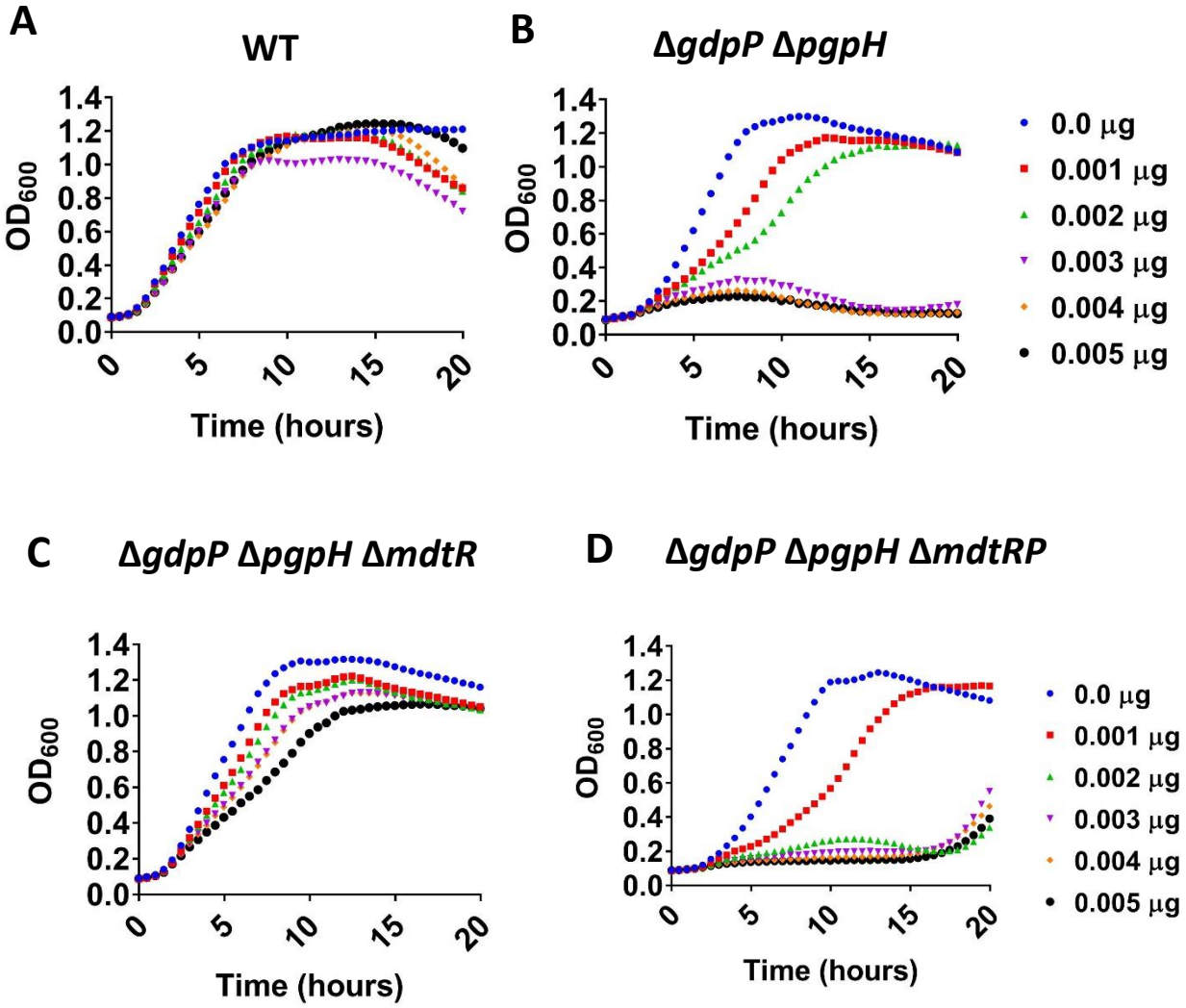

Figure 4.4: Growth curve analysis of WT, Δ*gdpP* Δ*pgpH*, Δ*gdpP* Δ*pgpH* Δ*mdtR* and Δ*gdpP* Δ*pgpH* Δ*mdtRP*. (A-D) CEF sensitivity testing was carried out by growth curve study in a bio screen analyzer. This is a representative growth curve of at least three biological replicates. CEF concentrations indicated in the figure are per 200 µl of MH medium in a 100 well plate.

4.3.4 *mdtP* is not induced when c-di-AMP levels are high in the cell.

To study if intracellular accumulation c-di-AMP induces *mdtP* expression, I analyzed *mdtP* expression by qRT-PCR analysis. I did not see any c-di-AMP dependent change in *mdtP* expression (Figure 4.5A). While I was trying to understand role of MdtP as c-di-AMP efflux pump, a new study demonstrated that *B. subtilis* secretes c-di-AMP, and this facilitates biofilm formation and plant attachment [20]. It was shown that two membrane bound transporters YcnB and YhcA contribute to the secretion of c-di-AMP in *B. subtilis*. This study further noted that *B. subtilis* has four paralogs of putative efflux transporters (including MdtP and ImrB) that all belong to the same family. Therefore, I next tested if any of these membrane associated transporters were induced in response to an intracellular accumulation of c-di-AMP. qRT-PCR analysis shows that there is no induction of *imrB*, *ycnB* and *yhcA* upon c-di-AMP accumulation in Δ*gdpP* Δ*pgpH* double mutant strain (Figure 4.5B-4.5D).

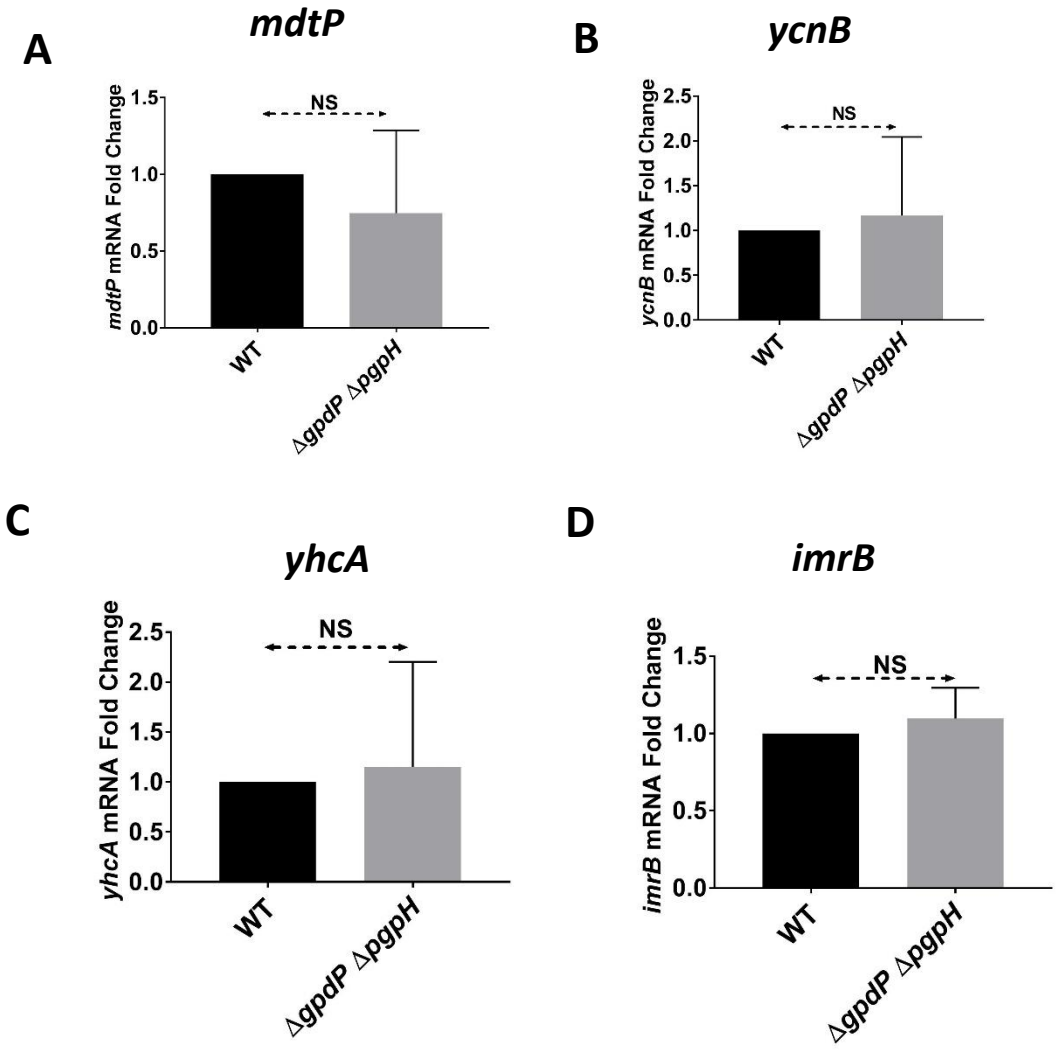

Figure 4.5: *mdtP* is not induced when c-di-AMP levels are high in the cell. (A-D) qRT-PCT analysis showing relative mRNA levels of *mdtP*, *ycnB*, *yhcA* and *imrB* in WT vs Δ*gdpP* Δ*pgpH*. Standard deviation (error bars) is based on at least three biological replicates. Statistical significance is determined by Tukey test where NS is non-significant (P >0.05).

4.4 Discussion and future directions

4.4.1 C-di-AMP and PG homeostasis:

In this study I show that the double PDE enzyme mutant Δ*gdpP* Δ*pgpH* is very sensitive to CEF due to toxic accumulation of c-di-AMP. An earlier study reported that Δ*gdpP* Δ*pgpH* accumulates more than two-fold levels of c-di-AMP compared to WT strain. I show that the deletion of the major vegetative DAC enzyme CdaA significantly reduces CEF susceptibility of Δ*gdpP* Δ*pgpH*. Earlier studies have showed that the deletion of the DAC enzyme gene *cdaA* resulted in severe beta-lactam sensitivity due to lowered c-di-AMP concentration [9]. Whereas a *gdpP* deletion has been shown to increase beta-lactam resistance [9]. Too little or too much c-di-AMP results in elevated beta-lactam sensitivity and therefore, c-di-AMP needs to be maintained at appropriate concentration.

Although a role for c-di-AMP in PG homeostasis is elusive, and there is no known receptor protein linking the two, it has always been suspected that the *cdaAR-glmMS* operon is important. GlmS and GlmM catalyze first and second PG precursor biosynthesis, respectively. In firmicutes, *glmS* expression is tightly regulated by a cis-acting ribozyme by negative feedback regulation [21]. CdaA, CdaR and GlmM co-localize on membrane and GlmM is known to modulate DAC activity of CdaA through direct protein -protein interaction, although details remain unclear [4, 17]. Moreover, an increase in c-di-AMP levels resulted in an increase in the level of the PG precursor UDP-acetylglucosamine in *Lactococcus lactis* [17]. In *Staphylococcus aureus gdpP* deletion increases PG cross linking in a lipoteichoic acid deletion strain [22]. It is likely that role of c-di-AMP in PG homeostasis is through the *cdaAR-glmMS* operon by controlling early steps in PG

precursor biosynthesis. A lack of enough PG precursors has been known to sensitize bacteria to PG synthesize inhibiting antibiotics [23-25].

Additionally, I show that by either deleting autolysins *cwlO* or *lytE* CEF susceptibility of the double PDE mutant can be significantly reduced. In an actively growing bacterial cell balanced activity of PG hydrolases allows newly synthesized precursors to integrate into the growing sacculus and elongate the cell without increasing the width of the cell. A perturbation in PG synthesis can result in increased cell lysis. It has been previously reported that Δ*gdpP* Δ*pgpH* strain has an increased cell lysis rate and that this can be attributed to a skewed balance of PG synthesis to PG hydrolysis [4].

4.4.2 C-di-AMP and potassium homeostasis

A recent review hypothesizes that effect of c-di-AMP cell wall integrity might be through an imbalance of osmolyte transport [26]. In *B. subtilis* and other organisms c-di-AMP controls potassium and other osmolyte homeostasis. In *B. subtilis*, the c-di-AMP dependent *ydaO* riboswitch controls expression of potassium uptake systems encoded by *ktrAB* and *kimA*. A recent study attributed essentiality of c-di-AMP to toxic accumulation of potassium in the cell leading to cell swelling and lysis due to unchecked expression of *kimA* and *ktrAB*. Increased availability of potassium also elevates *cdaA* and c-di-AMP levels. It is plausible that the c-di-AMP related cell wall phenotypes are indirectly linked to turgor pressure, and phenotypes associated with Δ*gdpP* Δ*pgpH* can be attributed to the shrinking of cells due to an inability to uptake potassium. Additionally, I do see that *ktrAB* mutant is more sensitive to CEF than WT (Figure 4.6). The link between osmolyte and cell-wall homeostasis, however, needs to be experimentally proven.

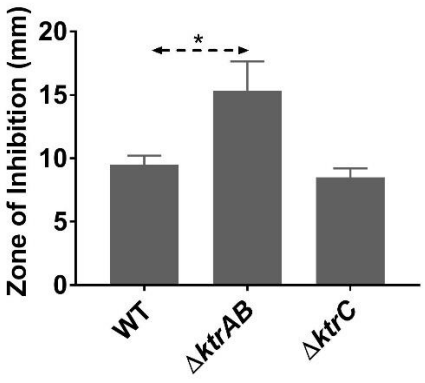

Figure 4.6: A *ktrB* deletion mutant is sensitive to CEF. Disc diffusion assay was carried out with 6 µg of CEF. Statistical analysis was carried out by Tukey's test and one asterisk represent $P < 0.05$.

4.4.3 C-di-AMP secretion by multidrug efflux pump:

As the name suggests multidrug efflux pumps provide a defense mechanism for bacteria by extruding antibiotics. It is worth noting that these efflux pumps can secrete a wide range of other compounds such as bacterial metabolites, heavy metals and quorum sensing signals [27]. Here I show that the multidrug efflux pump MdtP is an extracellular transporter of c-di-AMP by genetic analysis. *Listeria monocytogenes* is known to secrete c-di-AMP outside of the cell through multidrug efflux pumps. Consequently c-di-AMP binds to the host receptor protein stimulator of interferon genes (STING). In the host cell cytosol, when the STING is bound to c-di-AMP, it activates the host interferon response to suppress protective cell mediated immune response [28]. While I was studying the role of MdtP in c-di-AMP transport, a study came out that showed that, *B. subtilis* is also able secrete c-di-AMP through the YcnB and YhcA transporters [20]. These two transporters account for approximately 50% of c-di-AMP secretion in *B. subtilis*, suggesting that there is at least one more transporter that accounts for other 50% of c-di-AMP secretion. This study also shows that extracellular c-di-AMP is important for biofilm formation and plant root colonization and proposes that the secretion of c-di-AMP results in a quorum sensing like mechanism for cell to cell communication.

In conclusion, I show based on genetic analysis that MdtP is a putative c-di-AMP transporter in *B. subtilis*. In future studies, I will carry out extra-cellular c-di-AMP measurements in the WT and Δ*gdpP* Δ*pgpH* strains overexpressing MdtP. I will generate multiple mutants of four putative c-di-AMP transporters to determine their relative contribution to c-di-AMP secretion in *B. subtilis*. I also plan to explore a possible connection between c-di-AMP dependent potassium homeostasis disruption and beta-lactam sensitivity.

4.5 Methods

4.5.1 Bacterial strains and growth conditions

B. subtilis strains used in this study are derivative of strain 168. All *B. subtilis* strains are listed in Table 4.2. For cloning procedures, *Escherichia coli* strain DH5α was used. All the cultures were grown in lysogeny broth (LB) at 37^0 C with vigorous shaking. When necessary antibiotics were added to growth medium to following concentration, 100 μg/ml ampicillin, 10 ug/ml chloramphenicol, 100 ug/ml spectinomycin, 10 ug/ml kanamycin, and 1 μg/ml erythromycin and 25 μg/ml lincomycin.

4.5.2 Strain construction

All the in frame clean deletion strains of *B. subtilis* used in this study were derived from the *Bacillus* knock out erythromycin (BKE) collection obtained from bacillus genetic stock center (BGSC). Chromosomal DNA from BKE strain with desired mutation was transformed into lab *B. subtilis* str. 168 background. The erythromycin resistance cassette was removed using pDR244 [29], which produces Cre recombinase at the permissive temperature of 30^0 C, to generate in-frame

deletions. pDR244 was transformed into *B. subtilis* strain at 30^0 C and plated on LB plates with spectinomycin. Colonies were picked after two overnight incubations and patched three successive times on LB plates incubated at the non-permissive temperature 42^0 C overnight. Strains were then patched on spectinomycin- and erythromycin-containing plates to confirm the absence of both markers. *sigM*::*kan*, *mdtRP*::*kan*, *cdaA::tet* and *disA::spc* were generated by replacing coding region with antibiotic cassette using long flanking homology (LFH) PCR followed by DNA transformation [11].

For cloning procedure restriction digestion and ligation was carried out as per manufacturer's protocol (NEB). Cloned vector was then transformed in to competent DH5α cells. Cloning was confirmed by PCR followed by Sanger's sequencing. For *B. subtilis* transformation, cell were grown in minimal competence medium. DNA was added at OD_{600}-0.7-0.8 followed by incubation for one hour at 37^0 C shaker. Transformants were selected on LB agar plate with antibiotic of interest. *B. subtilis* strains overexpressing genes of interest at *amyE* locus was created using vector pPL82 carrying gene of interest followed by transformation into *B. subtilis* [30].

4.5.3 Antibiotic susceptibility test

Susceptibility test for antibiotic was carried out using disc diffusion assay. Strains of interest were grown in 5 ml LB medium with vigorous shaking to OD_{600}-0.4. 100 µl of cells were added to 4 ml of top agar (Mueller Hinton (MH) medium with 0.7 % agar) kept at 50^0 C. 1mM IPTG was also added when necessary. Top agar was then poured on premade MH base agar (1.5%) plate. After agar was solidified, a Whatman paper disc (7 mm) with was placed on top agar. 6 µg of CEF was added to the disc unless specified otherwise. Plates were incubated overnight at 37^0 C and zone of inhibition (ZOI) was measured the next days.

4.5.4 Growth assay:

CEF sensitivity growth curve was carried out in MH medium. Strains of interest were grown in 5 ml LB medium to OD_{600}-0.4. 2 µl cells (1:100 dilution) were added to 200 µl of MH medium in 100 well bio screen plate. CEF was added if required. Growth was monitored in bio screen growth curve analyze.

4.5.5 Transposon mutagenesis:

Mariner transposon mutagenesis in Δ*gdpP* Δ*pgpH* strain was carried out as described previously [31]. In brief, Δ*gdpP* Δ*pgpH* was transformed with pMarA plasmid. The resulting strain was grown in 5 ml LB to mid exponential phase. Various dilution of culture was prepared and plated on MH agar plate with varying concentration of CEF.

4.5.6 qRT-PCR:

Strains of interest were grown to an OD_{600} of ~0.5. 2 ml of culture was used for RNA extraction. RNA isolation (Qiagen, USA) and cDNA preparation (Thermofisher, USA) was carried out as suggested by the manufacturer. qRT-PCR was carried out using a Bio-Rad iTaq universal SYBR green super mix. 23S rRNA was used to normalize the cycle threshold (Ct) value.

Table 4.2 *B. subtilis* strains used in this study

Strains	Genotype	Source/reference
168	*trpC2*	Lab stock
HB10216	*trpC2 sigM::kan*	Luo and Helmann (2009)
HB10257	*trpC2 sigM::kan gdpP::mls*	Luo and Helmann (2012)
HB16799	*trpC2 sigM::kan pgpH*	This work
HB16800	*trpC2 sigM::kan gdpP::mls disA::spc*	This work
HB16801	*trpC2 sigM::kan gdpP::mls cdaA::tet*	This work
HB16804	*trpC2 sigM::kan gdpP::mls pgpH amyE::*$P_{spac(hy)}$ *pgpH*	This work
HB16813	*trpC2 gdpP*	This work
HB16818	*trpC2 gdpP pgpH*	This work
HB16861	*trpC2 gdpP pgpH yesJ::mls*	This work
HB16874	*trpC2 mdtR*	This work
HB16875	*trpC2 gdpP pgpH mdtR*	This work
HB16879	*trpC2 mdtP::mls*	This work
HB16882	*trpC2 lytE::mls*	This work
HB16886	*trpC2 gdpP pgpH mdtP::mls*	This work
HB16890	*trpC2 cwlO::kan*	This work
HB16891	*trpC2 gdpP pgpH cwlO::kan*	This work
HB16893	*trpC2 gdpP pgpH mdtR thrC::mdtR*	This work
HB16953	*trpC2 pgpH*	This work
HB16956	*trpC2 gdpP pgpH lytE::mls*	This work
HB16961	*trpC2 gdpP pgpH* $P_{spac(hy)}$ *pgpH*	This work
HB16992	*trpC2 gdpP pgpH amyE::*$P_{spac(hy)}$ *mdtP*	This work
HB21959	*trpC2 amyE::*$P_{spac(hy)}$ *mdtP*	This work
HB21961	*trpC2 mdtRP::kan*	This work
HB21964	*trpC2 gdpP pgpH mdtRP::kan*	This work

4.5.7 REFERENCES

1. Commichau FM, Heidemann JL, Ficner R, Stülke J. Making and breaking of an essential poison: the cyclases and phosphodiesterases that produce and degrade the essential second messenger cyclic di-AMP in bacteria. Journal of Bacteriology. 2018. doi: 10.1128/jb.00462-18.
2. Whiteley Aaron T, Pollock Alex J, Portnoy Daniel A. The PAMP c-di-AMP Is Essential for *Listeria monocytogenes* Growth in Rich but Not Minimal Media due to a Toxic Increase in (p)ppGpp. Cell Host & Microbe. 2015;17(6):788-98. doi: 10.1016/j.chom.2015.05.006.
3. Commichau FM, Dickmanns A, Gundlach J, Ficner R, Stülke J. A jack of all trades: the multiple roles of the unique essential second messenger cyclic di-AMP. Molecular Microbiology. 2015;97(2):189-204. doi: doi:10.1111/mmi.13026.
4. Gundlach J, Mehne FMP, Herzberg C, Kampf J, Valerius O, Kaever V, *et al*. An Essential Poison: Synthesis and Degradation of Cyclic Di-AMP in *Bacillus subtilis*. Journal of Bacteriology. 2015;197(20):3265-74. doi: 10.1128/jb.00564-15.
5. Oppenheimer-Shaanan Y, Wexselblatt E, Katzhendler J, Yavin E, Ben-Yehuda S. c-di-AMP reports DNA integrity during sporulation in *Bacillus subtilis*. EMBO reports. 2011;12(6):594-601. doi: 10.1038/embor.2011.77.
6. Mehne FMP, Schröder-Tittmann K, Eijlander RT, Herzberg C, Hewitt L, Kaever V, *et al*. Control of the Diadenylate Cyclase CdaS in *Bacillus subtilis*: AN AUTOINHIBITORY DOMAIN LIMITS CYCLIC DI-AMP PRODUCTION. Journal of Biological Chemistry. 2014;289(30):21098-107. doi: 10.1074/jbc.M114.562066.

7. Rao F, See RY, Zhang D, Toh DC, Ji Q, Liang Z-X. YybT Is a Signaling Protein That Contains a Cyclic Dinucleotide Phosphodiesterase Domain and a GGDEF Domain with ATPase Activity. Journal of Biological Chemistry. 2010;285(1):473-82. doi: 10.1074/jbc.M109.040238.

8. Huynh TN, Luo S, Pensinger D, Sauer J-D, Tong L, Woodward JJ. An HD-domain phosphodiesterase mediates cooperative hydrolysis of c-di-AMP to affect bacterial growth and virulence. Proceedings of the National Academy of Sciences. 2015;112(7):E747-E56. doi: 10.1073/pnas.1416485112.

9. Luo Y, Helmann JD. Analysis of the role of *Bacillus subtilis* σM in β-lactam resistance reveals an essential role for c-di-AMP in peptidoglycan homeostasis. Molecular Microbiology. 2012;83(3):623-39. doi: doi:10.1111/j.1365-2958.2011.07953.x.

10. Kaplan Zeevi M, Shafir NS, Shaham S, Friedman S, Sigal N, Nir Paz R, *et al*. *Listeria monocytogenes* Multidrug Resistance Transporters and Cyclic Di-AMP, Which Contribute to Type I Interferon Induction, Play a Role in Cell Wall Stress. Journal of Bacteriology. 2013;195(23):5250-61. doi: 10.1128/jb.00794-13.

11. Mascher T, Margulis NG, Wang T, Ye RW, Helmann JD. Cell wall stress responses in *Bacillus subtilis*: the regulatory network of the bacitracin stimulon. Molecular Microbiology. 2003;50(5):1591-604. doi: doi:10.1046/j.1365-2958.2003.03786.x.

12. Lazarevic V, Soldo B, Médico N, Pooley H, Bron S, Karamata D. *Bacillus subtilis* α-Phosphoglucomutase Is Required for Normal Cell Morphology and Biofilm Formation. Applied and Environmental Microbiology. 2005;71(1):39-45. doi: 10.1128/aem.71.1.39-45.2005.

13. Formstone A, Errington J. A magnesium-dependent mreB null mutant: implications for the role of mreB in *Bacillus subtilis*. Molecular Microbiology. 2005;55(6):1646-57. doi: doi:10.1111/j.1365-2958.2005.04506.x.

14. Leaver M, Errington J. Roles for MreC and MreD proteins in helical growth of the cylindrical cell wall in *Bacillus subtilis*. Molecular Microbiology. 2005;57(5):1196-209. doi: doi:10.1111/j.1365-2958.2005.04736.x.

15. Dajkovic A, Tesson B, Chauhan S, Courtin P, Keary R, Flores P, *et al*. Hydrolysis of peptidoglycan is modulated by amidation of meso-diaminopimelic acid and Mg2+ in *Bacillus subtilis*. Molecular Microbiology. 2017;104(6):972-88. doi: doi:10.1111/mmi.13673.

16. Mehne FMP, Gunka K, Eilers H, Herzberg C, Kaever V, Stülke J. Cyclic Di-AMP Homeostasis in *Bacillus subtilis*: BOTH LACK AND HIGH LEVEL ACCUMULATION OF THE NUCLEOTIDE ARE DETRIMENTAL FOR CELL GROWTH. Journal of Biological Chemistry. 2013;288(3):2004-17. doi: 10.1074/jbc.M112.395491.

17. Zhu Y, Pham TH, Nhiep THN, Vu NMT, Marcellin E, Chakrabortti A, *et al*. Cyclic-di-AMP synthesis by the diadenylate cyclase CdaA is modulated by the peptidoglycan biosynthesis enzyme GlmM in *Lactococcus lactis*. Molecular Microbiology. 2016;99(6):1015-27. doi: doi:10.1111/mmi.13281.

18. Barreteau H, Kovač A, Boniface A, Sova M, Gobec S, Blanot D. Cytoplasmic steps of peptidoglycan biosynthesis. FEMS Microbiology Reviews. 2008;32(2):168-207. doi: 10.1111/j.1574-6976.2008.00104.x.

19. Kim J-Y, Inaoka T, Hirooka K, Matsuoka H, Murata M, Ohki R, *et al*. Identification and Characterization of a Novel Multidrug Resistance Operon, mdtRP (yusOP), of *Bacillus subtilis*. Journal of Bacteriology. 2009;191(10):3273-81. doi: 10.1128/jb.00151-09.

20. Townsley L, Yannarell SM, Huynh TN, Woodward JJ, Shank EA. Cyclic di-AMP Acts as an Extracellular Signal That Impacts *Bacillus subtilis* Biofilm Formation and Plant Attachment. mBio. 2018;9(2). doi: 10.1128/mBio.00341-18.

21. Collins JA, Irnov I, Baker S, Winkler WC. Mechanism of mRNA destabilization by the glmS ribozyme. Genes & Development. 2007;21(24):3356-68. doi: 10.1101/gad.1605307. PubMed PMID: PMC2113035.

22. Corrigan RM, Abbott JC, Burhenne H, Kaever V, Gründling A. c-di-AMP Is a New Second Messenger in *Staphylococcus aureus* with a Role in Controlling Cell Size and Envelope Stress. PLOS Pathogens. 2011;7(9):e1002217. doi: 10.1371/journal.ppat.1002217.

23. Zhao H, Roistacher DM, Helmann JD. Aspartate deficiency limits peptidoglycan synthesis and sensitizes cells to antibiotics targeting cell wall synthesis in *Bacillus subtilis*. Molecular Microbiology. 0(0). doi: doi:10.1111/mmi.14078.

24. Patel V, Wu Q, Chandrangsu P, Helmann JD. A metabolic checkpoint protein GlmR is important for diverting carbon into peptidoglycan biosynthesis in *Bacillus subtilis*. PLOS Genetics. 2018;14(9):e1007689. doi: 10.1371/journal.pgen.1007689.

25. Irnov I, Wang Z, Jannetty ND, Bustamante JA, Rhee KY, Jacobs-Wagner C. Crosstalk between the tricarboxylic acid cycle and peptidoglycan synthesis in *Caulobacter crescentus* through the homeostatic control of α-ketoglutarate. PLOS Genetics. 2017;13(8):e1006978. doi: 10.1371/journal.pgen.1006978.

26. Commichau FM, Gibhardt J, Halbedel S, Gundlach J, Stülke J. A Delicate Connection: c-di-AMP Affects Cell Integrity by Controlling Osmolyte Transport. Trends in Microbiology. 2018;26(3):175-85.

27. Blanco P, Hernando-Amado S, Reales-Calderon JA, Corona F, Lira F, Alcalde-Rico M, *et al*. Bacterial Multidrug Efflux Pumps: Much More Than Antibiotic Resistance Determinants. Microorganisms. 2016;4(1):14. doi: 10.3390/microorganisms4010014. PubMed PMID: PMC5029519.

28. Archer KA, Durack J, Portnoy DA. STING-Dependent Type I IFN Production Inhibits Cell-Mediated Immunity to *Listeria monocytogenes*. PLOS Pathogens. 2014;10(1):e1003861. doi: 10.1371/journal.ppat.1003861.

29. Koo B-M, Kritikos G, Farelli JD, Todor H, Tong K, Kimsey H, *et al*. Construction and Analysis of Two Genome-Scale Deletion Libraries for *Bacillus subtilis*. Cell Systems. 2017;4(3):291-305.e7.

30. Quisel JD, Burkholder WF, Grossman AD. In Vivo Effects of Sporulation Kinases on Mutant Spo0A Proteins in *Bacillus subtilis*. Journal of Bacteriology. 2001;183(22):6573-8. doi: 10.1128/jb.183.22.6573-6578.2001.

31. Le Breton Y, Mohapatra NP, Haldenwang WG. In Vivo Random Mutagenesis of *Bacillus subtilis* by Use of TnYLB-1, a mariner-Based Transposon. Applied and Environmental Microbiology. 2006;72(1):327-33. doi: 10.1128/aem.72.1.327-333.2006.

APPENDIX 1

Characterizing role of σ^M regulon in beta-lactam resistance[2]

A 1.1 Abstract

The cell wall of bacteria is essential for maintaining cell shape and integrity and countering turgor pressure. However, it is also a target for various antimicrobial compounds. Thus, bacteria have evolved mechanisms to counteract such stress. In the gram-positive soil bacterium *Bacillus subtilis* the alternative sigma factor σ^M plays an important role in maintaining cell surface integrity under various kind of cell wall stress. A previous study from our lab showed that deletion of σ^M renders *B. subtilis* very sensitive to beta-lactam antibiotics. However, the underlying mechanism of σ^M dependent beta-lactam resistance is elusive. From previous work, we know the operons that are induced by σ^M. These studies showed that the activation of σ^M controls the stress-induced up-regulation of genes important for cell wall biosynthesis, cell shape determination and cell division. However, σ^M dependent expression of which gene(s) is the most important for the beta-lactam resistance is not characterized yet. To obtain insights into beta-lactam defense mechanism, we[2] have generated individual σ^M promoter mutations. Inactivation of σ^M promoter abolishes the stress dependent induction of the gene(s) it controls without affecting the σ^A dependent basal level expression. These mutant strains were tested for beta-lactam sensitivity. So far, we[2] have inactivated and tested σ^M promoters located

[2] Wen-Wen Zhou and Pete Chandrangsu contributed in the characterization of P_M-*maf* promoter.

inside genes *maf* and *murG* that induce *radC-mreBCD-minCD* and *murB-divIV* respectively. My preliminary data suggest that P_M -*maf* and P_M-*murG* contribute to beta-lactam resistance mechanism in *B. subtilis*. However, this does not account for complete resistance. These preliminary data suggest that the possible induction of multiple operons in *sigM* regulon contribute to beta-lactam resistance.

A 1.2 Introduction

In gram-positive bacterium *B. subtilis,* there are seven extra cytoplasmic sigma factors (ECF) that control induction of genes involved in protection against cell envelop stress response [1]. Roles for σ^M, σ^W, σ^X and σ^V have been implicated in cell wall stress response. A possible role for σ^Y, σ^Z and σ^{YlaC} are not well understood. Each σ factor is the first gene in the operon with the corresponding anti-σ factor being the next gene. Upon cell envelop stress, anti-σ factor is inactivated and the release of σ factor activates the regulon by binding to RNA polymerase. σ^M is induced when *B. subtilis* is exposed to heat, high salt, alcohol and some cell wall synthesis inhibiting antibiotics [2]. A *sigM* deletion mutant displays morphological defects when exposed to cell envelope stress [3]. Luo *et al.* have shown that the *sigM* deletion mutant is very sensitive to beta-lactam antibiotics cefuroxime (CEF) as well as aztreonam and cefixime [4]. The mechanism of the role of σ^M in beta-lactam resistance is not clear. σ^M regulon is well characterized by transcriptomics analysis [5]. There are over 30 operons and over 60 genes that are induced by σ^M. Intriguingly, σ^M controls the expression of many peptidoglycan (PG) biosynthesis enzymes including the Rod complex enzymes (RodA, MreB, MreC, MreD), major class A penicillin binding protein; PBP1and the cell division proteins (DivIB, DivIC, MinC, MinD). σ^M also induces

enzymes from cytoplasmic steps of PG biosynthesis (MurB, Ddl, MurF) and lipid II carrier protein BcrC. In addition, σ^M regulon controls expression of lipoteichoic acid (LTA) synthase, LtaS and the enzyme that attaches wall teichoic acid (WTA) to PG (TagT). LTA and WTA are negatively charged phosphate containing polymers that attached to cell membrane and PG respectively in gram positive bacteria [6, 7]. Moreover, c-di-AMP synthase DisA is also part of *sigM* regulon. It is known that increased concentration of c-di-AMP suppresses CEF sensitivity phenotype of *sigM* deletion mutant.

In this study, I aim to study the contribution of internal σ^M promoters in beta-lactam resistance. There are four σ^M promoters that are located inside a gene and that includes σ^M promoters inside *maf*, *murG*, *radC* and *ydbO* [5].To achieve my goal, we[2] have created an individual σ^M promoter mutations and tested for beta-lactam sensitivity. So far, the promoters inside genes *maf* and *murG* that controls expression of *radC-mreBCD-minCD* and *murB-divIB* respectively, have been inactivated. My initial analysis suggests that both of these promoters contribute in beta-lactam resistance. The P_M*-*maf* and P_M*- *murG* have additive beta-lactam (CEF) sensitivity. In future, I intend to characterize additional σ^M promoters controlling the expressions of genes that are important for PG biosynthesis and study their relative contribution to beta-lactam stress response in *B. subtilis*.

A 1.3 Results

σ^M promoter mutations inside *maf* was generated without affecting the open reading frame (ORF) (Figure A1.1A). These strains were then tested for CEF susceptibility using commercially available Mueller Hinton (MH) medium from Sigma. In the initial study carried out

by Wen-Wen Zhou, she observed that P_M*-*maf* strain exhibited significant CEF susceptibility, almost as sensitive as *sigM* deletion mutant (data not shown). The complementation experiments showed that the ectopic expression of *radC-mreBCD-minC* from native σ^M promoter completely restored the CEF sensitivity phenotype of P_M*-*maf*. Similarly, I generated σ^M promoter mutation inside *murG* without disturbing the ORF (Figure A1.1B). This promoter controls the expression of *murB-divIB*. P_M*-*murG* strain exhibited increased CEF susceptibility, however not as prominent as P_M*-*maf* (data not shown). CEF sensitivity of P_M*-*murG* can be complemented by the ectopic expression of *murB* from native σ^M promoter. However, these phenotypes were not reproducible in MH medium from any different batches obtained from Sigma that I tried. I also tried MH medium from different manufacturers, but I still couldn't reproduce our initial observations. Due to these inconsistencies, I decided to make a buffered growth medium by combining individual ingredients as described in the method section. I have carried out CEF susceptibility analysis by growth curve analysis in this lab made MH medium. *sigM* deletion mutant is highly sensitive to CEF and exhibited no growth at any CEF concentrations I tried. P_M*-*maf* strain exhibited intermediate sensitivity to CEF and that can be complemented by σ^M dependent expression of *radC-mreBCD-minC* at *thrC* locus (Figure A1.2 A and B). I was also able to reproduce to CEF sensitivity phenotype of P_M*-*murG* in the lab assembled growth medium (Figure A1.3 A and B). I generated P_M*-*maf* PM*-*murG* double promoter mutant and tested for CEF sensitivity by growth curve analysis. This mutant strain exhibits additive CEF sensitivity compare to the individual mutants.

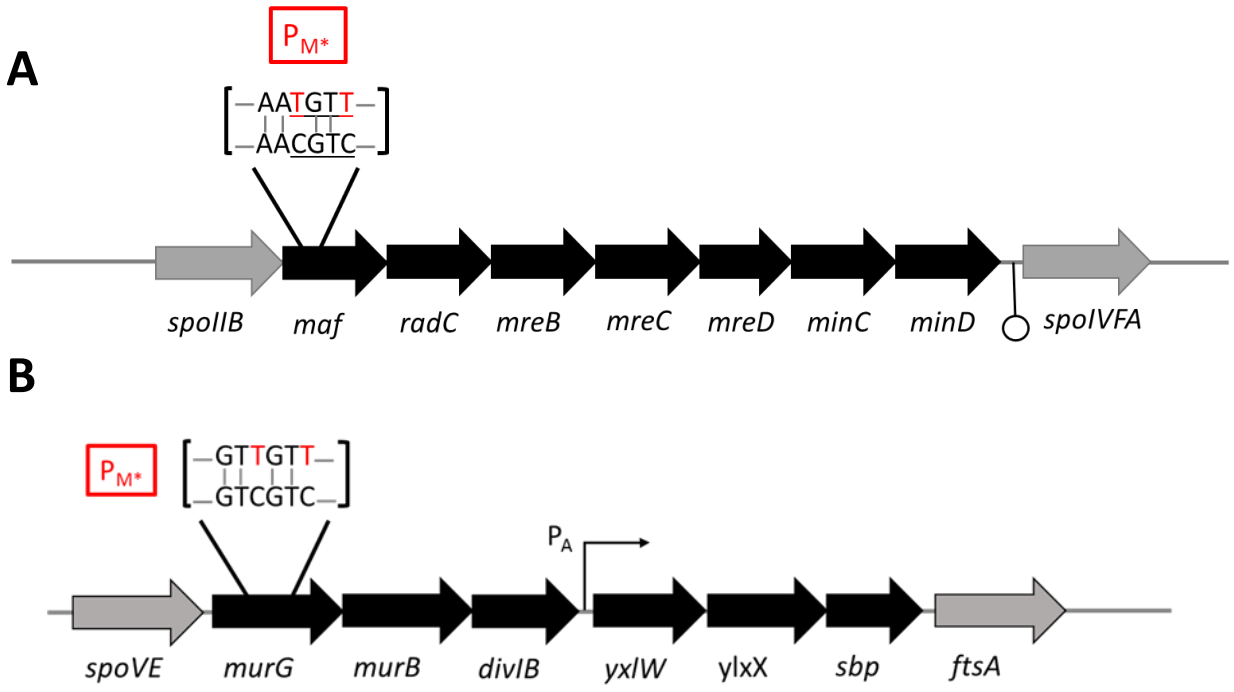

Figure A1.1: Operons controlled by internal σ^M promoters (A) P_M*-*maf* and (B) P_M*-*murG*. The σ^M promoters inside *maf* and *murG* were mutated by silent mutation. Red letters represent mutated nucleotides.

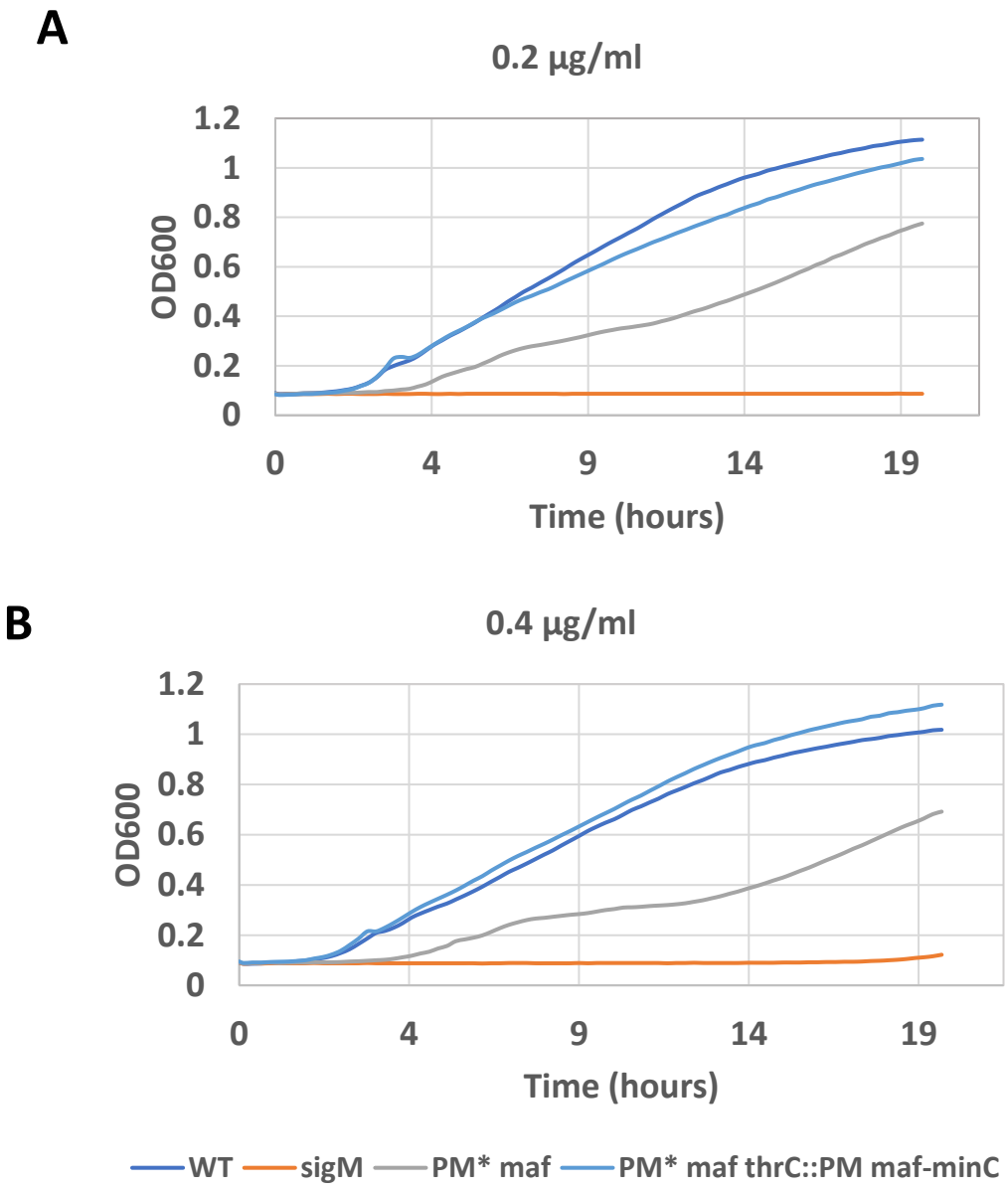

Figure A1.2: P_M*-*maf* is sensitive to CEF. The representative growth curve study from at least three biological replicates done with WT, *sigM*, P_M*-*maf* and P_M* *maf thrC*::P_M *maf-minC* done with (A) 0.2 µg/ml and (B) 0.4 µg/ml CEF

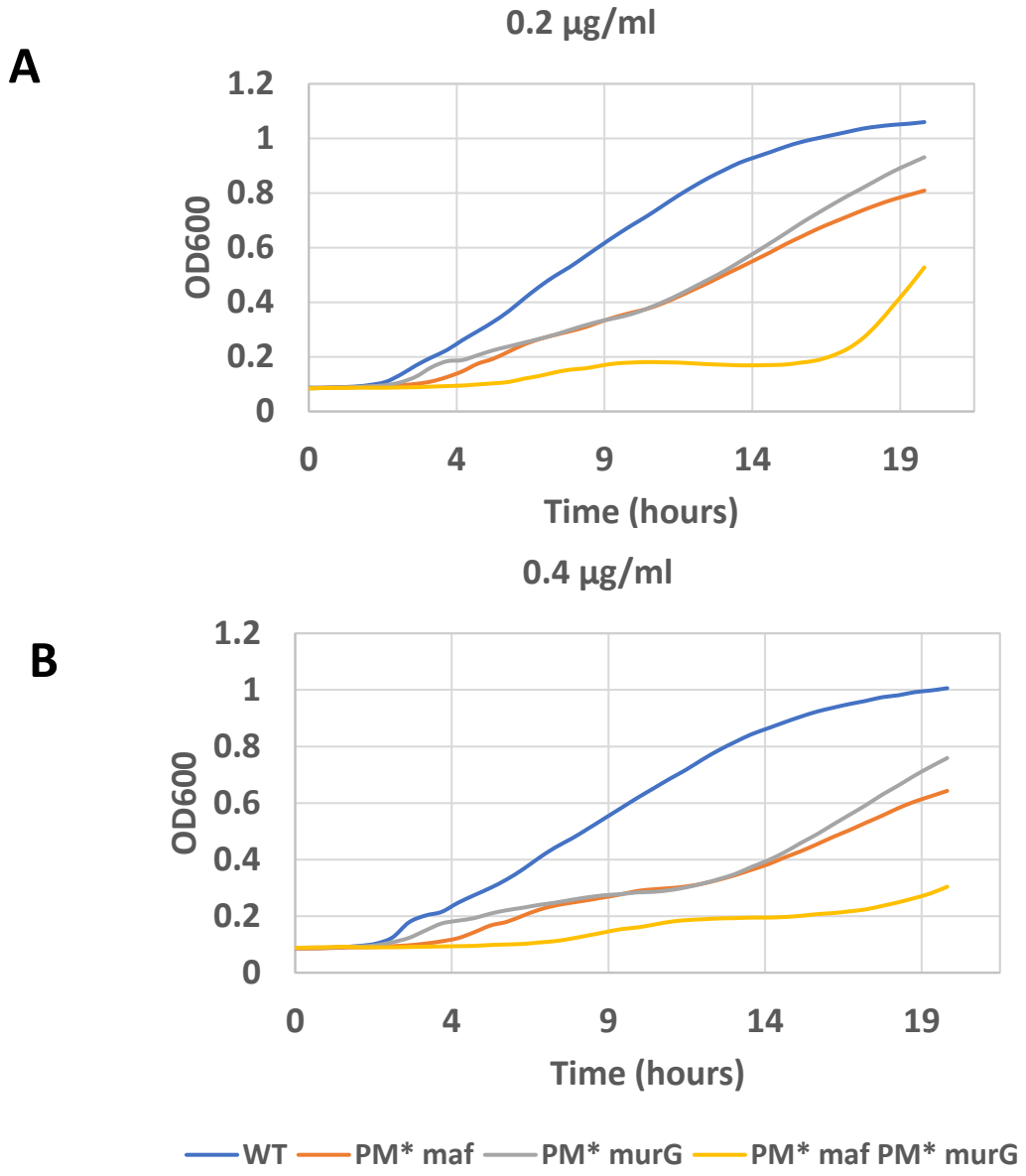

Figure A1.3: P_M*-*murG* is sensitive to CEF and P_M*-*murG* P_M*-*maf* double mutant exhibit additive CEF sensitivity**.** The representative growth curve study from at least three biological replicates done with WT, P_M*-*maf*, P_M*-*murG* and P_M* *maf* P_M*-*murG* done with (A) 0.2 µg/ml and (B) 0.4 µg/ml CEF.

A 1.4 Future directions

In the future, I plan to carry out all the experiments in the lab assembled growth medium for the strains that I have not tested yet. In addition to that I plan to generate σ^M promoter mutation inside genes *radA* and *ydbO* as well as combine these mutations with P_M*-*maf* and P_M*-*murG*. I also intend to extend this study to other promoters, especially those controlling expression of enzymes involved in PG biosynthesis.

A 1.5 Material and methods

A 1.5.1 Bacterial strains and growth conditions:

B. subtilis strains used are derived from strain 168 (*trpC2*). *E. coli* strain DH5α was used for cloning. Bacteria were cultured in LB broth. Antibiotics were added to growth media when required at the following concentrations: 100 μg/ml ampicillin, 10 μg/ml kanamycin, 10 μg/ml chloramphenicol, 5 μg/ml tetracycline, 100 μg/ml spectinomycin and 1 μg/ml erythromycin with 25 μg/ml lincomycin (erm; macrolide-lincomycin-streptogramin B resistance).

A 1.5.2 Cloning, transformation and strain construction:

The restriction digestion and ligation for cloning procedure was done as per manufacturer's protocol. Plasmids were then transformed into competent DH5α cells. Cloning was confirmed by polymerase chain reaction (PCR) followed by Sanger sequencing. pDG1731 was used for generating ectopic gene expression constructs.

A fragment of DNA with the mutation of interest was cloned into pMutin4 and confirmed with PCR and Sanger sequencing. The vector was transformed into *B. subtilis* where it integrated at locus by single crossover homologous recombination. Transformants were selected on plates with Erm and 40 µg/ml X-gal. After overnight incubation, a few blue color colonies were picked. Since pMutin4 integration is unstable, cells were grown without antibiotic selection three consecutive times with each time adding 1:100 dilution of cells from previous culture. Cells were then plated on LB plates with X-gal and white colonies were picked and sequenced to find those strains that retained the single nucleotide mutation of interest.

A 1.5.3 Growth assay:

For the growth studies, MH medium was made by combining 0.2 grams of beef heart infusion and 1.75 grams of casein hydrolysate in 100 ml in 0.8 mM MOPs buffer (pH 7.4). All the growth experiments were carried out in bioscreen growth analyzer. The strains of interest were grown in 5 ml LB medium up to OD_{600}-0.4. 2 µl of cell were then added to a 100 well plate with 200 µl of MH medium and CEF if needed. Experiment was run at 37^0 C with constant shaking for 24 hours.

Table A1.1 *B. subtilis* strains used in this study

Strains	Genotype	Source/Ref
168	*trpC2*	Lab stock
HB10216	*trpC2 sigM::kan*	Luo *et al.* 2012
HB17934	*trpC2* P_M*-*maf*	This work
HB17945	*trpC2* P_M*-*maf amyE::radC-mreBCD-minC*	This work
HB16780	*trpC2* P_M*-*murG*	This work
HB16812	*trpC2* P_M*-*maf* P_M*-*murG*	This work

A 1.6 REFERENCES

1. Helmann JD. Bacillus subtilis extracytoplasmic function (ECF) sigma factors and defense of the cell envelope. Current Opinion in Microbiology. 2016;30:122-32.
2. Thackray PD, Moir A. SigM, an Extracytoplasmic Function Sigma Factor of *Bacillus subtilis*, Is Activated in Response to Cell Wall Antibiotics, Ethanol, Heat, Acid, and Superoxide Stress. Journal of Bacteriology. 2003;185(12):3491-8. doi: 10.1128/jb.185.12.3491-3498.2003.
3. Horsburgh MJ, Moir A. σM, an ECF RNA polymerase sigma factor of Bacillus subtilis 168, is essential for growth and survival in high concentrations of salt. Molecular Microbiology. 1999;32(1):41-50. doi: doi:10.1046/j.1365-2958.1999.01323.x.
4. Luo Y, Helmann JD. Analysis of the role of Bacillus subtilis σM in β-lactam resistance reveals an essential role for c-di-AMP in peptidoglycan homeostasis. Molecular Microbiology. 2012;83(3):623-39. doi: doi:10.1111/j.1365-2958.2011.07953.x.
5. Eiamphungporn W, Helmann JD. The Bacillus subtilis σM regulon and its contribution to cell envelope stress responses. Molecular Microbiology. 2008;67(4):830-48. doi: doi:10.1111/j.1365-2958.2007.06090.x.
6. Percy MG, Gründling A. Lipoteichoic Acid Synthesis and Function in Gram-Positive Bacteria. Annual Review of Microbiology. 2014;68(1):81-100. doi: 10.1146/annurev-micro-091213-112949. PubMed PMID: 24819367.
7. Brown S, Santa Maria JP, Walker S. Wall Teichoic Acids of Gram-Positive Bacteria. Annual review of microbiology. 2013;67:10.1146/annurev-micro-092412-155620. doi: 10.1146/annurev-micro-092412-155620. PubMed PMID: PMC3883102.

APPENDIX 2

Identification of c-di-AMP receptor protein in *Bacillus subtilis*.

A 2.1 Introduction

Cyclic diadenosine monophosphate(c-di-AMP) is a secondary messenger molecule produced in bacteria. C-di-AMP is a relatively newer addition to well-studied signal molecules like cyclic-adenosine monophosphate (cAMP), cyclic diguanylate monophosphate(c-di-GMP) and guanosine tetra or pentaphosphate ((p)ppGpp)[1]. Prior studies show that intracellular or environmental changes alter the levels of cAMP, c-di-GMP and (p)ppGpp [1]. In general, these molecules regulate many important cellular processes such as biofilm formation, cell-cycle control, stringent response, virulence and alternate sugar utilization. c-di-AMP was serendipitously discovered bound to one of the c-di-AMP synthase DNA integrity scanning protein (disA) from *Thermotoga maritima* during structural study by Witte *et al.* [2]. Since its discovery, c-di-AMP has been found in many important bacteria. Bioinformatics study predicts presence of c-di-AMP in many more prokaryotes that mostly include gram positive bacteria and some gram-negative bacteria and archaea as well [3]. Signaling nucleotides function by allosterically changing its receptor protein or riboswitch and thus modulating specific cellular pathway in response to a stimulus. In *B. subtilis*, c-di-AMP has been linked to many phenotypes like DNA damage sensing, cell wall homeostasis and potassium uptake [4-6]. In this study I looked for c-di-AMP protein receptors in *B. subtilis* by carrying out affinity pull down experiments. When I began this study, no *B. subtilis* c-di-AMP receptor was identified. I identified one c-di-AMP receptor called YaaQ

(also referred to as DarA and PstA), a protein of unknown function. YaaQ specifically binds to c-di-AMP and exhibited no binding to cAMP and c-di-GMP.

A 2.2 Results and discussion

B. subtilis BSU00290 (YaaQ) is a cyclic-di-AMP receptor protein.

I carried out affinity pull down experiments to search for c-di-AMP receptors in *B. subtilis* as described in the methods section. I observed one distinct protein bound to c-di-AMP as shown in Figure A2.1. In order to confirm that the protein only binds to c-di-AMP specifically and not to other nucleotides, I carried out a competition assay. In the assay, once c-di-AMP immobilized streptavidin beads were treated with cell lysate, I tried eluting protein bound to the beads with excess of c-di-AMP, c-di-GMP and cAMP. A polypeptide was only eluted with c-di-AMP (Figure 2.2). I then cut the band from the gel and sent it for mass spectrometry analysis. The analysis identified this protein as BSU0029 which is designated as YaaQ in databases. Protein databases list that YaaQ has a domain (DUF970) that is conserved in Firmicutes. DUF970 has no known function.

While I was working on this project, other groups also identified YaaQ as a c-di-AMP receptor protein in *B. subtilis*, *L. monocytogenes* and *S. aureus* [7-9]. These studies also included the structural analysis of the YaaQ bound to c-di-AMP. The structural studies suggest that when bound to c-di-AMP, YaaQ undergoes conformational change. The physiological function of YaaQ remains to be investigated. The bioinformatic analysis suggest that it is a PII like signal transduction molecule. PII proteins function in a signal transduction pathway and they are known regulate activity of a target protein by protein-protein interaction. The vast majority of PII proteins

are involved in nitrogen metabolism. It is possible that YaaQ is also involved in nitrogen metabolism; however, this remains to be investigated.

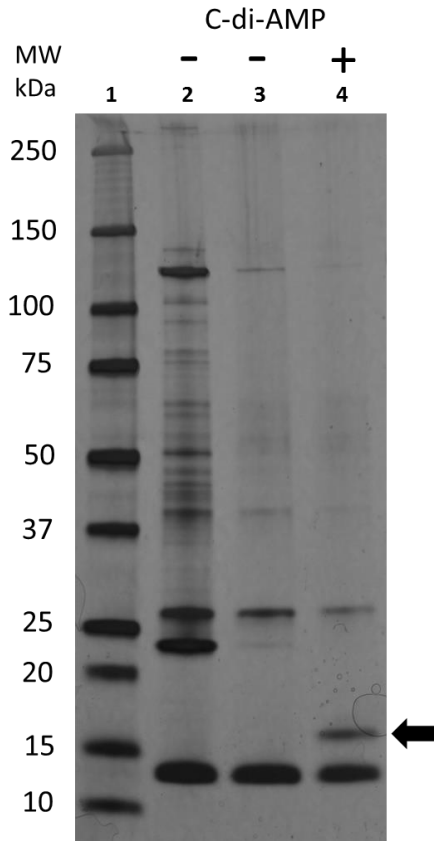

Figure A2.1: Identification of *B. subtilis* YaaQ (BSU00290) as c-di-AMP binding receptor. Silver stained SDS-PAGE gel of proteins bound to streptavidin beads in the presence and absence of biotinylated c-di-AMP. Lanes showing (1) Protein marker, (2) proteins from beads not immobilized with biotin or c-di-AMP, (3) Proteins from beads blocked with biotin, no c-di-AMP, (4) Proteins from beads immobilized with c-di-AMP and blocked with biotin. Arrow around 15 kDa shows c-di-AMP bound YaaQ.

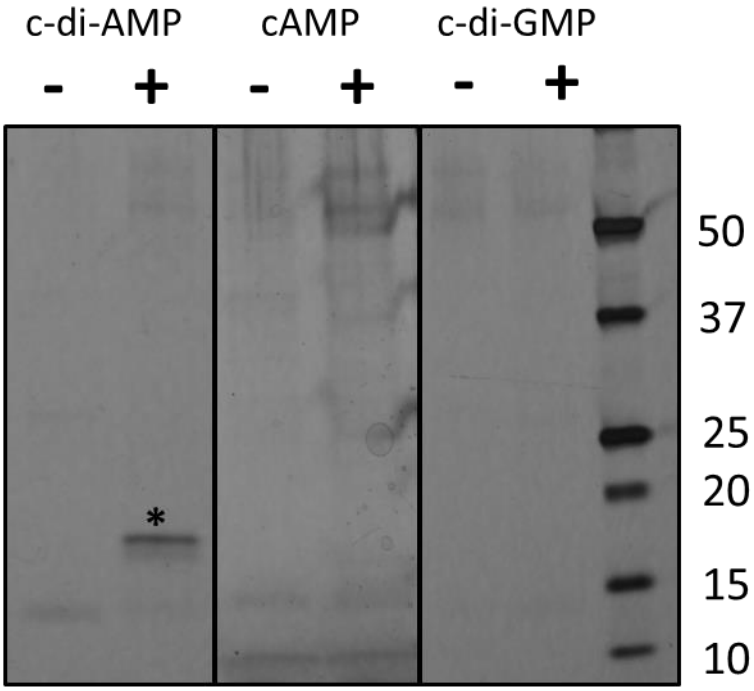

Figure A2.2: Competition assay to confirm c-di-AMP interaction with YaaQ. Above silver stained SDS-PAGE gel shows proteins eluted in absence and presence c-di-AMP, cAMP and c-di-GMP that were retained on c-di-AMP immobilized streptavidin beads from affinity pull down assay. Asterisk shows YaaQ eluted with c-di-AMP.

A 2.3 Methods

A 2.3.1 Bacterial strains and growth conditions

The *B. subtilis* strains used were derived from strain 168 (*trpC*) and are listed in Table 1. All *B. subtilis* strains were grown in lysogeny broth (LB) medium at 37 ^{o} C.

A 2.3.2 Pull-down assay

B. subtilis 168 was grown at 37 ^{o}C in LB medium until culture reached OD_{600} of approximately 1.0. 50 ml of cells for each set of experiments were harvested and suspended in lysis buffer containing 50 mM Tris-HCl pH 7.5, 150 mM NaCl, 0.1% tween 20 and 1% Triton X-100 supplemented with freshly made 80 $mg.ml^{-1}$ lysozyme to final concentration of 20 $\mu g.ml^{-1}$. The samples were kept at 37^{o} C for lysis till solution became clear. Then samples were subjected to sonication for 5 x 10 seconds to disrupt DNA. Post sonication, crude lysate was centrifuged for 10 minutes at 13000 rpm to remove cell debris. Supernate was moved to a fresh tube. On the other hand, 40 mg of streptavidin-coated magnetic beads (Pierce) were incubated with 0.6 µg of biotinylated c-di-AMP (2'-[Biotin]-AHC-c-di-AMP, Biolog). After c-di-AMP immobilization, streptavidin beads were incubated with 1 mg of biotin to reduce non-specific protein interaction with streptavidin. After two washes of wash binding (WB) buffer (50 mM Tris-HCl, pH 7.5, 150 mM NaCl, 0.1% tween 20), c-di-AMP immobilized streptavidin beads were incubated overnight with the supernate at 4^{o} C. After removal of cell lysate, beads were washed with 500 µl of WB buffer followed by 1 ml high salt buffer wash (50 mM tris-HCl, 0.5 M NaCl, 0.1% tween 20). Two 1 ml WB buffer washes were given to remove excess salt. Streptavidin beads were then suspended in 50 µl of 1X Laemmli buffer (50mM 1M Tris-HCl pH 6.8,2% SDS, 10% glycerol, 1% beta-mercaptoethanol,12.5mM EDTA, 0.02% bromophenol blue) and heated at 95^{o} C for 15 minutes.

Two µl of sample was electrophoresed on a precast 4-20% gradient polyacrylamide gel (BIO-RAD). The gel was stained with silver stain kit (Pierce) as per manufacturer's protocol.

A 2.3.3 Competition Assay:

C-di-AMP receptor was pulled down by using the method mentioned above. After high salt and wash-binding buffer washes each set of beads were divided into two parts consisting 20 mg beads each. To one set of beads, 6 µg of c-di-AMP (Courtesy-Dr. Joshua Woodward lab. Should go to acknowledgements), c-di-GMP (Invivogen) and cAMP (Sigma) were added; whereas WB buffer was added to the second set for negative control. These samples were incubated on ice for 3 hours with frequent, gentle shaking. The elution was transferred to a separate tube and 100% TCA was added to 1/10 final volume. Samples were incubated on ice overnight. Next day the TCA precipitated samples were centrifuged at 13000 rpm for 30 minutes. The supernate was removed and pellet was washed twice with 500 µl of ice-cold acetone. Subsequently, the pellet was suspended in 25 µl 1X Laemmli buffer and 2 µl of samples were electrophoresed as mentioned above.

A 2.3.4 Protein identification:

For the identification of protein, the samples were electrophoresed as above and then stained with Coomassie brilliant blue R250 in 50% methanol and 10% Acetic acid. Destaining was done with 30% Methanol and 10% acetic acid solution for one hour. The protein band of interest was cut from the gel and was sent to Cornell Proteomics and Mass Spectrometry Facility for protein identification. The protein was identified by nano-HPLC ms/ms with an orbitrap mass analyzer.

Table A2.1 *B. subtilis* strains used in this study

Strain	Genotype	Source
168	*trpC2*	Laboratory stock

A 2.5 REFERENCES

1. Kalia D, Merey G, Nakayama S, Zheng Y, Zhou J, Luo Y, *et al*. Nucleotide, c-di-GMP, c-di-AMP, cGMP, cAMP, (p)ppGpp signaling in bacteria and implications in pathogenesis. Chemical Society Reviews. 2013;42(1):305-41. doi: 10.1039/C2CS35206K.
2. Witte G, Hartung S, Büttner K, Hopfner K-P. Structural Biochemistry of a Bacterial Checkpoint Protein Reveals Diadenylate Cyclase Activity Regulated by DNA Recombination Intermediates. Molecular Cell. 2008;30(2):167-78.
3. Römling U. Great Times for Small Molecules: c-di-AMP, a Second Messenger Candidate in Bacteria and Archaea. Science Signaling. 2008;1(33):pe39-pe. doi: 10.1126/scisignal.133pe39.
4. Bejerano-Sagie M, Oppenheimer-Shaanan Y, Berlatzky I, Rouvinski A, Meyerovich M, Ben-Yehuda S. A Checkpoint Protein That Scans the Chromosome for Damage at the Start of Sporulation in *Bacillus subtilis*. Cell. 2006;125(4):679-90. doi: 10.1016/j.cell.2006.03.039.
5. Gundlach J, Herzberg C, Kaever V, Gunka K, Hoffmann T, Weiß M, *et al*. Control of potassium homeostasis is an essential function of the second messenger cyclic di-AMP in *Bacillus subtilis*. Science Signaling. 2017;10(475). doi: 10.1126/scisignal.aal3011.
6. Luo Y, Helmann JD. Analysis of the role of *Bacillus subtilis* σM in β-lactam resistance reveals an essential role for c-di-AMP in peptidoglycan homeostasis. Molecular Microbiology. 2012;83(3):623-39. doi: doi:10.1111/j.1365-2958.2011.07953.x.
7. Gundlach J, Dickmanns A, Schröder-Tittmann K, Neumann P, Kaesler J, Kampf J, *et al*. Identification, Characterization, and Structure Analysis of the Cyclic di-AMP-binding PII-like Signal Transduction Protein DarA. Journal of Biological Chemistry. 2015;290(5):3069-80. doi: 10.1074/jbc.M114.619619.

8. Choi PH, Sureka K, Woodward JJ, Tong L. Molecular basis for the recognition of cyclic-di-AMP by PstA, a PII-like signal transduction protein. MicrobiologyOpen. 2015;4(3):361-74. doi: doi:10.1002/mbo3.243.
9. Campeotto I, Zhang Y, Mladenov MG, Freemont PS, Gründling A. Complex Structure and Biochemical Characterization of the *Staphylococcus aureus* Cyclic Diadenylate Monophosphate (c-di-AMP)-binding Protein PstA, the Founding Member of a New Signal Transduction Protein Family. Journal of Biological Chemistry. 2015;290(5):2888-901. doi: 10.1074/jbc.M114.621789.